DIPLOMARBEIT

Titel der Diplomarbeit

Determination of the provenance of prehistoric wood by isotopic fingerprinting

Verfasserin

Monika Horsky

angestrebter akademischer Grad

Magistra der Naturwissenschaften (Mag. rer. nat.)

Wien, 2010

Table of Contents

Acknowledgements

First of all I would like to express my gratitude to my supervisor Thomas Prohaska for giving me the opportunity to write my diploma thesis about this topic and to become part of his working group. Beyond that I especially acknowledge the constant precious support in every stage of this thesis and his motivating encouragement. I could benefit a lot in many respects, both analytically and 'outside the box' of chemistry.

Sincere thanks go to Hans Reschreiter and Kerstin Kowarik whose archaeological finds and associated questions provided the basis for this study. The interdisciplinary collaboration and their enthusiasm were always enriching. I owe them special gratitude for the trip to the Hallstatt salt mine providing insight into prehistoric mining and today's archaeological activity.

The working atmosphere in the lab was both constructive and pleasant which is due to the members of the VIRIS working group anno 2009: Christopher, David, Johanna, Lindi, Lubna, Magda, Marion, Martin, Steffi and guests. However, fun times did not miss out either, be it in coffee breaks or at off-lab activities. I greatly appreciate the mutual assistance in many respects with my favourite fellow diploma students Lindi and Magda. Special thanks also go to Johanna who considerately introduced and supervised me. Furthermore I acknowledge the (technical) support of several other colleagues in the AGAC laboratory in Muthgasse, especially Alexandra Pederzolli, in the course of sample preparation.

Besides, I am obliged to my parents for their support which enabled me to focus on my studies. And last but not least, the backing of my private environment was essential for me and consequently for my work's progress, too. Huge thanks to Alexandra, Christian, Franzi, Sabrina, Violeta et al. for just being there, offering diversion, patience and moral support during the last year.

Finally I apogolize to anyone I may have forgotten to mention by name and thank you, dear reader, for your attention and your interest in this work.

Abstract

Prehistoric organic material like wood and textiles has been preserved for about 3000 years in the special environment of a salt mine in Hallstatt, Upper Austria. These finding present a unique information source on past structures of industry, society and trade. Their plain existence gives evidence of human sub-surface mining activities as early as the Bronze Age, but major questions like provenance or trading are not answered, yet. This information is maybe concealed within the chemical composition. Strontium isotopes as well as multi-element signatures can act as fingerprints of geographical origin. Unfortunately, in this case, the conserving salt mine environment led to the contamination of organic material and consequently masking of the original inorganic signatures.

In a first step, wood samples were screened for NaCl and other salt content applying laser ablation – inductively coupled plasma mass spectrometry (LA-ICP-MS) to monitor diagenetic alteration. Depth profiles of drill cores of massive timber samples revealed full penetration of secondary material. In order to cope with this challenge, a decontamination procedure was developed involving ultrasonic leaching with purified water as well as diluted nitric acid. Prior to analysis by ICP-MS dried wood samples were digested in a microwave oven using HNO_3/H_2O_2. The cleaning approach proved itself successful for Sr^{2+} and other easily soluble ions in a quantitative multi-element determination using a quadrupole instrument (ICP-QMS), while measurement of rare earth element content on a high resolution – ICP-MS showed elevated levels compared to modern wood samples. The latter were sampled in the direct proximity of the mine in order to define the local signature in wood. These 29 samples were measured for comparison reasons with all applied methods. Furthermore, surrounding material from the mine environment was extracted by NH_4NO_3 solution allowing the investigation of the elemental and isotopic composition of contaminants.

Sr was separated from the matrix by an ion extraction procedure prior to determination of the high precision $^{87}Sr/^{86}Sr$ isotope ratio by multiple collector – ICP-MS. Ratios of samples from the mine environment define a small range of low values, while both recent and prehistoric wood dominantly exhibit higher ratios. A spike experiment with ^{84}Sr on modern wood, surveyed by LA-ICP-MS, should confirm the applicability of the developed methods, but showed that secondary Sr could not be fully removed. Consequently, the assumption of non-exhaustive leaching with respect to diagenetic Sr was included into evaluation and a mixing theory was adopted to extract the natural Sr isotopic composition.

Zusammenfassung

Die besonderen Lagerungsbedingungen im Hallstätter Salzbergwerk in Oberösterreich ermöglichten die Erhaltung von organischem Material aus prähistorischer Zeit über 3000 Jahre hinweg. Diese Funde stellen daher eine einzigartige Informationsquelle über vergangene Strukturen von Industrie, Gesellschaft und Handel dar. Allein ihre Existenz beweist Bergbauaktivitäten unter Tage, die bis in die Bronzezeit zurückreichen. Fragestellungen über Handel und Herkunft sind aber weitgehend ungelöst. Über die chemischen Zusammensetzung hat man nun einen möglichen Zugang zu dieser Information. Strontium-Isotopenverhältnisse sowie die elementare Zusammensetzung können als Fingerabdruck des geographischen Ursprungs dienen. Die konservierenden Bedingungen eines Salzbergwerks zeigen in dieser Hinsicht jedoch auch eine Schattenseite, da eindringende anorganische Salze die organischen Funde kontaminieren und in Folge die ursprünglichen Isotopen- und Elementsignaturen maskieren.

Der erste Schritt dieser Arbeit umfasste ein Screening der Holzfunde in Hinblick auf ihren Gehalt an NaCl und anderen Salzen mittels induktiv gekoppelter Plasma – Massenspektrometrie mit Probeneinführung durch Laserabtragung (LA-ICP-MS). Die erhaltenen Tiefenprofile massiver Bauholzproben offenbarten die komplette Durchdringung des Materials mit Salzen. Um dieser Herausforderung beizukommen, wurde eine Reinigungsmethode mit Hilfe von ultraschall-unterstützer Extraktion mit entionisiertem Wasser und verdünnter Salpetersäure entwickelt. Vor der Analyse mittels ICP-MS wurden die getrockneten Holzproben einem Mikrowellen-aufschluss mit HNO_3/H_2O_2 unterzogen. Die Dekontaminationsstrategie erwies sich durch quantitative Multi-Elementanalyse an einem Quadrupol-Gerät (ICP-QMS) als erfolgreich für Sr^{2+} und andere leichtlösliche Ionen. Eine Bestimmung des Gehalts an Seltenen Erden mittels hochauflösender ICP-MS zeigte jedoch erhöhte Werte verglichen mit heutigen Holzproben. Zusätzlich wurden nämlich 29 Bäume in der direkten Umgebung des Bergwerks beprobt und mittels aller angewandten Methoden zum Vergleich analysiert, um lokale Signaturen zu definieren. Weiters wurde das die Proben direkt umgebende Material, genannt Heidengebirge, mit NH_4NO_3-Lösung extrahiert, um die elementare und Isotopenzusammensetzung der Kontamination zu bestimmen.

Eine Sr selektive Extraktion wurde angewandt, um Sr von der Probenmatrix abzutrennen, eine Voraussetzung für hochpräzise Isotopenverhältnismessungen mittels Multikollektor – ICP-MS. Die gemessenen $^{87}Sr/^{86}Sr$-Verhältnisse des Umgebungsmaterials definieren einen engen Bereich mit niedrigen Werten, während sowohl prähistorische als auch moderne Holzproben großteils höhere Verhältnisse aufweisen. Ein Spike-Experiment mit ^{84}Sr wurde an rezentem Holz durchgeführt und mittels LA-ICP-MS überwacht, mit dem Ziel, die Anwendbarkeit der entwickelten Methode zu bestätigen. Es zeigte sich jedoch, dass sekundäres Sr nicht zur Gänze entfernt werden konnte. Deshalb wurde die Annahme, dass die Extraktion des diagenetischen Sr unvollständig stattfand, in die Auswertung integriert. Mit Hilfe einer Mischungslinie konnte so die natürliche Sr-Isotopenzusammensetzung gewonnen werden.

I   Introduction

I.1   Objective of the pilot study

The present pilot study was assessing the applicability of multi-element patterns and Sr isotope ratio measurements for the determination of provenance of wooden findings. The storage conditions of these findings inside a former salt mine guaranteed on the one hand their preservation, but on the other hand present an obstacle with regard to inorganic contaminations. A method had to be developed to remove these masking diagenetic salts in order to obtain the original signal, using established procedures for sample preparation and measurement by (multiple collector) inductively coupled plasma mass spectrometry. The feasibility of this approach was investigated as well.

Furthermore, a basis for the determination of origin had to be established by defining the local signal. First steps were accomplished on the way to geographical mapping of Sr and trace element signatures in wood in the region of interest for the creation of local isoscapes.

I.2   Archaeological background

This chapter shortly summarises the current archaeological knowledge on the Bronze Age salt mining industry in Hallstatt with an emphasis on previous examinations on the findings investigated during this study.

Hallstatt in Upper Austria is a UNESCO World Cultural Heritage Site. Its location in the Northern Calcareous Alps stands out due to its geology [Rohn et al., 2005]. In a simplified description it is characterized by the so-called 'Haselgebirge' below some limestone layers. 'Haselgebirge' signifies alternating belts of sodium chloride rich rock and of interburden composed of gypsum, anhydrite, clay and sandstone (see also I.5). The village Hallstatt is located next to a steep hillside at the edge of the lake Hallstättersee (508 m asl), while the mine entrances are uphill in a hanging valley about 350 m above the lake and higher. Therefore the valley is not easy accessible and not hospitable, either, but nonetheless there is evidence of human presence as long as 7000 years ago. Presumably this was even back then due to the precious salt deposits below the surface of the valley. Mining activities are proven from the 15th century BC, but at

that time the subsurface mines were already extensive and required highly developed techniques. This thesis focuses on findings from one of the oldest of the so far known prehistoric galleries at the site 'Christian von Tuschwerk', which are one of the focuses of the current excavation and examination activities of the archaeologists of the Department of Prehistory from the Museum of Natural History, Vienna. [Barth, 2009]

Two further independent prehistoric mines are known as well, which both date from the Iron Age, when Hallstatt emerged as a cultural and economical metropolis in Central Europe. The findings of the site are of such importance, that the era from 800 to 400 BC was named 'Hallstatt period'. While comprehensive findings, not only from subsurface mines, but also from a huge burial ground allow researchers to get a versatile picture of life at the Hallstatt Age, the Bronze Age mining conception is mainly based on finds from inside the mine. So far, no Bronze Age settlements or burial grounds were located due to the fact, that the surface from that period is today covered by some meters of debris from mass movements in the meantime. [Reschreiter et al., 2009; Rohn et al., 2005]

Today's researchers owe their unique finds originating from Bronze Age mining on the one hand to the special environment inside the salt mine preventing the degradation of organic material for some thousand years and on the other hand to the practice of prehistoric workers to leave behind their waste inside the mine. They applied a dry-mining process in huge halls and while they proceeded the cavity was filled from the floor with mining leftovers. This material is called 'Heidengebirge' and comprises mainly burnt-down illumination chips, worthless rocks (clay and gypsum) and broken material: burst tool handles and other wooden gadgets, ripped textiles, skin and fur pieces as well as ropes. Furthermore, human excrements, food remains and charcoal from burning can be found. Although the pressure exerted by the mountain led to closure of most cavities, their former existence is traceable due to these extensive mining leftovers. Additionally surface material like tree trunks with roots, soil, limestone and clay is found inside the shafts and halls providing the basis for the theory, that Bronze Age mining was maybe ended by a debris avalanche that led to the collapse of the galleries. [Ehret, 2009; Reschreiter and Kowarik, 2009a; Reschreiter and Kowarik, 2009b]

The presumable end of Bronze Age mining activities can even be dated to a certain year: 1245 BC. This assumption relies on the fact, that so far no timber that was felled later than that has

been excavated. Futhermore it is known, that working on fresh green wood is far easier when using bronze axes, so building probably followed felling immediately. The year-precise dating of wooden finds is based on dendrochronology. Grabner et al. established a chronology based on annual tree rings for the Salzkammergut region ranging back until 1523 BC. It relies on preserved tree trunks from a lake and a bog, wood from the salt mine, timber from historical buildings, and recent trees. Thus 128 samples from the gallery Christian von Tuschwerk could be dated: the trees had been felled between 1458 and 1245 BC. Among the samples was timber from a very spectacular finding: the world's oldest known preserved wooden staircase, dating to the years 1344 and 1343 BC. [Grabner et al., 2007] The dendrochronology approach improves dating precision a lot compared to previous trials on some Hallstatt findings via ^{14}C measurements using accelerator mass spectrometry providing only a rough estimate [Rom et al., 1999].

But archaeological research on the finds goes far beyond dating of wood. The diverse organic findings are examined thoroughly applying a wide range of methods, from basic visual investigation to modern analytical approaches in order to conclude on their provenance and proposed usage. From the group of organic material, so far woollen textile findings have been under examination. High performance liquid chromatography with photo diode array detection (HPLC-PDA) as well as scanning electron microscopy coupled to energy dispersive X-ray spectroscopy (SEM/EDS) were applied for dyestuff and mordant analysis [Joosten et al., 2006]. Future research on the findings will cover, for example, DNA analysis on animal skins, human excrements and maybe human remains on tool handles [Uzunoglu-Obenaus et al., 2009].

The results from all these scientific considerations will be put into a larger context in order to create a model of prehistoric life, technology and organisation. Many questions shall be answered, ranging from very practical ones arising from the design of tools to more general ones concerning for example infrastructure, division of labour and lifestyle. The evident well-developed mining industry required good organisation, especially in the rather difficult location in the Alps. In order to supply the mining enterprise and the workers with all required goods (nutrition, equipment, Bronze tools) subcontracted supply was necessary. But how were the trade routes, what was the size of the trading area? What was traded – only parts or whole tools and pieces of equipment? Which steps were outsourced, were there specialized suppliers or was the mine part of an industrial complex involving all preliminary production processes

and supply tasks? This is where this pilot study links in with its aim to solve the question of origin of wooden findings. [Kowarik, 2009]

I.3 Geochemical methods in archaeometry

One approach in archaeometry is the use of geochemistry as a key to information on the past, stored in archaeological findings. Geochemistry is usually based on processes on large timescales, so in comparison the ages of humanity from prehistory until today are a very short period. This stability provides a good basis for its application to archaeological questions. Nonetheless, biogeochemical processes have to be taken into account, if we want to decipher geochemistry related patterns in biological material. These processes are dependent on environmental conditions and thus not necessarily comparable between today and prehistoric times.

I.3.1 Isotopic systems

I.3.1.1 Strontium and other heavy stable isotopes

Strontium is an alkaline earth element and consequently very similar to calcium, one of the most abundant elements in the earth's crust and an important nutrient for living organisms. Sr acts as a proxy for Ca and therefore participates in geochemical and biogeochemical processes. [Capo et al., 1998] It features four naturally occurring stable isotopes (Tab. 1), one of which is radiogenic. ^{87}Sr is produced by radioactive β^- decay of ^{87}Rb with a decay constant of $1.42{\cdot}10^{-11}$ a^{-1} (corresponding to a half-life of $48.8{\cdot}10^{9}$ a) [Steiger and Jäger, 1977]. Hence the proportion of ^{87}Sr is not constant, but varies with the age of a rock and its (initial) relative Rb content. Sr is a 'heavy' element, so relative mass differences between isotopes are small. As a consequence, fractionation occurs only to negligible extents in biological processes. Thus, the isotopic composition acts as a fingerprint of the geological material the Sr originates from. [Capo et al., 1998] Usually it is expressed by the ^{87}Sr/^{86}Sr ratio, which exhibits values varying between 0.702 and 0.750 in the continental crust. [Bentley, 2006]

Typical concentration ranges for Sr are reported to be 370 µg g^{-1} earth crust average, 8 – 2500 µg g^{-1} in wood and 0.7 – 383 µg L^{-1} in rain water. [Capo et al., 1998]

element	mass number	isotopic abundance [atom %]
Sr	84	0.56
	86	9.86
	87	7.00
	88	82.58
Rb	85	72.17
	87	27.83

Tab. 1 Representative isotopic composition of Sr and Rb [Rosman and Taylor, 1998]

For all these reasons, the Sr isotope system renders useful for diverse applications, ranging from geochronology [Müller, 2003] and geology [Spötl and Pak, 1996] over ecology [Åberg, 1993; Horstwood, 2005; Poszwa et al., 2004; Stewart et al., 1998] to food authentication [Swoboda et al., 2008], forensic science [Aggarwal et al., 2008] and migration studies with archaeological [Prohaska et al., 2002] and biological background [Balter et al., 2008].

The application of Sr as a tracer of provenance of e.g. plants or artefacts produced from plants is based on its cycling through ecosystems. Primarily Sr becomes mobile by being released from geological material via weathering processes. The mobile fraction in the soil is then bioavailable to plants via root uptake. Furthermore, mixing processes may occur if Sr from different sources is present. Potential additional inputs to the soil mobile fraction are the decomposition of organic matter (e.g. from litterfall), atmospheric deposition via precipitation and streaming water. Precipitation contains Sr from its evaporation source (e.g. the oceans), but can also wash out Sr from atmospheric dust, either from anthropogenic sources or soil erosion. [Åberg, 1993; Berger et al., 2006]

Another heavy stable isotope system applied in a similar context is e.g. the lead isotopic system. It is mainly used to trace environmental pollution sources, but also as provenance indicator. [Komarek et al., 2008; Prohaska et al., 2005; Schultheis et al., 2004]

High precision methods for the measurement of these isotope ratios of interest are mainly thermal ionisation mass spectrometry (TIMS) and multiple collector inductively coupled plasma mass spectrometry (MC-ICP-MS; see chapter I.6). [Yang, 2009]

I.3.1.2 Light stable isotopes

The term 'light stable isotopes' or 'bioelements' refers to isotopic systems of the constituent elements of organic material, i.e. hydrogen, carbon, oxygen, nitrogen and sulphur. All of them have at least two stable isotopes, the lighter/lightest of which has the highest abundance.

Typically the following ratios are investigated: ^{2}H/^{1}H, ^{13}C/^{12}C, ^{18}O/^{16}O, ^{15}N/^{14}N and ^{34}S/^{32}S, which exhibit high relative mass differences between 6.3 and 100%. These differences affect their thermodynamic and kinetic properties resulting in the accumulation of the heavier isotope in the thermodynamically favoured state or component. Consequently, significant fractionation effects occur during all physical and chemical processes. Commonly, these ratios are reported relative to an international reference such as, for example, the Vienna Standard Mean Ocean Water (VSMOW) for hydrogen, using the delta notation in per mil. [Lee-Thorp, 2008; Sulzman, 2007]

Light stable isotope analysis expands the range of covered processes toward organic and biochemical context. The field was pioneered by earth scientists, but has been adopted by diverse sciences such as ecology or animal migration studies due to the capability to integrate biochemical processes such as photosynthesis (δ^{13}C) or nitrogen fixation (δ^{15}N). δ^{34}S reflects geological differences, too. [Lee-Thorp, 2008; Martínez del Rio et al., 2009] Dendroclimatology utilises the fact, that conclusions on (palaeo-)climate concerning temperature and precipitation are possible based on δ^{13}C, δ^{18}O or δ^2H analysis of tree rings. [Loader et al., 2008; Nakatsuka et al., 2004]. Regional climatic differences also provide a basis for geographical provenancing of plants. [Ehleringer et al., 2000; Horacek et al., 2009; Keppler and Hamilton, 2008; Stern et al., 2006]

The analytical method mainly applied for the determination of these isotope ratios is isotope ratio mass spectrometry (IRMS). A typical continuous flow instrument consists of an elemental analyser converting the sample into the desired gas (CO_2, N_2, H_2 or SO_2, respectively) and purifying it by integrated gas chromatography. The gas is subsequently ionised by electron impact, ions are separated in a magnet and detected simultaneously in Faraday cups. [Sulzman, 2007] An alternative method is optical detection via infrared spectrometry. A high sensitivity advancement of this technique is cavity ring down spectroscopy (CRDS), which increases the optical path length via a resonant optical cavity. [Kerstel and Gianfrani, 2008]

I.3.2 Multi-element patterns

I.3.2.1 Rare Earth Elements

According to IUPAC nomenclature [IUPAC, 2005], the group of rare earth elements (REE) comprises scandium, yttrium and the lanthanoids (La, Ce, Pr, Nd, Pm, Sm, Eu, Gd, Tb, Dy, Ho, Er, Tm, Yb and Lu). They feature very high similarity in their chemical properties like preferred oxidation degree +III and ionic radii. Therefore, they usually occur jointly. Their abundance in the earth's crust is not as rare as the name suggests, but they usually occur in accessory minerals like phosphates, carbonates, fluorides and silicates rather than forming ores. Depending on the parent material as well as on soil properties like pH, weathering state and content of organic matter and clays, concentration in soils can vary significantly. [Tyler, 2004]

name	symbol	atomic number	stable isotopes (mass numbers)[a]	earth's crust abundance[b] [$\mu g\ g^{-1}$]	CI chondrite concentration[c] [$ng\ g^{-1}$]
scandium	Sc	21	45	25	5920
yttrium	Y	39	89	31	1570
lanthanum	La	57	139	35	237
cerium	Ce	58	140	66	613
praseodymium	Pr	59	141	9.1	92.8
neodymium	Nd	60	142, 143, 145, 146, 148	40	457
promethium	Pm	61	-	$4.5 \cdot 10^{-20}$	-
samarium	Sm	62	144, 149, 150, 152, 154	7.0	148
europium	Eu	63	151, 153	2.1	56.3
gadolinium	Gd	64	154,155,156,157,158	6.1	54.6
terbium	Tb	65	159	1.2	36.1
dysprosium	Dy	66	156,158,160,161,162,164	4.5	246
holmium	Ho	67	165	1.4	54.6
erbium	Er	68	162, 164, 166, 167, 168, 170	3.5	160
thulium	Tm	69	169	0.5	24.7
ytterbium	Yb	70	168, 170, 171, 172, 173, 174, 176	3.1	161
lutetium	Lu	71	175	0.8	24.6

Tab. 2 REE data from [IUPAC, 2005], [a] from Seelmann-Eggebert et al. [1981], [b] from Greenwood and Earnshaw [1990] and [c] from McDonough and Sun [1995]

There are various studies on the uptake mechanisms of REE from soil to plants resulting in different observations of involved fractionation effects. Uptake differs among species and among elements. Enrichment of HREE or of LREE can occur as well as W- or M-type patterns (tetrad effect) of chondrite normalized values. Complexation with organic ligands plays an important role in REE biogeochemistry, both for their bioavailability in soils and transport and fixation due to adsorption to cell walls inside the plant organism. [Fu et al., 2001; Liang et al., 2008]

The accurate quantitative measurement of these elements is not trivial. Mainly two methods are applied for environmental and biological samples: ICP-MS following digestion and occasionally preconcentration and/or separation, [e.g. Djingova et al., 2001; Fu et al., 2001; Ivanova et al., 2001; Pearson et al., 2009; Spalla et al., 2009; Xu et al., 2003] as well as neutron activation analysis (NAA) [Wyttenbach et al., 1998a; Wyttenbach et al., 1998b; Xiao et al., 2003]. The application of the latter is limited due to higher limits of detection than ICP-MS: in a study of peat bog profiles, the authors report LoDs of about one order of magnitude higher for INAA of 8 g peat sample compared to ICP-QMS of 200 mg digested sample [Krachler et al., 2003]. As far as ICP-MS measurements are concerned, the advance of sector field mass analysers improved their detectability due to enhanced sensitivity (in low resolution mode) and the possibility to remove at least part of the interfering species (e.g. oxides) in medium or high resolution mode.

Another problem derives from surface contaminations with dust or soil, which are hard to remove and may distort analytical results. [Wyttenbach and Tobler, 2002]

I.3.3 Provenance studies of organic archaeological findings

Tab. 3 gives an overview over provenance studies of organic archaeological findings via isotopic tracing.

reference	archaeo-logical samples	modern samples	storage conditions	analytes	method	decontamination method	focus
Benson et al., 2003	maize	synthetic soil water		$^{87}Sr/^{86}Sr$; Ba/Sr, Mg/Sr, Y/Yb	TIMS; ICP-MS		sourcing
Benson et al., 2006	textiles (willow, tule)	water, synthetic soil solution, modern plant samples	cave	$^{87}Sr/^{86}Sr$; $\delta^{18}O$; trace metals	TIMS; IRMS; ICP-MS, ICP-AES	scrubbing	plant sourcing
Benson et al., 2008	maize	mice bone, synthetic soil water; modern maize, soil water		$^{87}Sr/^{86}Sr$; trace metals, REE	TIMS; ICP-MS, ICP-AES		method development/ evaluation for sourcing
Benson et al., 2010	maize	synthetic soil water		$^{87}Sr/^{86}Sr$; trace metals, REE	TIMS; ICP-MS, ICP-AES	acid leaching	decontamination
Durand et al., 1999	timber	wood		multi-element	ICP-MS, ICP-AES		sourcing
English et al., 2001	timber	wood, soil, bedrock, stream water		$^{87}Sr/^{86}Sr$	TIMS	surface discarded	sourcing

reference (continued)	archaeological samples	modern samples	storage conditions	analytes	method	decontamination method	focus
Frei et al., 2009a	woollen textiles	sheep hair, soil samples	peat bog	$^{87}Sr/^{86}Sr$	TIMS	HF attack	method establishment decontamination, origin tracing
Frei et al., 2009b	plant fibre, woollen textile, human skin	sheep hair, bog	peat bog	$^{87}Sr/^{86}Sr$	TIMS	HF attack	differentiation between origins
Heier et al., 2009	carbonized grain	charred and uncharred grain		$^{87}Sr/^{86}Sr$	TIMS	HCl leaching	retrieval of biogenic signal (after chalk immersion)
Reynolds et al., 2005	timber	wood		$^{87}Sr/^{86}Sr$	TIMS		sourcing
Stern et al., 2006	birch bark tar	birch bark		$\delta^{13}C$, $\delta^{18}O$, $\delta^{2}H$	IRMS	H_2O, brush	geographical discrimination
von Carnap-Bornheim et al., 2007	leather, wool, fur	bog samples	peat bog	$^{87}Sr/^{86}Sr$	TIMS	rehydration	decontamination

Tab. 3 Literature on provenancing of organic archaeological findings via isotopic methods

Alternative strategies applied in wood provenance studies apart from isotopes consider e.g. wood anatomy or genetics. The determination of timber species from anatomical investigation combined with historical texts is an approach to draw conclusions on possible origin of old wooden artefacts. [Romagnoli et al., 2007]. Tree ring investigation allows not only the dating of wood samples, but also the assignment of samples to the provenance of trees or even to one same tree stem. [Bernabei et al., 2010; Haneca et al., 2009; Haneca et al., 2005] Population distribution maps or databases using chloroplast DNA markers provide another tracing approach for modern timber. [Deguilloux et al., 2003; Finkeldey et al.; Tnah et al., 2009]. Another molecular method uses FTIR spectroscopy to discriminate between wood from different origins. [Brunner et al., 1996; Rana et al., 2008]

I.4 Wood chemistry

A given analytical problem always requires the consideration of the sample matrix and its relevant properties. In this case, the structure, ultrastructure and chemical composition of wood as well as a possible alteration due to ageing processes or storage conditions have to be taken into account. Furthermore, the analyst needs to understand the possible desired or undesired modification of the sample's nature during the sample preparation procedure. This

chapter will give a short introduction to wood chemistry with a focus on the inorganic components (comprising our analytes) and their integration in the organic matrix.

Wood is a perennial vascular tissue in plants (xylem) fulfilling several functions: transport of water and nutrients, storage and mechanical support. [Myburg and Sederoff, 2001]

Roughly, a distinction between softwoods (conifers) and hardwoods (deciduous trees) is necessary. Focusing on one living stem a differentiation is possible between heartwood and sapwood, and within both of them the separation of annual rings is visible to the naked eye (in trees growing in temperate regions). The growth rings themselves are again divided into an earlywood and a latewood region. [Fengel and Wegener, 1989] All these macroscopic discriminations affect the properties and thus for example the analyte concentrations. Regarding especially small scale analysis, like the use of LASER ablation (see chapter I.6.3) which allows the sampling of very small amounts of wood from a distinct spot on the original sample, these differences have to be taken into account. The spatially resolved analysis of elemental composition in tree rings is called dendrochemistry and is often applied, e.g. to answer ecological questions or for environmental monitoring. [Barrelet et al., 2006; Barrelet et al., 2008; Burnett et al., 2007; Hoffmann et al., 1997; Monticelli et al., 2009; Pearson et al., 2005; Prohaska et al., 1998; Watmough et al., 1997]
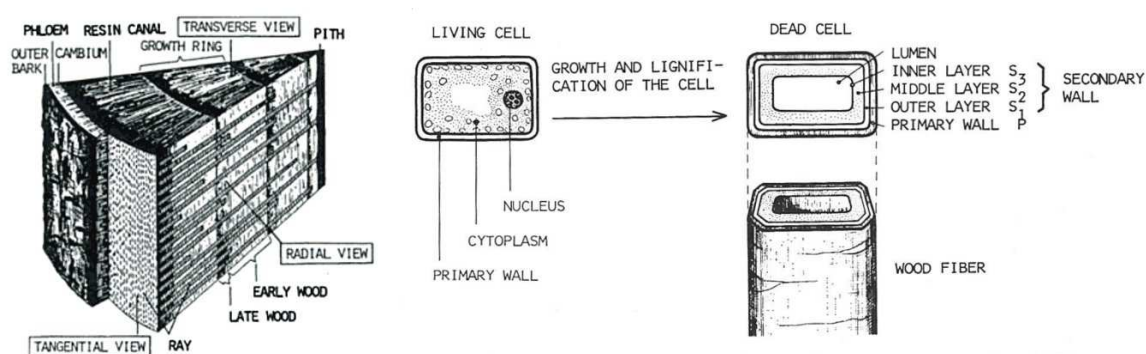
Fig. 1 Wood structure (left, 'Sections of a four-year old pine stem') and ultrastructure (right, 'Development of the living cell to wood fiber'), [Sjöström, 1981]

Trees exhibit different types of cells for different functions, depending on the species as well. Among the cell types occurring in wood are vascular cells as well as longitudinal and ray parenchyma cells, all of which – except for the very latter – are oriented parallel to the stem axis resulting in the wood's fibrous texture. In contrast to softwood hardwood shows pores (conducting vessels) embedded in a tissue of shorter fibres with thicker cell walls and smaller

lumina compared to the softwood's tracheids. The length of tracheids and fibres amounts to a few millimeters, while hardwood vessels measure in the range of 10^{-1} m. Some conifer species additionally have resin canals, surrounded by epithelial cells. After their death due to heartwood formation or felling of the tree all mentioned types of cells show basically the same structure and ultrastructure (Fig. 1) as can be observed using scanning electron microscopy: They consist of a cell wall built from concentrically arranged cell wall layers surrounding the lumen. In more detail, the composition of these layers depends again on the type of wood and the former function of the cell, but roughly they are similar. A middle lamella between two neighbouring cells acts as a glue. Next to it there is the primary wall, followed by two (or three, for parenchyma cells only) secondary wall layers (S1, S2, S3). The innermost layer bordering the lumen is the tertiary layer, in some cases covered with warts. [Fengel and Wegener, 1989]

The cell wall layers with their distinct structure provide the cell with ruggedness and flexibility, especially during its growth. The layers differ on the one hand concerning their chemical composition and thickness, but more importantly in the arrangement of the macromolecular constituents on the other hand. The cellulose fibrils, which provide the structure, are oriented in different angles and show different degrees of order. The S2 layer makes up the main part of the cell wall's thickness. Without digging too deep into the details, it should anyhow be mentioned, that there are functional elements in the cell walls, so-called pits, that occur in different forms related to their conducting function in the living cells. After the cell's death, in those pits in parenchyma cell walls next to vascular cells the formation of tyloses occurs. A tylosis is a thin membrane growing into the lumina preventing the water from streaming through it.

Finally and most interestingly for our analytical problem, wood needs to be examined on a molecular level. Its main constituents are the macromolecules cellulose, various hemicelluloses (polyoses) and lignin. Furthermore, there are substances with low molecular weight which can be subdivided into organic and inorganic species.

Cellulose is a linear polysaccharide consisting only of β-D-glucose monomers and presents the major component. (Fig. 2A) The other polysaccharides differ between hardwoods and softwoods – basically glucomannans and xylans occur, the first in a higher proportion in conifers, the latter in deciduous trees. [Zhong and Ye, 2009] Xylans are of particular interest

concerning the bonding of the mineral elements as they exhibit acid groups (Fig. 2B). The basic structure is a homopolymer backbone of xylose monomers, some of which carry O-acetyl substituents at C2 or C3. Furthermore it is branched and includes 4-O-methylglucuronic acid units and other monomers depending on the kind of wood. The third macromolecular component is lignin (Fig. 2C), a highly cross-linked aromatic polymer built from phenylpropane units. [Fengel and Wegener, 1989]
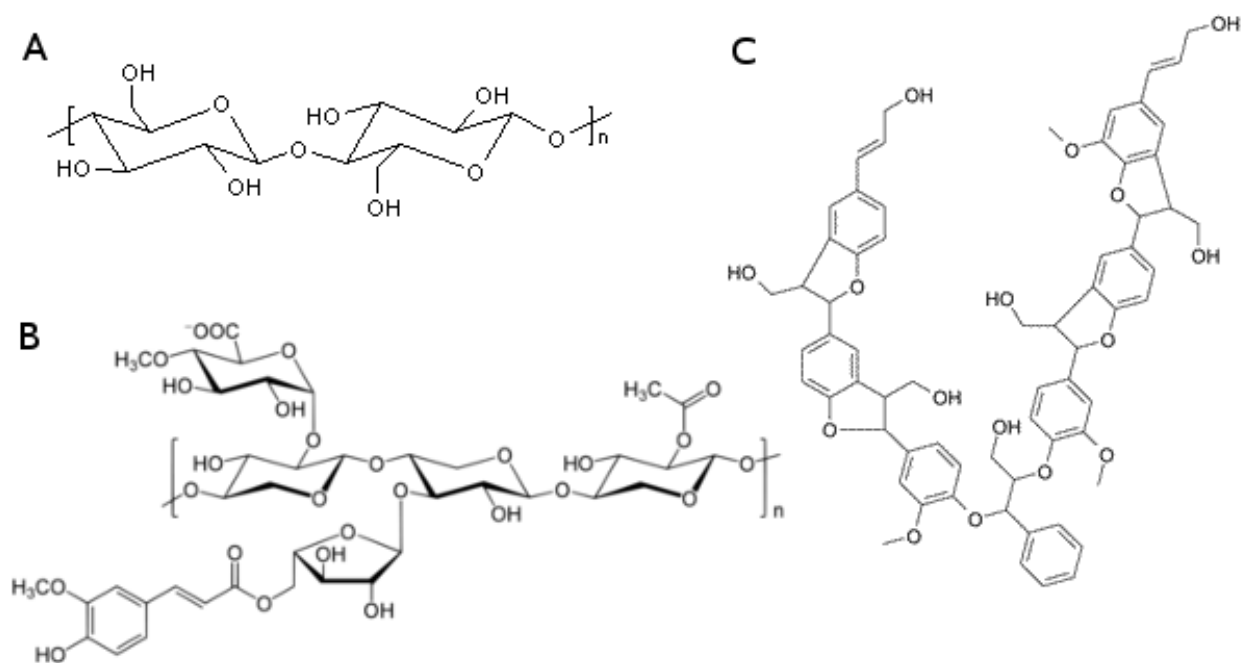
Fig. 2 Structural formulae of selected macromolecular wood constituents. A: cellulose, source: Kratzert [2000]; B: lignin (detail), source: Steen [2010]; C: xylan, source: N.N. [2009]

I.5 Geology of the investigated site

The Northern Calcareous Alps are a geologically diverse region. Mesozoic marine carbonates are widespread, but rock ages range between Permian (Haselgebirge) and Eocene (Gosau Group), while Triassic rocks dominate. Lithology covers salt-bearing claystones, marlstones, limestones, dolostones, sandstones and conglomerate rocks. 'Haselgebirge' signifies Permian and Triassic evaporites and consists of siliciclastic mudrocks, siltstones and variable fractions of calcium sulfates, halites, carbonates, sandstones and volcanic rocks. [Rohn et al., 2005; Spötl and Pak, 1996]

Spötl and Pak [Spötl and Pak, 1996] investigated and compared the Sr and S isotopic composition in $CaSO_4$ evaporites (gypsum and anhydrite) from various spots in the Northern Calcareous Alps including Hallstatt. Their Sr isotope data are discussed in III.5.3.

I.6 Inductively coupled plasma – mass spectrometry

I.6.1 Principle

Inductively coupled plasma – mass spectrometry (ICP-MS) is an analytical technique enabling the quantitative determination of trace elements and isotope ratios. Like every mass spectrometric method it is based on the separation of ions according to their mass/charge ratio (m/z). The ion source is an inductively coupled Ar plasma which generates preferably singly positively charged atomic ions. Thus the differentiation not only between elements but also between isotopes is possible allowing the measurement of isotope ratios. An ICP-MS instrument basically consists of the following parts: sample introduction system, ion source, interface, ion optics, mass analyser and detector (Fig. 3).
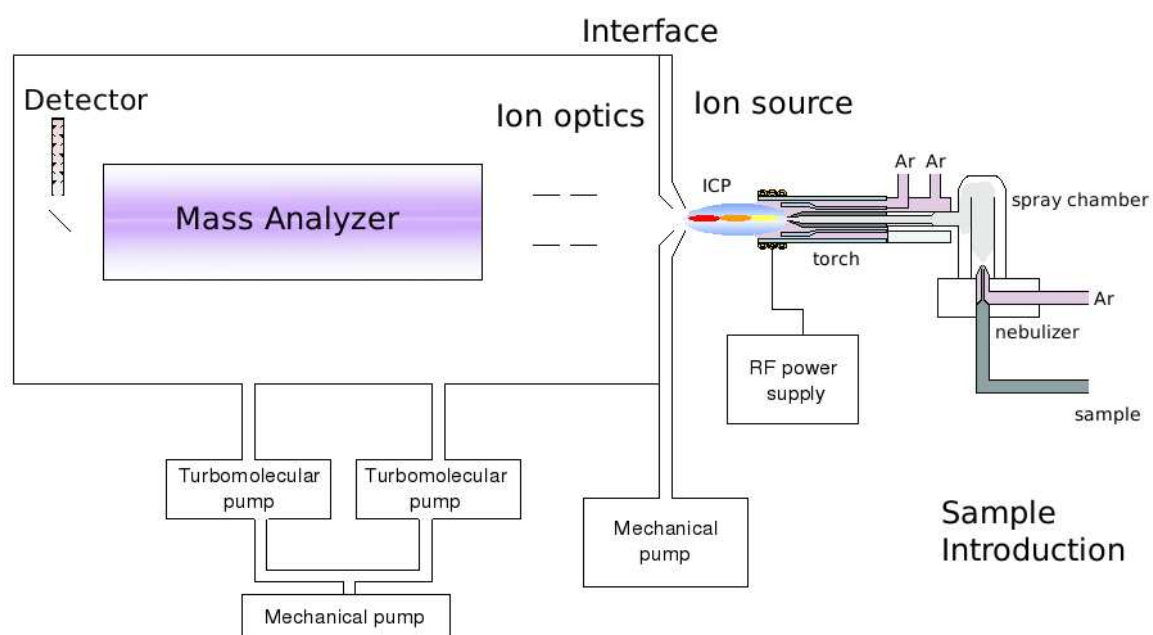
Fig. 3 Schematic view of an ICP-MS instrument, modified from Thomas [2001a] and Swoboda [2008]

I.6.1.1 Sample Introduction

The purpose of the sample introduction system is the generation of an aerosol of droplets or solid particles of appropriate size to guarantee ionization efficiency in the following ICP.

Aerosol formation is accomplished by a nebulizer when liquid samples are investigated. Different strategies are applied. The most common designs are the concentric and the crossflow nebulizer. Both use a gas flow, concentric to the liquid flow or rectangular to it, respectively, to break up the liquid into small droplets. Microflow nebulizers are based on the concentric design, but made of polymer materials, e.g. PFA, allowing a thinner capillary and higher gas pressures, resulting in lower uptake-rates. [Thomas, 2001a] An alternative to these pneumatic nebulizers is ultrasonic nebulization, which uses a scintillating quartz to generate aerosol droplets. [Thomas, 2003]

The pneumatic nebulizer sprays the aerosol into a spray chamber which selects the droplets of suitable size by removing too large ones. The Scott double pass design is based on gravity: heavier droplets will hit the walls of a central tube and are drained, while the smaller ones pass through and enter the injector tube to the plasma torch. Another design relies on the centrifugal force: the cyclonic spray chamber creates a vortex; too large droplets again hit the wall and are removed via a drain tube. The additional use of membrane desolvation systems in advanced nebulizers allows the reduction of water load into the plasma. [Thomas, 2001a]

A different sample introduction strategy allows the direct measurement of solid samples: the ablation using a laser beam (see chapter I.6.3). It generates an aerosol consisting of solid μm-sized particles. Another approach which is applicable to soild samples, too, is electrothermal vaporisation (ETV). It involves drying, ashing and vaporisation of a sample by heating. [Thomas, 2002; Thomas, 2003]

I.6.1.2 Ion Generation

The aerosol needs to be dried (in case of liquid droplets), atomized and ionized in order to create (singly) positively charged (atomic) ions that can be separated in a mass analyser. These processes take place in an argon plasma: a highly excited partially ionized gas. The plasma discharge is built from an Ar gas flow through the middle tube of a quartz torch. Further necessary components are a grounded radio frequency coil and a radio frequency generator (power supply). It applies an alternate current of 27 or 40 MHz with a power between 750 and 1500 W thus creating an electromagnetic field within the coil. A high voltage spark is created and ionizes Ar atoms releasing electrons. These are accelerated in the field producing further collision induced ionization. These processes result in a plasma discharge, visible by the

emission of light and sustained by continuous inductive coupling. It includes different heating zones with temperatures between 6000 and 10000 K. [Thomas, 2001b]

I.6.1.3   Interface

The plasma region is under atmospheric pressure while all mass separation devices require high vacuum (between 10^{-6} and 10^{-8} mbar). The role of the interface region is the realization of this transition including the efficient, reproducible and representative (stoichiometric) sampling of the generated ions from the plasma to the ion optics. It consists of a cooled interface housing containing two metal cones named sample and skimmer cone (usually made of Ni, Al or Pt) with small orifices below 1 mm. Between the cones the pressure is reduced to about 1 mbar by a rotary pump.

I.6.1.4   Ion focussing

The ion beam has to be focused before the mass analyser. This is achieved by an ion optic consisting of a set of lenses. The system can be rather simple or more advanced and depends on the requirements of the mass analyser and detector. An extraction lens is applied for accelerating the ions to the mass analyser, enhancing ion transmission. Negative extraction voltages range from a few to ~100 V for quadrupole instruments which require ions with low eV kinetic energies (rendering an extraction lens optional) and typically about 2000 V for sector field and TOF instruments, where ion kinetic energies in the keV range are necessary. Ion acceleration and beam geometry shaping is usually performed by additional lenses. In addition, neutral species and photons are hindered from reaching the detector by a photon stop or by off-axis design.

I.6.1.5   Mass analyser

The heart of an ICP-MS instrument is, of course, the mass analyser. The following three types are mainly applied in commercial instruments: (i) quadrupole, (ii) double-focusing sector field and (iii) time-of flight.

The most common type uses a quadrupole for the separation of ions. It consists of four parallel rods, to which a symmetric constant potential is applied as well as an additional alternating potential with high frequency. Depending on the two voltages, only ions with m/z in a certain

range are stable as can be seen from Mathieu stability diagrams. [Horstwood, 2005] The settings are chosen in a way that only a band pass of ~1 amu can get through at a time. Then the quadrupole is scanned over the desired m/z range (or hops between distinct values) resulting in a sequential analysis of isotopes. High scan speeds enable a quasi-simultaneous multi-element measurement.

The double focusing sector field analyser requires high vacuum of about 10^{-8} mbar. Ions have to be accelerated to about 10kV before entering. It consists of an electrostatic and a magnetic sector, either in this sort order (Nier-Johnson geometry) or in reversed order (reverse Nier-Johnson). The magnetic field strength and the kinetic energy of the ion determine its curved path through the field. Magnetic force and centripetal force counteract, resulting in a separation according to m/z in space. The electrostatic field accomplishes energy focusing. [Prohaska, 2005]

I.6.1.6   Detector

Different detectors can be applied in mass spectrometers. The simplest design is a Faraday cup, a plain electrode, where the resulting voltage is measured. It is only suitable for high ion count rates. Secondary electron multipliers have better sensitivity and are consequently capable of measuring lower count rates. They are available in two different designs, the 'channeltron' and the discrete dynode electron multiplier. The latter can be operated in dual mode by switching between analog and pulse counting mode. Thus, a dynamic range of nine orders of magnitude can be achieved. [Thomas, 2001d]

A multiple collector (MC) instrument includes more than one detector allowing the simultaneous detection of ions with different m/z after separation by a magnetic sector. Hence precision of isotope ratio measurements is improved by one order of magnitude because instabilities of intensities due to plasma fluctuations are compensated. MC-ICP-MS instruments use Nier-Johnson geometry, as can be seen in Fig. 4. [Horstwood, 2005; Rehkämper et al., 2001; Vanhaecke et al., 2009]
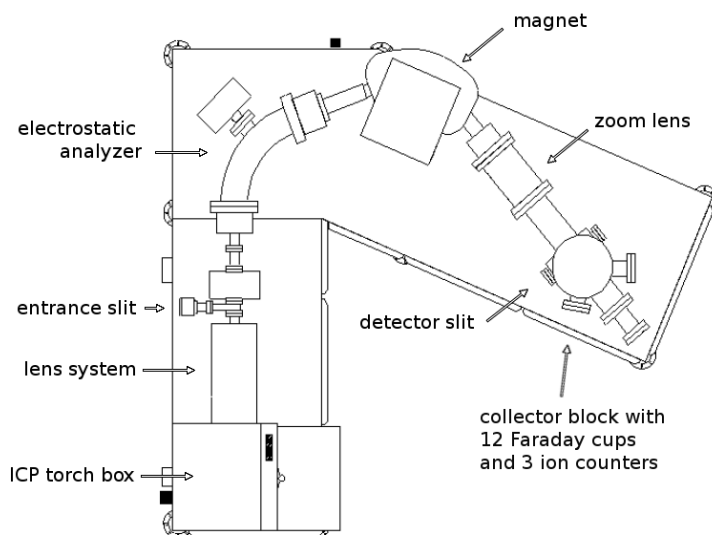
Fig. 4 Schematic view of the Nu Plasma MC-ICP-MS [Nu Instruments, 2007]

I.6.2   Problems and solution strategies

I.6.2.1   Interferences

The probably most vital problem to consider for accurate measurement results in ICP-MS is spectral interferences. The term describes species that result in a signal superimposing the analyte signal. Spectral interferences can be subdivided into four categories. The first group covers isobaric interferences. Isobars are atoms with identical nominal mass, e.g. ^{87}Sr and ^{87}Rb. The second group covers multiply charged atoms. Doubly charged atomic ions overlap with singly charged ions of half their mass. The third category comprises polyatomic interferences or molecular interferences. Either analyte, matrix or solute ions may not be fully atomized or reactions between these and/or plasma gas ions occur because of discharges in the ICP or recombinations take place in the supersonic jet after the cone In addition, peak tailing from very high adjacent peaks can be seen as another source of interferences. [Prohaska, 2005]

Several strategies can be applied in order to overcome interference problems. In quantitative elemental analyses the easiest approach to overcome isobaric interferences is choosing another isotope, which is less interfered. Furthermore, mathematical corrections can be calculated by determining the contribution of an isotope via another isotope of the respective element and known abundances. Another possibility is to apply matrix separation during sample preparation procedures by e.g. using chromatography techniques. The following instrumental strategies are applied additionally:

- Membrane desolvation reduces solute molecules and consequently decreases solute derived polyatomic interferences such as oxide species significantly.

- Collision/reaction cell technology includes a chamber into the instrument prior to the mass analyser, which is filled with a gas. The strategy is based on collisions, which decrease the kinetic energy of larger polyatomic interferences on the one hand. If a reactive gas like O_2 or NH_3 is used, collision induced reactions will occur additionally, which can shift either interfering ions or analyte ions to another mass. [Thomas, 2001c]

- High resolution is a feature of sector field instruments, which are therefore also referred to as high resolution (HR)-ICP-MS. The mass resolution R is defined as

$$R = \frac{m}{\Delta m}$$
<div align="right">**Equ. 1**</div>

where m is the nominal mass of an isotope and Δm is the mass difference between two peaks that can be resolved. The resolution of a sector field instrument is defined by adjusting the width of two slits through which the ion beam passes prior to the analyser and prior to reaching the detector, respectively. Achievable high resolution with a SF instrument is about 10 000. This value is sufficient to separate molecular and doubly charged species. Isobaric interferences often feature lower mass differences, however, and cannot be separated. [Prohaska, 2005]

I.6.2.2 Mass bias

Mass bias describes mass fractionation effects that occur in the instrument. Ions with higher mass are preferentially transmitted resulting in inaccurate measured isotope ratios. The crucial step is the sampling of ions from the plasma and their extraction through the interface. The space charge effect in this region appears to have a major influence. The underlying processes are not fully understood, however. Nonetheless, corrections are required in order to receive better estimates of the true isotope ratio. Various laws are applied like the linear law, the power law and the exponential law. The latter is used in this work and given on the example of Sr in Equ. 2 in chapter II.2.2.3. It is based on the assumption, that the fractionation factor is mass independent. A mass dependence could be observed by some researchers, however. [Albarede et al., 2004; Heumann et al., 1998; Meija et al., 2009; Niu and Houk, 1996]

I.6.3 LASER Ablation

Laser ablation allows direct solid sampling and spatially resolved analysis of surfaces down to 3 μm. Fig. 1 shows the principle: A pulsed laser beam is focused onto the sample surface resulting in an energy transfer to its chemical bonds which leads to their breakup and evaporation of analytical volume. Thus a gaseous aerosol is produced in an airtight cell which is directly transported by a carrier gas to the ICP. [Pisonero et al., 2009] The underlying processes of ablation have not been fully understood, but the influence of several parameters has been investigated, e.g. the wavelength of laser light. Shorter wavelengths were found advantageous on particle size distribution and signal stability. [Guillong et al., 2003]
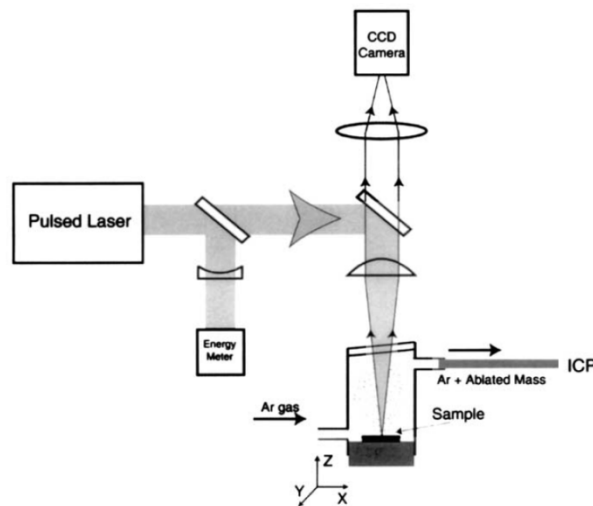
Fig. 5 LASER ablation schematic, adapted from Russo et al. [2002]

One of the main limitations of LA-ICP-MS is derived from laser induced isotopic and elemental fractionation. Consequently, quantification presents a challenge, as matrix matched standards are required. [Russo et al., 2002] LA-ICP-MS has also been applied to isotope ratio measurement in various sciences. [Pickhardt et al., 2005] A shorter pulse duration provided by lasers producing ultra-short femtosecond pulses proved advantageous with respect to fractionation. [Sylvester, 2008] Tab. 4 summarizes different available laser systems, their wavelength properties and possible applications.

LASER	λ [nm]	pulse duration	selected applications	references
Ruby	694	ns	(fundamental research)	Ward et al., 1992
Nd:YAG	1064	ns	geology authentication	Boulyga and Heumann, 2005 Watling, 1998
Nd:YAG	532	ns	archaeology	Wanner et al., 1999
Nd:YAG	266	ns	material science environmental science biology	Koch et al., 2002; Pickhardt and Becker, 2001 Lee et al., 2003 Feldmann et al., 2002
Nd:YAG	213	ns	archaeology biomonitoring	Prohaska et al., 2002 Kylander et al., 2007
Nd:YAG	193	ns	geology	Jochum et al., 2009
XeCl	308	ns	geology	Bea et al., 1996
ArF	193	ns	geology, industry geochronology	Delmdahl and von Oldershausen, 2005 Horn et al., 2000
F_2	157	ns	(fundamental research)	Telouk et al., 2003
Ti:Sapphire	~800	fs	geology	Freydier et al., 2008
Ti:Sapphire	196	fs	geology	Steinhoefel et al., 2009

Tab. 4 Laser types, wavelengths and selected applications of LA-ICP-MS

As a quasi-non-destructive method with sample consumption in the µg range [Russo et al., 2002] it proves especially advantageous in archaeometry, where samples are highly valuable. [Resano et al., 2010]

II   Experimental Section

Sampe preparation and ICP-SFMS measurements were performed in the VIRIS laboratory at the University of Applied Life Sciences, 1190 Vienna, Muthgasse 18, which provides two different clean rooms (class 10 000 and 100 000) with air filtration. ICP-QMS and MC-ICP-MS analysis were performed at the VIRIS laboratories at the University of Vienna, Althanstraße 14, 1090 Vienna.

II.1   Materials

II.1.1   Laboratory equipment

All laboratory vessels and other equipment that got in contact with (liquid) samples were made of synthetic polymers. The polyethylene vials and polypropylene test tubes as well as pipette tips were only used once and underwent a washing procedure that comprised 24 hours in a 10% nitric acid bath, 24 hours in a 1% nitric acid bath and rinsing with purified water (resistivity $> 18\,M\Omega\,cm$, SG, Wasseraufbereitung und Regenerierstation GmbH, Barsbüttel, Germany) followed by air drying in a digestor in a class 100 clean room workbench.

PTFE digestion bombs were cleaned by alternately running a nitric acid digestion without samples between sample digestions applying the same microwave program.

Sample preparation tools for solid samples such as a stainless steel knife and tweezers were rinsed with isopropanol between handling of different samples to avoid cross contamination. Standard dilutions were prepared gravimetrically using an analytical balance (Sartorius BP 210 D, Sartorius AG, Göttingen, Germany).

II.1.2   Reagents and standards

All liquid standards, blanks and samples were prepared in about 2% w/w nitric acid. P.a. grade nitric acid (Merck KGaA, Darmstadt, Germany) was purified in a subboil distillation quartz apparatus (MLS DuoPur, MLS, Leutkirch im Allgäu, Germany) in two steps. Likewise, the water used for diluting was purified water from a purification system, which underwent one step of

sub-boiling distillation (MLS DuoPur, MLS, Leutkirch im Allgäu, Germany). H_2O_2 (p.a. grade, Merck KGaA, Darmstadt, Germany) was used as the second reagent for digestions.

Indium was used as internal normalisation standard for all liquid concentration measurements. The required solution was prepared from a 1000 mg L^{-1} standard (Merck KGaA). External calibration for the liquid multi-element measurements was performed using nine dilutions of the ICP Multi-Element Standard Solution VI (CertiPUR®, Merck KGaA). The accuracy of the calibration was controlled by measurement of a certified water reference material: either TM-28.3 or TM-25.3 (both: Environment Canada, Burlington, Ontario, Canada) were used.

Calibration standards for REE measurements were prepared from REE multi-element Solution 1 (Claritas PPT, SpexCertiPrep, Metuchen, USA), while two geological CRMs were used for quality control: BCR-2 (Basalt, Columbia River, United States Geological Survey, Denver, USA) and BHVO-2 (Basalt, Hawaiian Volcanic Observatory, USGS).

The CRM applied in Sr isotope ratio measurements was a digest of NIST SRM 987 $SrCO_3$ (National Institute for Standards and Technology, Gaithersburg, USA). A [84]Sr spike solution ("BERN", 7.9 µg g^{-1} Sr, 99.895% [84]Sr) was provided by Prof. Urs Klötzli.

II.1.3 Samples

II.1.3.1 Prehistoric wood

Small parts of wooden archaeological findings from the Bronze Age were provided by the Museum of Natural History, Vienna, Department of Prehistory. The finds originate from the prehistoric gallery Christian von Tuschwerk in the Hallstatt salt mine, Upper Austria. The samples were stored in the museum's inventory after their recovery and subsequent leaching in water to prevent them from establishing a salt crust on their surface due to higher air humidity outside the mine compared to inside. Depending on the size of the whole wood parts, they were soaked for between a few days and a few weeks.

Five drill cores were obtained from different whole stems of timber in a first step. (Tab. 5) After surveying the depth of penetration of secondary salts into these massive tree stems six splinters of tool shaft wood of about 1-2 g were sampled (Tab. 6), as well as parts of remains of three illumination chips (Tab. 7). The tree species covered are spruce (*Picea abies*, 4 timber drill

cores), fir (*Abies alba*, 1 timber drill core, 3 illumination chips), beech (*Fagus sylvatica*, 1 timber, 3 tool handles) and oak (*Quercus robur*, 3 tool handles). The determination of species had been carried out previously [Grabner et al., 2007; Klein, 2006].

sample name	inventory no. / find no.	find spot	tree species	length [cm]
T01	04/135	Tusch/Ost	spruce	15.5
T02	216	Tusch/Ost	spruce	11.4
T03	04/172	Tusch/Ost	fir	14.5
T04	02/054	Tusch/Ost	spruce	5.4
T05	04/121	Tusch/Ost	beech	4.6

Tab. 5 Sample list of timber drill cores

sample name	inventory no. / find no.	find spot	tree species	mass [g]
S01	113 029 or 028	Tusch/Nord	oak	2.54
S02	113 094	Tusch/Ost	oak	1.61
S03	113 125	Tusch/Ost	oak	1.40
S04	113 463	Tusch/Westend	beech	2.40
S05	113 110	Tusch/Ost	beech	1.61
S06	113 497	Tusch/Westend	beech	1.45

Tab. 6 Sample list of tool handle splinters

sample name	inventory no. / find no.	find spot	tree species	mass [g]
F01	113.435/29 / 02.012	Tusch/West	fir	1.57
F02	113.435/31 / 02.012	Tusch/West	fir	1.04
F03	113.435/32 / 02.012	Tusch/West	fir	2.10

Tab. 7 Sample list of illumination chips

II.1.3.2   Recent wood

Some recent wood samples were obtained from carpenters for method development. Furthermore, modern wood samples from living trees growing in the proximity of the mine were drilled using an increment borer. The three main tree species growing there, as well as three different bedrocks according to the geotechnical map shown below were taken into account in all possible combinations. This resulted in 28 drill cores and one branch. (Tab. 8)

Fig. 6 gives a detail of the geotechnical map created by Ehret in the course of his diploma thesis. The German legend is given only in extracts; for further information I refer to [Ehret, 2002]. The map was used as a basis for the selection of recent trees for sampling in order to define a local signal and taking into account different bedrocks in the proximity of the mine. The sampling spots of the trees are shown in the map. They belong to three location types: (A) salt-bearing claystones (Haselgebirge Formation; indicated by petrol coloured areas), (B) limestone-marl alternations (Allgäu-Zlambach Formation; indicated by orange coloured areas) and (C) old rockslide material >25 m^3 ('lime stone run'; indicated by larger black triangles).
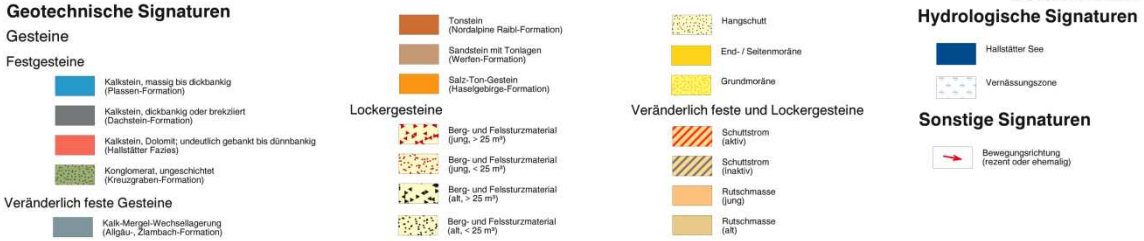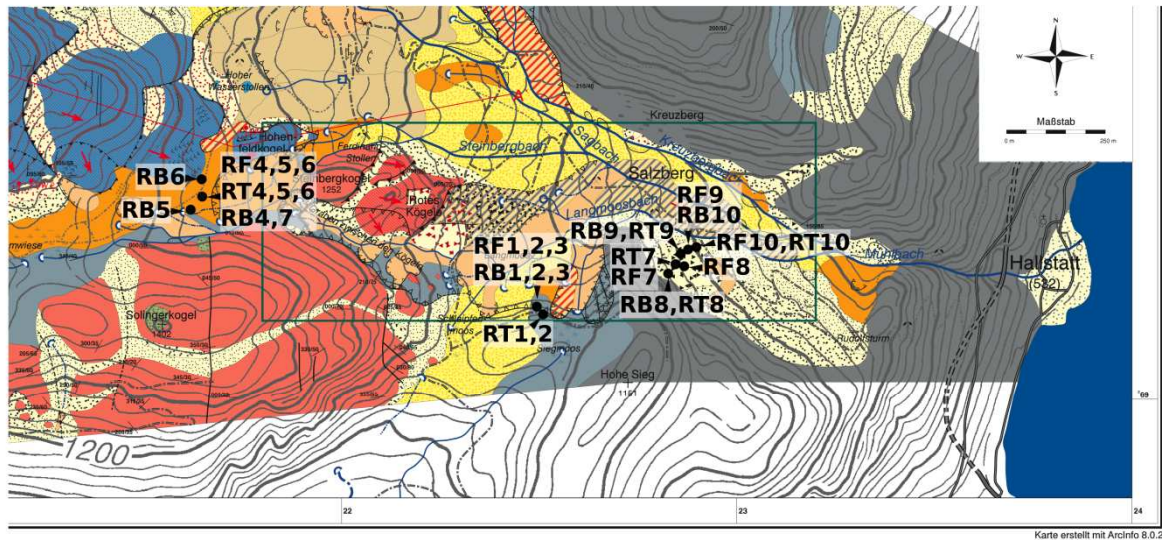
Fig. 6 Geotechnical map of Hallstatt mine surroundings (detail) from Ehret, 2002 with sampling spots

sample name	tree location	bedrock	tree species	length [cm]
RF1	path to Hohe Sieg	marl	spruce	27.5
RF2	path to Hohe Sieg	marl	spruce	26.5
RF3	path to Hohe Sieg	marl	spruce	26
RF4	path to Dammwiese	claystone	spruce	26.5
RF5	path to Dammwiese	claystone	spruce	26
RF6	path to Dammwiese	claystone	spruce	26
RF7	behind Alte Schmiede	limestone	spruce	26
RF8	behind Alte Schmiede	limestone	spruce	23
RF9	behind Alte Schmiede	limestone	spruce	26
RF10	behind Alte Schmiede	limestone	spruce	25
RB1	path to Hohe Sieg	marl	beech	20
RB2	path to Hohe Sieg	marl	beech	18
RB3	path to Hohe Sieg	marl	beech	19.5
RB4	path to Dammwiese	claystone	beech	17
RB5	path to Dammwiese	claystone	beech	20
RB6	path to Dammwiese	claystone	beech	7.5
RB7	path to Dammwiese	claystone	beech	(branch)
RB8	behind Alte Schmiede	limestone	beech	21
RB9	behind Alte Schmiede	limestone	beech	22.5
RB10	behind Alte Schmiede	limestone	beech	21.5
RT1	path to Hohe Sieg	marl	fir	25
RT2	path to Hohe Sieg	marl	fir	26
RT4	path to Dammwiese	claystone	fir	23.5
RT5	path to Dammwiese	claystone	fir	25
RT6	path to Dammwiese	claystone	fir	20
RT7	behind Alte Schmiede	limestone	fir	25
RT8	behind Alte Schmiede	limestone	fir	29
RT9	behind Alte Schmiede	limestone	fir	25
RT10	behind Alte Schmiede	limestone	fir	22

Tab. 8 Sample list of recent wood drill cores

36

II.1.3.3 Surrounding mine material

Eleven samples of the material surrounding the wooden findings in the mine environment were also provided by the Museum of Natural History (Tab. 9). The material is called 'Heidengebirge' and comprises remains of rock salt, gypsum, clay, wooden splinters from illumination chips and other leftovers from prehistoric mining

sample name	inventory no. / find no.	find spot	type	mass [g]
SM01	113 609 / 03.019	Tusch/Ost	Heidengebirge (HG)	~30
SM02	113 336 / 02.079	Tusch/Ost	HG	~100
SM03	113 779 / 03.126	Tusch/Ost	HG +surface material	~50
SM03A	113 779 / 03.126	Tusch/Ost	HG +surface material	~30
SM04	2000/LFM 7.55-7.70	Tusch/West	HG	~70
SM05	04/135	Tusch/Ost	surface material	~40
SM06	04/103 Nr.1/2	Tusch/Westend	HG	~50
SM07	05/020	Tusch/Ost	HG	~35
SM08	07/099	Tusch/Ost	HG + surface material	~90
SM09	91.936	Tusch/Nord	HG	~40
SM10	03/026	Tusch/Ost/Nordquerschlag 2	HG	~70

Tab. 9 Sample list surrounding mine material ('Heidengebirge')

II.2 Methods

II.2.1 Sample Preparation

II.2.1.1 Preparation of solid samples for Laser Ablation-ICP-MS

The drill cores and the carpenter's wood leftovers were cut into parts of maximum 3 cm length to fit the laser cell using a stainless steel knife. Then they were fixed onto glass slides via a layer of plasticine. The drill cores had been cut longitudinally resulting in a plain surface, perfectly suitable for laser ablation. In one case this had not been done, so part of the curved surface was removed using the stainless steel knife in order to obtain a planar area of a few mm width along the drill core.

II.2.1.2 Spike experiment

In order to confirm the applicability of the analytical procedure a spike experiment was performed. The exposure to secondary salts in the mine environment should be simulated by subjection of recent wood parts to a similarly concentrated Sr spike solution with 99.9% [84]Sr which enables the distinction of primary and secondary Sr in the wood. The process of spiking and subsequent leaching was surveyed using LA-ICP-MS.

Spruce, oak and beech wood (80-100 mg) was cut into three small splinters each and weighed into Eppendorf vials. The 7.9 $\mu g\,g^{-1}$ ^{84}Sr spike was neutralized / slightly alkalinized using aqueous NaOH and 700 μL were added to each vial. Three blanks were prepared equally, but with 2% w/w HNO_3 instead of the spike solution. After ten days of exposure under room temperature the wood samples were dried for 2 h at 70 °C. Then the samples were screened applying Laser Ablation-ICP-MS using the same setup and method as described in II.2.2.1, but measuring the isotope ^{84}Sr in addition.

Furthermore, the developed leaching procedure (see chapter II.2.1.4) was applied to test its ability to selectively remove the secondary cations. According to the therein mentioned routine drying and measurement were performed again.

II.2.1.3   Extraction of mine material

In order to get a picture of the mine environment's influence during the storage of the wood samples geological samples were collected from the proximity of the wooden findings. An extraction procedure which is usually applied to soils aiming at simulating the soil mobile phase and the bio-available fraction of the minerals was adopted. The advantage of using an ammonium nitrate solution for leaching is its slightly acidic pH value facilitating the dissolution of many (basic) salts. However, a disadvantage for ICP-MS analysis results from the high salt content.

The obtained material had to be reduced to smaller pieces using a stainless steel mortar and a hammer. The resulting small stones and dust were sieved to remove particles of more than 2 mm size. These procedures were performed in a geology laboratory at the Department of Lithospheric Research (University of Vienna) that also supplied the necessary equipment. 20 g of the ground material was weighed into 100 mL PE bottles and 50 mL of 1 M ammonium nitrate solution were added. The suspension was shaken for 2 h at 20 rpm in a GFL 3040 overhead rotator (GFL Gesellschaft für Labortechnik GmbH, Burgwedel, Germany) at the Department of Forest and Soil Science, University of Natural Resources and Applied Life Science. After allowing the solids to settle the extracts were filtered using folded filters (Munktell Filter AB, Falun, Sweden). The first 5 mL were discarded, the rest collected in PE bottles.

Prior to the measurements the extracts were filtered again using syringes (B. Braun Injekt 5 ml, B. Braun Melsungen AG, Melsungen, Germany) and compatible filters (Minisart-RC/SRP 0.45μm, Sartorius, Göttingen, Germany).

II.2.1.4   Ultrasonic leaching of prehistoric wood samples

In order to remove secondary salts from the prehistoric samples originating from their storage in a salt mine environment for about 3000 years a leaching procedure was developed.

In a first trial a selection of the samples from the laser ablation screening were taken as a whole. One prehistoric (timber drill core part) and one recent (carpenter's leftover) spruce and beech sample were weighed and covered with 20 mL sub-boiled water in a 50 mL PE bottle each and exposed to ultrasound in an ultrasonic bath (Transsonic 780, Elma GmbH & Co KG, Singen, Germany) for 30 minutes. Subsequently they were dried in an oven (WTB Binder, Binder GmbH, Tuttlingen, Germany) at 70°C overnight and screened using LA-ICP-MS. This procedure was repeated four times.

Due to preliminary results obtained from evaluating this procedure (see chapter III.1.4) it was modified as follows and tested on two prehistoric samples (spruce timber drill core and oak tool shaft) and recent carpenter's wood of corresponding species.

About 600 mg of the wood samples were first cut into smaller splinters using the stainless steel knife and weighed. Then three ultrasonic leaching steps of 30 minutes each were performed using quantities of 8, 5 and 3 mL of subboiled water, respectively, in PP test tubes. The wood samples were left in the third step's solution overnight. Thereafter two analogue steps followed, but using 5 and 3 mL of 0.1 M HNO_3, respectively. The samples were not dried in-between, but after the five steps. The leaching solutions were weighed, filtered and stored for multi-element measurement. Water leaching solutions were acidified to about 1% HNO_3.

This procedure was applied to all prehistoric wood samples.

II.2.1.5   Microwave digestion

The microwave digestion procedure was first tested on recent samples. 300 – 350 mg of dry wood were weighed into a PTFE bomb and 3 mL concentrated doubly subboiled nitric acid (65% w/w) and 1 mL hydrogen peroxide were added. In case not all the solid wood splinters were

covered with liquid, an extra mL of HNO_3 was added. An immediate reaction occurred, visible by foaming and emission of nitrous gases. After it faded away, the batch of six bombs including one blank was fixed to a rotor and placed into the microwave (mls 1200 mega, MLS, Leutkirch im Allgäu, Germany) applying the following program.

time [min]	power [W]
2	250
2	0
6	250
5	400
5	600
10	0

Tab. 10 Microwave digestion programme

The resulting digests were clear. After cooling down the digests were filled into 50 mL PE bottles including meticulous rinsing of the remains. The final weight (between 9 and 10 g) of the diluted digest was determined.

II.2.1.6   Sr/matrix separation

As the measurement of the isotopic ratio $^{87}Sr/^{86}Sr$ are disturbed by interferences originating from matrix elements, mainly by the isobaric interference of ^{87}Rb, a separation of Sr and matrix is performed prior to the measurement. A solid phase extraction procedure was adopted from [Swoboda et al., 2008]. It involves a Sr specific crown ether resin (Sr Resin, Eichrom Technologies, Inc., Lisle, USA), which is composed of 4,4'(5')-di-t-butylcyclohexano 18-crown-6 in 1-octanol immobilized on an inert substrate. The resin was slurred in 1% w/w HNO_3. About 0.5 mL were filled into 3 mL PP columns equipped with filters (pore size 10 µm), both of which were washed in 5% w/w and stored in 1% w/w nitric acid. After four washing steps of 0.5 mL H_2O subb. the resin was preconditioned using 6M HNO_3. Subsequently 2 mL of sample were applied. If necessary the sample was acidified to about 8M HNO_3 beforehand. The flow rate was manually controlled to be below 1 mL min^{-1} for conditioning and sample application via drop-wise addition. About 12 washing steps followed using 0.5 mL 8M HNO_3 each, resulting in the elution of rubidium and other matrix elements such as calcium. Finally Sr was eluted from the column using 2.5 mL of sub-boiled water.

The success of the separation concerning Sr recovery and removal of Rb was controlled by screening of the separated samples via ICP-QMS applying the same method as for multi-element measurements with a few modifications.

II.2.1.7   Preparation of liquid samples for measurement

The stability of solutions (as one prerequisite for reproducible analyses) requires an acid concentration of optimum 1-2% w/w HNO_3, so all digests had to be diluted by minimum factor 10.

Indium was selected as internal standard for the concentration measurements due to its negligible natural abundance and mass in the medium range of the spectrum. A 110 or 11 ng g^{-1} In solution, respectively, was added volumetrically to each sample, blank and standard in order to obtain a concentration of 10 ng g^{-1} (quadrupole instrument) or 1 ng g^{-1} (sector field instrument) in the measured solution.

The samples for isotope ratio measurements were diluted according to the instrument's actual current sensitivity to ensure signals between 1 and 8 V.

II.2.2 Instrumentation

II.2.2.1   The ICP-quadrupole MS instrument (ICP-QMS ELAN DRC-e)

All multi-element measurements on different matrices comprising wood digests (HNO_3/H_2O_2), water and diluted nitric acid leaching solutions of wood, and aqueous ammonium nitrate extracts of mine material were performed on the ELAN DRC-e quadrupole mass spectrometer (PerkinElmer, Waltham, Massachusetts, USA) in standard mode. The instrument is equipped with an auto-sampler (PerkinElmer AS93plus). The instrumental setup is summarized in Tab. 11. (In case of Sr-Rb-screenings, a PFA nebulizer was used and pump speed accordingly reduced to 10 rpm.) The instrument is controlled via the software ELAN Version 3.4 (PerkinElmer SCIEX).

The instrument was optimized daily. The adjusted parameters were the torch x/y position, the nebulizer gas flow and if necessary as well the autolens calibration. The requirements of successful tuning were maximum sensitivity for indium ($> 5 \cdot 10^4$ cps (ng g^{-1})$^{-1}$), while the oxide formation rate should be low ($CeO^+/Ce^+ < 5\%$) as well as the formation of doubly charged ions,

which was monitored on the example of barium, an element with low second ionization potential (10.0 eV [Chan et al., 2001]). The ratio Ba^{2+}/Ba^+ should be below 4%.

nebulizer type	concentric
spray chamber design	cyclonic
sampler cone material	nickel
skimmer cone material	nickel
nebulizer gas flow [L min^{-1}]	~1
plasma gas flow [L min^{-1}]	15
auxiliary gas flow [L min^{-1}]	0.6
RF power [W]	1250
pump speed during analysis [rpm]	20
number of sweeps/reading	8
number of readings/replicate	1
number of replicates	4
dwell time/amu [ms]	50
scan mode	peak hopping
detection mode	dual
analog stage voltage [V]	-1875
pulse stage voltage [V]	1100

Tab. 11 ELAN DRC-e parameters

Quantification was performed via external calibration using nine gravimetric dilutions of a multi-element standard including thirty elements covering a working range of about 0.05 to 100 ng g^{-1} in the measured solution for most of them (Li, Na, Mg, Al, K, V, Cr, Mn, Co, Ni, Cu, Ga, Rb, Sr, Mo, Ag, Cd, Te, Ba, Tl, Pb, Bi, U), while some elements were present in a concentration of a factor of 10 higher (Be, B, Fe, Zn, As, Se) and the Ca content was a factor of 100 higher. A new calibration was measured for each sequence. An appropriate regression (fit) was chosen for each element – in most cases a weighted linear regression was most suitable. The basic quantification calculation was done by the ELAN software. Its weighted linear regression uses the square reciprocal standard concentration of the corresponding standard as weighting factor for each point (see II.2.3.4) guaranteeing a better fit in the lower concentration range compared to a simple linear fit. In some cases the working range was limited on the lower side due to high instrumental LoDs (e.g. Fe).

The accuracy of the calibration was controlled by repeated measurements of a water reference material certified for 25 or 26 trace elements, respectively, after every twenty samples and immediately following a blank measurement. Either TM-25.3 or TM-28.3 was applied as QC standard. If the measured result of an element including an estimated relative expanded uncertainty of 10% overlapped with the certified range of the reference material, the measurement of the respective element was considered accurate; if not the values were discarded or considered only semi-quantitative estimates, respectively.

II.2.2.1 Laser Ablation Setup (LA)

The New Wave UP 193 Solid-State Laser Ablation System (New Wave Research Inc, Fremont, USA) was used for direct solid sample introduction. This flash lamp-pumped Nd:YAG sytem generates radiation at 1064 nm which is then shifted to a UV wavelength of 193 nm. It offers flat beams of high irradiance (>2 GW cm^{-2}). The system is equipped with a colour charge coupled device (CCD) camera and a mass-flow controller. [New Wave Research, 2005] The device is controlled by the software 'Laser Ablation System V. 1.9.0.2'. Its operating parameters are summarized in Tab. 12.

parameter [unit]	value
wavelength [nm]	193
pulse duration [ns]	<3
repetition rate [Hz]	10
fluence [J cm^{-1}]	~2-5
ablation mode	line scan
spot size [µm]	120
scan speed [µm s^{-1}]	100
carrier gas	Ar
carrier gas flow rate [L min-1]	~1.0

Tab. 12 Laser ablation parameters

The laser ablation system was hyphenated to a quadrupole ICP-MS, which was optimized in the same way as for liquid measurement (see chapter II.2.2.1) and operated using basically the same parameters. In this case, however, a data-only method was used: only intensities versus time were recorded and reported by the software. Further data processing steps such as internal standardization and quantification were calculated 'manually' in spreadsheets.

The laser ablation parameters were chosen based on test measurements using wood leftovers to yield high (and preferably uniform) intensities for the analytes of interest. Lines of about 8 mm length were drawn along the radial axis of each investigated timber stem (i.e. along the length of the drill core) resulting in an ablation time of approximately 1:40 min. The isotopes ^{12}C, ^{13}C, ^{23}Na, ^{32}S, ^{34}S, ^{35}Cl, ^{37}Cl, ^{42}Ca, ^{43}Ca, ^{44}Ca, ^{88}Sr and ^{208}Pb were analysed in peak hopping mode with a dwell time of 40 ms. Analysis time should be 2 min, so the number of readings was chosen accordingly (254). Number of replicates and sweeps were both put 1. Before and after ablation, the gas background was recorded, averaged and subtracted from the analyte signal for blank correction. Furthermore, before, after and during each sequence additional gas blanks were measured to survey the stability and air tightness of the system.

This screening should only give a rough insight into penetration depth of inorganic contamination into timber samples in the salt mine. For simplicity reasons quantification was accomplished via internal standardization to ^{12}C and one-point calibration. An approximate sensitivity was calculated for each isotope using the reference material 'NCS DC 73348 – bush branches and leaves'. The comparability to the sample matrix was compromised as it is a powdered material.

II.2.2.2 The sector field instrument (ICP-SF-MS ELEMENT2)

The measurement of rare earth elements was carried out on the high resolution ICP-MS instrument ELEMENT2 (Thermo Scientific, Bremen, Germany) equipped with an ESI SC 4 autosampler (Elemental Scientific Inc., Omaha, USA), a PFA microconcentric nebulizer (glass nebulizer for NH_4NO_3 extracts) and a peltier cooled cinnabar spray chamber (PC³; Elemental Scientific, Inc., Omaha, USA). The instrumental parameters are summarized in Tab. 13. The instrument was tuned for maximum In intensity and low UO_2^+/U^+. The instrument is equipped with a discrete dynode detector.

nebulizer type	PFA
spray chamber design	PC^3
sampler cone material	aluminium
skimmer cone material	aluminium
nebulizer gas flow [L min^{-1}]	0.97
plasma gas flow [L min^{-1}]	16
auxiliary gas flow [L min^{-1}]	1.15
DAC cool gas flow [L min^{-1}]	0.47
RF power [W]	1300
number of runs	3
number of passes	3
pump speed during analysis [rpm]	6.35
sample uptake rate [μL min^{-1}]	100

Tab. 13 ELEMENT2 operating parameters

Quantification was achieved using a 9-point external calibration in a working range between 0.001 ng g^{-1} and 1 ng g^{-1} in the measured solution. Calibration standards were prepared from REE Multi-element Solution 1 (Claritas PPT, SpexCertiPrep, Metuchen, NJ, USA). Indium was added to blanks, standards and samples in a concentration of 1 ng g^{-1} for internal standardization.

The sector field instrument offers the possibility to measure with medium (~3000) or high (~10000) mass resolution (m Δm^{-1}) which enables the separation of many interferences. For that reason, certain isotopes were measured additionally in high resolution what goes at the

expense of sensitivity. Indium intensities were up to $1.4 \cdot 10^6$ cps in low resolution, about $7 \cdot 10^5$ cps in medium and $\leq 10^5$ cps in high resolution for 1 ng g^{-1}. Due to the fact that analyte count rates were very low in high resolution (e.g. below 100 cps for a typical sample solution) resulting in high intensity RSDs, most of these data was not taken into account for evaluation.

The measured isotopes in each resolution mode are listed in Tab. 14.

mass resolution mode	low	medium	high
measured isotopes	^{89}Y, ^{115}In, ^{137}Ba, ^{138}Ba, ^{139}La, ^{140}Ce, ^{141}Pr, ^{147}Sm, ^{149}Sm, ^{143}Nd, ^{145}Nd, ^{146}Nd, ^{151}Eu, ^{153}Eu, ^{165}Ho, ^{166}Er, ^{167}Er, ^{169}Tm, ^{171}Yb, ^{172}Yb, ^{173}Yb, ^{155}Gd, ^{175}Lu, ^{159}Tb, ^{161}Dy, ^{163}Dy, ^{232}Th	^{45}Sc, ^{115}In	^{65}Ho, ^{115}In, ^{166}Er, ^{167}Er, ^{169}Tm, ^{171}Yb, ^{172}Yb, ^{173}Yb, ^{157}Gd, ^{175}Lu, ^{159}Tb, ^{161}Dy, ^{163}Dy, ^{232}Th

Tab. 14 Isotopes measured by ICP-SF-MS and resolution modes

The accuracy of the calibration was controlled using digested geological reference materials (BCR-2 and BHVO-2, United States Geological Survey, Denver, USA).

II.2.2.3   The multiple collector sector field instrument (MC-ICP-(SF)MS Nu Plasma)

The Nu Plasma (Nu Instruments Ltd., Wrexham, UK) is a double focusing sector field instrument with Nier-Johnson geometry. Its multiple collector, consisting of 12 Faraday cups and three full size discrete dynode ion-counters on fixed spots, makes it a high precision instrument for isotope ratio analysis. It is equipped with an ESI SC 4 autosampler (Elemental Scientific, Inc., Omaha, USA). A membrane desolvation system (DSN-100, Nu Instruments Ltd, Wrexham, UK) dries liquid samples prior to ionization in the ICP. Operating parameters are summarized in Tab. 15.

The instrument was tuned daily by adjusting a range of parameters including DSN temperatures, gas flows, torch position and lens voltages, in order to achieve maximum sensitivity for Sr and maximum precision for Sr isotope ratios.

nebulizer type	PFA/membrane desolvation
sampler cone material	nickel
skimmer cone material	nickel
nebulizer back pressure [psi]	~30
plasma gas flow [L min-1]	13
auxiliary gas flow [L min-1]	1.2
DSN-100 hot gas flow [L min-1]	~0.3
DSN-100 membrane gas flow [L min-1]	~3
DSN-100 membrane temperature [°C]	115
DSN-100 spray chamber temperature [°C]	115
RF power [W]	1300
axial m/z	86
mass resolution m/Δm	300
measurements / block	10
number of blocks	6
dwell time [s]	5
sample uptake rate [µL min-1]	40

Tab. 15 Nu Plasma operating conditions

The following Faraday collector block arrangement results from choosing axial mass 86 and a mass separation of 0.5 (Tab. 16). Ion-counters have not been used in the course of this work.

cup	L5	L4	L3	L2	L1	Ax	H1	H2	H3	H4	H5	H6
mass	82	83	84	85		86		87		88		89
analyte			^{84}Sr			^{86}Sr		^{87}Sr		^{88}Sr		
interference	^{82}Kr	^{83}Kr	^{84}Kr	^{85}Rb		^{86}Kr		^{87}Rb				

Tab. 16 Faraday collector block arrangement and possible isobaric interferences

Tab. 16 also lists the isobaric interferences on the measured masses. Kr is a noble gas and will not occur in liquid samples. It might, however, be present as a contamination in the Ar supply, but blank correction accounts for these interferences. Rb has to be removed in the course of sample preparation, but a minor fraction may remain in the samples. Consequently, mathematical corrections are necessary, which are calculated by the instrument's software using a NICE file. It includes correction for Rb interference as well as internal mass bias correction via the ^{88}Sr/^{86}Sr ratio (see below). For each calculation step, the calculation procedure eliminates outliers and calculates a standard deviation. Further possible interferences include doubly charged REEs and polyatomic species, but the Sr separation should separate any matrix elements and the DSN reduces solution based interferences (H, O).

A blank and a CRM certified for its ^{87}Sr/^{86}Sr ratio are measured before every five samples. The blank is measured using an 'on-peak-zero' method and defines the background voltage for each cup, which is consequently subtracted from all measured voltages. The CRM is evaluated like a sample and reveals, if mass bias correction results in accurate isotope ratios and if precision requirements are met.

The first step after blank subtraction is the calculation of the fractionation factor (Equ. 2) to account for mass fractionation according to the exponential law [Albarede et al., 2004] using the measured $^{86}Sr/^{88}Sr$ ratio, which is assumed to be stable and not interfered. The value used was 0.1194. U signifies the measured voltages on the respective masses, while m is the mass of the respective isotope.

$$f = \log\left(\frac{U_{86}}{U_{88}}\left(\frac{^{86}Sr}{^{88}Sr}\right)^{-1}_{true}\right) \cdot \left(\log\left(\frac{m_{Sr86}}{m_{Sr88}}\right)\right)^{-1} \qquad \textbf{Equ. 2}$$

Assuming a constant fractionation factor for Rb and Sr, this factor can also be applied to calculating the signal on mass 87, which is caused by ^{87}Rb, as described in Equ. 3.

$$U_{Rb87} = 0.38506 \cdot U_{85} \cdot \left(\frac{m_{Rb85}}{m_{Rb87}}\right)^{f} \qquad \textbf{Equ. 3}$$

Subtraction of U_{Rb87} from the total signal on mass 87 gives the net signal for ^{87}Sr:

$$U_{Sr87} = U_{87} - U_{Rb87} \qquad \textbf{Equ. 4}$$

Finally, mass bias correction can be applied to the Rb corrected ratio:

$$\frac{^{87}Sr}{^{86}Sr} = \frac{U_{Sr87}}{U_{86}}\left(\frac{m_{Sr87}}{m_{Sr86}}\right)^{f} \qquad \textbf{Equ. 5}$$

II.2.3 Method validation parameters

In the course of this diploma thesis, no full method validation according to CITAC/EURACHEM [EURACHEM, 1998] was carried out, primarily due to the lack of suitable certified reference material. Nonetheless, some validation parameters were determined as a prerequisite for data evaluation and interpretation.

II.2.3.1 Limit of Detection

The limit of detection (LoD) or 'detection limit' indicates the lowest detectable analyte concentration. An estimate of it was calculated according to Equ. 6, which strictly speaking only

allows the distinction from the noise with about 99.85% probability assuming normally distributed data and constant variance.

$$LoD = 3 \cdot \sigma_{blank}$$

If applicable, the method's limit of detection was calculated from the standard deviation of the concentration measurements of at least three independent method blanks. This takes into account the variation in the background resulting from the sample preparation procedure as well as the instrumental contribution to variations. If too few method blanks were available, the LoD was calculated from measurement blanks, which gives no information about the sample preparation procedure and hardly includes the variations from the addition of internal standard, but may result in higher LoD values, though. As the analyte concentration in the sample is in the range of the method blank or above it makes more sense to compare it to the method LoD. The values below the calculated LoD were sorted out for statistical evaluation and marked '<LoD'.

LoDs in ammonium nitrate extracts could not be calculated as suggested above due to the lack of more than one method blank. Additionally, in this case the matrix was slightly different to the calibration standards, so matrix effects could not be ruled out. Consequently, the concentration values measured on different days but from the same blank were used for the calculation of the LoD and LoQ. If, like in case of the REE measurement, only two values were available, their difference was substituted for the standard deviation in Equ. 6.

II.2.3.2 Limit of Quantification

Furthermore and accordingly the limits of quantification were calculated in order to identify the values that could not be determined with a reliable uncertainty.

$$LoQ = 10 \cdot \sigma_{blank}$$

II.2.3.3 Sensitivity

Sensitivities for quantitative determinations were calculated from the slope of the calibration curve. As calibration curves were created from unit-free net intensities, the sensitivity in the unit cps (ng g^{-1})$^{-1}$ was obtained from Equ. 8, where m is the number of calibration standards

and the slope k has the dimension $(ng\ g^{-1})^{-1}$. $Int_{IS}^{std_i}$ is the intensity in cps of the internal standard in each calibration standard i.

$$sensitivity = k \cdot \frac{1}{m} \sum_{i=1}^{m} Int_{IS}^{std_i}$$ **Equ. 8**

II.2.3.4 Model Equation

The model equation for the determination of the concentration of the analyte A in wood

$$c_A^{sample} = \left(\frac{Int_A^{sample}}{Int_{IS}^{sample}} - \frac{1}{n} \cdot \sum_{i=1}^{n} \frac{Int_A^{blank_i}}{Int_{IS}^{blank_i}} \right) \cdot \frac{1}{k} \cdot \frac{V_{digest} + V_{dilution}}{V_{digest}} \cdot \frac{m_{digest}}{m_{wood} \cdot (1 - LD)}$$ **Equ. 9**

Int_a^b intensity of analyte a in solution b

blank   method blank

n number of method blanks

IS internal standard (^{115}In measured in the respective resolution mode)

k slope of the linear regression from external calibration

V_{digest} volume of digest applied for dilution

$V_{dilution}$ volume of 1% HNO_3 for dilution

m_{digest} total weight of the digest

m_{wood} weight of the wood prior to digestion

LD loss on drying of solid wood, if wood was not dried prior to digestion (else: LD=0)

The slope k of quantitative measurements using the quadrupole instruments was calculated by the instrument's software using Equ. 10 describing a weighted linear regression (*wlr*) for one analyte A. The weighting factors are the reciprocal analyte concentrations of the m standards.

$$k_{wlr} = \frac{S \cdot S_{xy} - S_x \cdot S_y}{S \cdot S_{xx} - S_x^2} = \frac{\sum_{i=1}^{m} w_i \cdot \sum_{i=1}^{m} w_i \cdot c_i \cdot y_i - \sum_{i=1}^{m} w_i \cdot c_i \cdot \sum_{i=1}^{m} w_i \cdot y_i}{\sum_{i=1}^{m} w_i \cdot \sum_{i=1}^{m} w_i \cdot c_i^2 - \left(\sum_{i=1}^{m} w_i \cdot c_i \right)^2}$$ **Equ. 10**

with the weighting factor w_i for each standard i

$$w_i = \frac{1}{c_i^2}$$

<div align="right">**Equ. 11**</div>

and with the net-intensity y_i of analyte A

$$y_i = \left(\frac{Int_A^{std_i}}{Int_{IS}^{std_i}} - \frac{Int_A^{blank}}{Int_{IS}^{blank}} \right)$$

<div align="right">**Equ. 12**</div>

and c_i being the concentration of analyte A in calibration standard i. *'blank'* refers to the instrumental blank in this case.

The sector field instrument ELEMENT2 uses simple linear regression, which means that w_i in Equ. 10 is 1 for all i.

The equation for wood leaching solutions and other extracts is very similar to Equ. 10. Only the word 'digest' has to be replaced by 'extract' and the word 'wood' by 'solid material' (if not wood was leached). Loss on drying is set zero.

II.2.3.5   Measurement uncertainty

Total combined uncertainties for quantitative multi-element measurements were calculated using the model equation (II.2.3.4) and applying the Kragten approach for error propagation.

Using the spreadsheet approach gives a good estimate of the values that would result from exact Gaussian error propagation. Additionally the individual contributions of the input parameters on total combined uncertainty can easily be evaluated giving insight into the relevant steps in the measurement and sample preparation procedures which need to be taken care of.

Total combined uncertainties of REE concentrations were calculated by a slightly simplified spreadsheet approach. First the estimated standard uncertainty of the slope of the calibration line was calculated as follows: First, the standard uncertainty of the net intensies was determined by Gaussian error propagation involving the standard deviation of the intensities of the respective analyte and of the internal standard. The relative error of the concentrations of the calibration standards from their certified stock solution by gravimetric preparation were

determined to be about 0.5% or below. A maximum slope was then calculated by adding one SD to the net intensity value (y), while subtracting one SD from the concentration value (x) for the highest three calibration standards because this way a maximum shift of the slope could be observed. The difference between the 'mean' slope of the calibration curve and the maximum slope was used as estimated uncertainty of the slope in the further calculations.

The contributions of the different terms of the model equation to the total combined uncertainty were evaluated for a few examples. Based on the finding, that the weights of digest and sample and the IS intensity of the method blank gave only minor contributions, the calculation was simplified by excluding these terms. The error from pipetting the internal standard solution to all standards, blanks and samples was accounted for by including it into the uncertainty of the IS intensity of the sample. The uncertainties were calculated for all successfully measurable analytes for all wood samples individually.

Uncertainty of Sr isotope ratio measurements:

Uncertainty calculation of Sr isotope ratio measurements took into account the influence of the measurement precision and of the mathematical corrections for each sample individually in a spreadsheet. The standard deviations for the measured voltage ratios were calculated by the Nu Plasma software, which also eliminates outliers. The influence of mass bias correction was calculated using a spreadsheet and therein, certified mass value uncertainties were found to make no significant difference. The main contributor to this uncertainty was the measured signal ratio of mass 87 / mass 86. The contribution of blank and rubidium correction was determined separately. Certified Rb isotope abundances were not taken into account (regarded as constants) as they are not a variable of the measurement. The influence on the combined uncertainty of these corrections is dependent on the measured voltages (which depend on the Sr and Rb content as well as the instrument's sensitivity).

II.2.4 Statistical data evaluation

Two different chemometric techniques were applied in order to statistically evaluate the large datasets resulting from multi-element analysis. Furthermore chemometrics help to achieve a simplification by reducing the number of variables and facilitate visualization of multivariate datasets.

II.2.4.1 Principal component analysis

Principal Component Analysis (PCA) is a useful tool for exploratory data analysis. Its aim is to reduce the dimension of a multivariate data set. This is achieved by calculation of principal components, i.e. linear combinations of the measured variables. Thus a data set of correlated variables is converted into a set of uncorrelated principal components. This new dataset should best represent the original variance of the datapoints. In a first step, however, data are usually centered or autoscaled / standardized resulting in a matrix **A.** The latter removes the influence of different scales of measurands, which is very sensible in case of elemental contents, especially if macro and trace elements are combined.

Then the covariance or correlation matrix, respectively, is calculated as $(n-1) \cdot \mathbf{A}^T \cdot \mathbf{A}$. The procedure of finding the principal component equals the determination of eigenvectors and eigenvalues of that covariance or correlation matrix. [Henrion and Henrion, 1995]

The calculations were accomplished using the software SPSS 16.0 (SPSS Inc., Chicago, Illinois, USA). It provides not exactly PCA but factor analysis, which is a model based method, but gives similar results if PCA is used for the extraction of the factors and no factor rotation is applied. The correlation matrix was analysed (i.e. standardized data) and extraction was restricted to eigenvalues > 1. The higher the eigenvalue the higher proportion of the total variance is explained by the respective factor. A Scree plot gives insight into the variance contribution of the factors and consequently into the number of significant factors.

II.2.4.2 Linear discriminant analysis

Another conventional technique for multivariate data analysis is linear discriminant analysis (LDA). It is a supervised learning technique and aims at optimum linear separation of groups. Nevertheless, its procedure resembles PCA. Only in this case, the linear combinations are chosen in order to achieve maximum separation between pre-defined groups of samples. [Henrion and Henrion, 1995] The different bedrocks from the mine surroundings in Hallstatt were chosen as groups in order to test the classification potential of wood samples grown on different bedrocks by the performed analysis. Furthermore, a LDA was carried out for the separation of different tree species, only for comparison reasons in order to assess the influence of the species.

Again, calculations were performed using SPSS 16.0. In this case the measured values were not standardized. The within-groups covariance matrix was analysed and prior probabilities were set equal for all groups.

III Results and Discussion

III.1 Laser ablation screening

III.1.1 Reference material 'bush branches and leaves'

As LA-ICP-MS measurements were carried out in order to screen the contents of some inorganic salts of prehistoric wood and the success of a developed leaching procedure concerning reduction of contamination, accurate quantification was not the major focus and only relative differences were of interest. In order to give estimate values for concentrations, a reference material with known contents was ablated and an approximate sensitivity was obtained. Tab. 17 shows the results from 18 measurements throughout all days of measurement. Average values were calculated and RSDs refer to the variation between individual measurements. SDs were considerably high and so were consequently the uncertainties of sensitivities, but still sufficient for an estimation of the elemental quantity.

element	certified concentration [µg g^{-1}]	isotope mass [amu]	average intensity [cps]	RSD of normalized data	average sensitivity [cps (µg g^{-1})$^{-1}$]	LoD [µg g^{-1}]
C		12	400000			
		13	5000	13%		
S	3200	32	90000	25%	27 ± 7	900
		34	5000	29%	1.6 ± 0.5	900
Ca	22200	44	400000	39%	19 ± 7	2000
		42	100000	43%	6.0 ± 2.5	700
		43	30000	43%	1.3 ± 0.6	4000
Cl	11300*	37	10000	30%	1.3 ± 0.4	20000
		35	20000	31%	1.6 ± 0.5	2000
Na	11000	23	1600000	33%	150 ± 50	10
Sr	345	88	400000	54%	1300 ± 700	0.4
		84	5000	33%	15 ± 5	1000
Pb	7.1	208	7000	47%	1000 ± 500	0.3

* indicative value

Tab. 17 Results from ablation of NCS DC 73348

LoDs given are calculated from the background of the RM measurement. They show large differences of many orders of magnitude depending on isotope abundance, ionisation energy and 'stability' of interferences. They are of course also depending on the determined sensitivity with its uncertainty. LoDs as exclusion criterion for values were determined for every individual sample and varied, e.g. due to airtightness difficulties.

III.1.2 Comparison of LA and digestion of modern wood

Recent wood samples of different species were ablated in order to optimize the laser parameters and evaluate the performance and detection possibilities. Between 10 and 15 lines were ablated on different days for each of the three samples, which were leftovers provided by carpenters. As sample provenance was unknown and sample preparation involved sawing in a non-cleanroom environment, contamination cannot be excluded. The obtained values were therefore not used for comparison purposes to prehistoric samples. Sample parts were digested, too, and measured applying the liquid setup in order to compare results. Approximate concentrations from LA measurement with RSDs, LoDs for LA and results from the measurement of digests with total combined uncertainties (k=2) are summarized in Tab. 18.

ele-ment	isotope mass [amu]	LoD LA [µg g^{-1}]	concentration [µg g^{-1}]								
			spruce			beech			oak		
			LA result	RSD*	result (dig.)	LA result	RSD*	result (dig.)	LA result	RSD*	result (dig.)
S	32	400	< LoD			< LoD			< LoD		
	34	300	< LoD			< LoD			< LoD		
Ca	44	500	1800	26%		1600	16%		1400	16%	
	42	200	1500	26%		1400	17%		1000	19%	
	43	1000	1600	19%	790 ± 50	1300	16%	640 ± 40	< LoD		510 ± 30
Cl	37	5000	< LoD			< LoD			< LoD		
	35	400	600	32%		600	43%		2200	57%	
Na	23	3	308	33%	4.8 ± 0.8	808	53%	43 ± 7	1909	52%	18 ± 3
Sr	88	0.1	9.6	14%	8.4 ± 0.9	5.5	9%	4.3 ± 0.5	3.0	25%	2.2 ± 0.3
Pb	208**	0.1	14.1	51%	0.039 ± 0.007	1.7	45%	0.22 ± 0.04	7.8	47%	0.032 ± 0.006

*RSD calculated from average values of all measured lines,
** for LA only, liquid measurement: [207]Pb, based on better results for water CRM

Tab. 18 Laser ablation results for recent wood and comparison to results from liquid measurement

These data clarify the capabilities and difficulties in the quantitative determination applying laser ablation. Sulfur could not be determined due to low contents in not-contaminated wood and the oxygen interferences giving high background levels. An approach to deal with that might be the use of a dynamic reaction cell by shifting the analyte signal to higher masses after reaction with O_2. Calcium is not easy to measure using ICP-MS, either. Its isotopes with mass numbers 42, 43 and 44 were measured as a compromise between low isotopic abundances (between below one and 2%) and less pronounced Ar related interferences. Due to the latter's disproportionate presence as plasma gas, LoDs are very high. Furthermore, results from liquid measurement, which cannot be claimed reliable because of lacking quality control and suffer

from the same interference problems, do not agree very well. The difference is about 50%, but LA appears to give a passable estimate of the order of magnitude of contents.

An argon based interference also affects ^{37}Cl resulting in high LoDs, but ^{35}Cl presents an alternative with factor 10 lower detection limits, but no comparison values to the liquid setup are available for modern carpenter's wood.

Sodium, strontium and lead show similar LoDs for liquid and LA setup. However, results from both measurements differ strongly for Pb and Na. Even correlation between both measurement strategies on the three samples is low. Differences are in the range between one and almost three orders of magnitude. One possible explanation could be sample surface contamination by touching (NaCl) or sawing and environmental influences from the carpenter's shop (Pb?) as the sample history is not known for these pieces.

Fortunately, the best agreement can be observed for strontium quantification. The LoD is about 100 ng g^{-1} and RSDs between ablated lines are satisfactory.

III.1.3 Depth-profiling of prehistoric timber

Drill cores of five timber stems from the salt mine were ablated in pieces resulting in an image of the radial distribution of analyte concentration from the surface to the innermost region of the stem. The aim was an assessment of the penetration depth of salts prior to sampling of wooden artefacts. Fig. 7 and Fig. 8 show two exemplary depth profiles for a thicker spruce and a thinner beech stem. Each ablated 8000 µm line was evaluated individually resulting in about 190 values per analyte corresponding to ablation along 1 cm length (or depth of the stem, respectively). Each 10 consecutive values were summarized by averaging and the resulting values were plotted against the length (calculated from ablation time and scan speed). The approximate spatial resolution of the resulting plots is therefore about 0.5 mm. Analyte names in the legend refer to the measured isotope, while values correspond to the respective element.
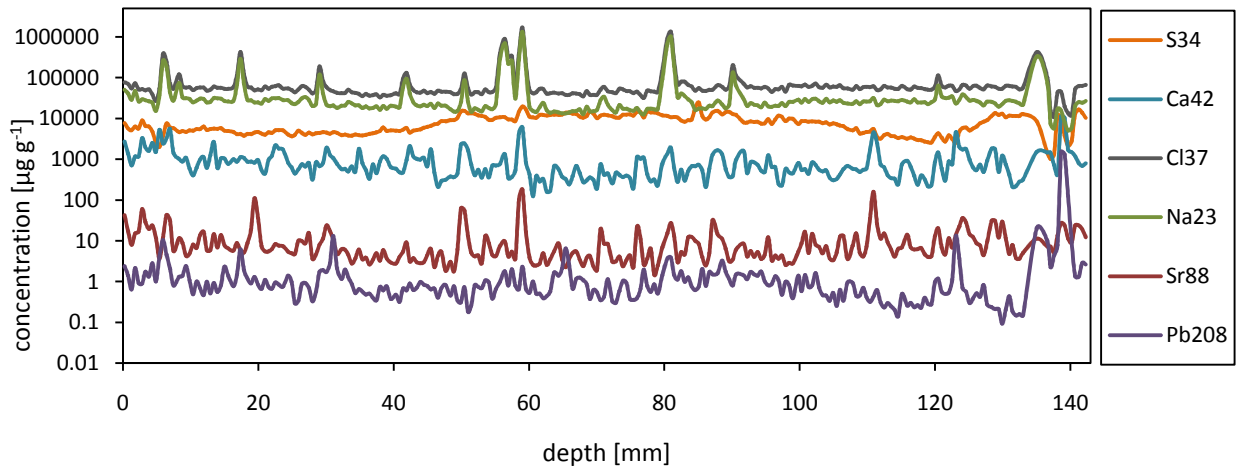
Fig. 7 Depth profile from LA screening for timber T01 (spruce)
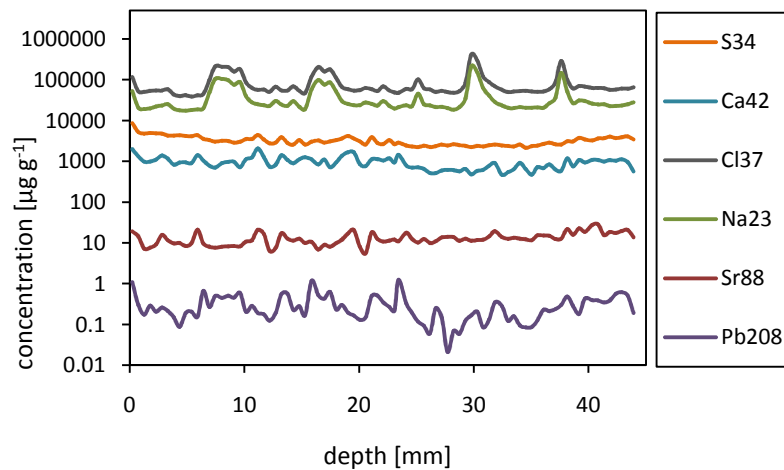
Fig. 8 Depth profile from LA screening for timber T05 (beech)

The resulting patterns show distinct local maxima where salt was crystallized in cavities in the wood. Where analyte concentrations approach 100%, internal standardization against ^{12}C cannot deliver accurate results, strictly speaking. Therefore, the median for a certain section was calculated and reported in Tab. 19. Thus local maxima were not weighted too highly. The depth profiling revealed full penetration of inorganic salts into wooden material. Furthermore, strong correlation between Na and Cl abundance, as expected from the occurrence of NaCl, as well as between Ca and Sr, as expected from their chemical similarity as earth alkaline elements, can be observed. Furthermore, all five samples covering spruce, fir and beech show roughly similar contents.

	approximate median concentration [μg g^{-1}]					
sample name	Na	Cl	Ca	Sr	Pb	S
T01	20000	50000	500	5	0.5	7000
T02	20000	60000	900	9	2	7000
T03	40000	90000	1000	10	1	5000
T04	20000	60000	1000	10	2	9000
T05	20000	60000	800	10	0.2	3000

Tab. 19 Concentration results from LA screening of timber drill cores prior to leaching

Tab. 22 in the appendix shows more detailed screening results with median values for each section of about 3 cm, which was individually measured in the laser cell (but still in several lines of about 8 mm). Latin numerals refer to sections with i being the outermost.

As no decline in contamination content with depth could be found, any splinter from an artefact could be sampled disregarding its degree of splitting, and decontamination prior to analysis was found inevitable.

III.1.4 Monitoring of the leaching procedure

The first approach towards decontamination in full pieces and with water only was surveyed by line ablation of wood pieces after each leaching step and drying. Modern wood leftovers were leached, too, in order to assess the leachable fraction of natural element contents. Results are given in Tab. 20 Results from LA screening of leaching procedureTab. 20. The major part of contaminating ions seems to be removed in the first leaching step. Modern wood releases significant fraction of total element content, too, especially for Na and Cl. Leaching of Sr and Ca results in similar contents for recent and prehistoric samples. Lead is present in similar or higher concentration in modern wood of the same species. Sulfur contents cannot be interpreted well because of natural contents below LoD, but leaching could at least achieve a drop below the LoD value for wood from the salt mine.

All these values are suitable for intercomparison, but do not represent accurate quantitative values (as stated above). The liquid measurement of leaching waters and digests after the fourth leaching supports the basic conclusions from laser ablation. These data are given in Tab. 23 in the appendix. (The second leaching approach was surveyed the same way and results obtained from that are discussed in more detail in III.2.4.)

sample name	number of leaching steps	approximate median concentration [µg g^{-1}]						number of ablated lines
		Na	Cl	Ca	Sr	Pb	S	
T02ii	0	20000	50000	2000	10	2	5000	4
	1	2000	3000	100	1	0.3	900	4
	2	400	600	100	1	0.2	500	4
	3	60	< LoD	200	1	0.2	100	4
	4	30	< LoD	< LoD	1	0.2	< LoD	4
spruce	0	300	400	1000	8	8	< LoD	2
	1	100	90	300	2	2	< LoD	2
	2	10	60	400	2	1	< LoD	2
	3	7	10	300	1	1	< LoD	2
	4	4	< LoD	400	1	2	< LoD	2
T05i	0	20000	70000	900	10	0.2	3000	3
	1	8000	10000	300	3	0.1	1000	3
	2	6000	6000	300	2	0.1	1000	3
	3	1000	1000	300	2	0.1	700	3
	4	200	< LoD	< LoD	1	< LoD	< LoD	3
beech	0	700	600	2000	6	2	< LoD	2
	1	50	100	300	2	0.8	< LoD	2
	2	20	< LoD	400	2	0.4	< LoD	2
	3	8	< LoD	200	1	0.3	< LoD	2
	4	6	< LoD	300	1	0.2	< LoD	2

Tab. 20 Results from LA screening of leaching procedure

III.2 Multi-element measurements

III.2.1 Validation parameters

III.2.1.1 Limit of detection and sensitivity

Limits of detection were determined for every sequence and used as a criterion for exclusion of values. Instrumental limits of detection were determined by measuring a 1% HNO$_3$ with internal standard. Values given in Tab. 21 refer to the measured solution. Instrumental LoDs are between 0.1 pg g^{-1} and 0.1 ng g^{-1} for most (trace) elements. Method LoDs are given in Tab. 24, Tab. 25, Tab. 26, Tab. 27, Tab. 28, Tab. 29 and Tab. 30 with the quantitative results. These detection limits have the same units as concentrations given there, i.e. they refer to solid wood in case of wood digests or leaching solutions of wood.

Sensitivities for all measured isotopes on a typical day of measurement with determined expanded SU (k=2) are listed in Tab. 21 on page 60. Values are dependent on the isotopic abundance and on the ionisation potential of the element as well as on the detector response curve. [115]In sensitivity was typically between 6·10^5 and 10^6 cps (ng g^{-1})$^{-1}$.

analyte	mass	instrumental LoD [ng g^{-1}]	sensitivity[a] [cps (ng g^{-1})$^{-1}$]	TM-28.3 certified range[b] [µg L^{-1}]	measurement result[c] [ng g^{-1}]
Li	7	0.008	2800 ± 100	4.12 ± 0.42	3.59 ± 0.35
Be	9	0.007	1020 ± 30	3.34 ± 0.45	3.80 ± 0.22
B	10	2	247 ± 4	10.4 ± 3.3	13.2 ± 0.7
B	11	2	970 ± 20	10.4 ± 3.3	13.4 ± 0.7
Na	23	20	11900 ± 200	n.c.	6090 ± 490
Mg	24	2	8500 ± 500	n.c.	4660 ± 330
Mg	26	2	1920 ± 40	n.c.	4420 ± 290
Al	27	0.06	18000 ± 1000	51.3 ± 5.6	56.0 ± 3.7
V	51	0.3	24000 ± 2000	3.07 ± 0.39	3.72 ± 0.29
Cr	52	0.2	20000 ± 1000	4.83 ± 0.77	5.65 ± 0.38
Mn	55	0.02	34300 ± 500	6.90 ± 0.52	7.58 ± 0.35
Fe	56	60	22000 ± 1000	16.5 ± 3.7	< LoD
Fe	57	20	810 ± 20	16.5 ± 3.7	87.3 ± 9.0
Co	59	0.002	32200 ± 400	3.53 ± 0.52	3.91 ± 0.22
Ni	58	0.1	17000 ± 1000	9.80 ± 1.16	10.9 ± 0.6
Ni	60	0.02	7100 ± 300	9.80 ± 1.16	11.6 ± 0.7
Cu	63	0.2	16000 ± 1000	6.15 ± 0.86	7.13 ± 0.41
Cu	65	0.02	7600 ± 400	6.15 ± 0.86	7.07 ± 0.39
Zn	66	0.05	4700 ± 700	27.5 ± 3.4	33.8 ± 1.6
Zn	68	0.08	3300 ± 400	27.5 ± 3.4	33.7 ± 1.5
Ga	69	0.009	28000 ± 2000	n.c.	0.711 ± 0.061
As	75	0.02	4600 ± 200	6.22 ± 0.85	7.25 ± 0.36
Se	77	0.1	390 ± 30	4.31 ± 0.92	5.23 ± 0.19
Se	82	0.1	510 ± 50	4.31 ± 0.92	5.06 ± 0.27
Rb	85	0.001	39000 ± 5000	0.42*	0.455 ± 0.014
Sr	88	0.002	38000 ± 1000	69.7 ± 5.5	75.3 ± 2.2
Mo	98	0.002	13000 ± 1000	3.82 ± 0.46	4.33 ± 0.14
Ag	107	0.003	25000 ± 1000	3.79 ± 0.44	3.84 ± 0.08
Ag	109	0.002	24000 ± 1000	3.79 ± 0.44	3.80 ± 0.08
Cd	111	0.003	6100 ± 200	1.91 ± 0.23	2.00 ± 0.03
Cd	114	0.003	15000 ± 1000	1.91 ± 0.23	1.99 ± 0.02
In	115	n.d.	87000 ± 1000	n.c.	n.d.
Te	128	0.005	6300 ± 500	n.c.	< LoD
Te	130	0.007	6900 ± 600	n.c.	< LoD
Ba	137	0.005	10000 ± 400	15.5 ± 1.4	15.9 ± 0.2
Ba	138	0.005	58000 ± 7000	15.5 ± 1.4	16.0 ± 0.1
Tl	203	0.0005	24000 ± 2000	3.89 ± 0.33	3.90 ± 0.03
Tl	205	0.0001	56000 ± 7000	3.89 ± 0.33	3.87 ± 0.05
Pb	207	0.1	19100 ± 500	3.97 ± 0.57	3.89 ± 0.04
Pb	208	0.1	41000 ± 5000	3.97 ± 0.57	3.91 ± 0.05
Bi	209	0.0006	51000 ± 13000	2.51 ± 1.10	1.79 ± 0.06
U	238	0.0001	95000 ± 12000	6.00 ± 0.46	6.21 ± 0.10
Ca	42	300	210 ± 20	n.c.	18400 ± 1700
Ca	43	3	50 ± 5	n.c.	16800 ± 1500
Ca	44	30	670 ± 80	n.c.	17200 ± 1500
K	39	10	15000 ± 3000	n.c.	727 ± 68

n.c. not certified, n.d. not determinable

[a] cps for one isotope relative to ng g^{-1} of the element

[b] value and 2-sigma limit for an individual measurement

[c] average and SD of 6 measurements in one sequence

* for information only

Tab. 21 Instrumental LoD, sensitivity and quality control data for multi-element measurements

III.2.1.2 Quality control

Repeated measurement of TM-28.3 or TM-25.3 during each sequence delivered results in good agreement with certified concentration ranges. (Tab. 21) An expanded uncertainty of 10% was assumed for the measurement of the CRM. In case two isotopes were measured, the one delivering more accurate results was identified on the basis of CRM measurements. Difficulties occurred with iron because its concentration in the CRM is in the range of the instrumental LoQ for ^{57}Fe, while significantly below that for ^{56}Fe. High detection and quantification limits are due to high background signals from polyatomic Ar-O interferences. Results for iron are given in the tables, but with reservations.

This quality control only covers the general accuracy of the calibration, but no sample preparation steps or matrix effects. Results for element concentrations, for which the CRM is not certified, are given with reservations, too.

III.2.1.3 Measurement uncertainty

The total combined uncertainty for the quantitative determination of a wide range of elements in wood digests was determined applying a spreadsheet approach. A sample was chosen, in which most elements were present above LoQ and the uncertainty was calculated for each isotope individually. As sample specific contributions were not insignificant, but similar for most samples (e.g. measurement precision of analyte and internal standard), the obtained RSU for each isotope was then applied to all samples of the same kind. Leaching solutions were calculated separately, but sample preparation steps such as gravimetric or volumetric procedures had in general only minor effect compared to intrinsic measurement features such as measured intensities or the slope of the calibration curve. The slope of the calibration curve and its uncertainty were calculated by the ELAN software. Coverage factor (k) was chosen to be two.

Fig. 9 shows the average uncertainty contributions of all input parameters for a digest of recent wood, only taking into account analytes with less than 40% RSU (k=2). Contributions were strongly analyte dependant, though. Due to different slope uncertainties its contribution differed between lower than 10% and above 90%. Accordingly, the other contributions varied,

too, especially the analyte intensity in the sample. In case of lower analyte intensities consequently the contribution of the method blank was more pronounced.
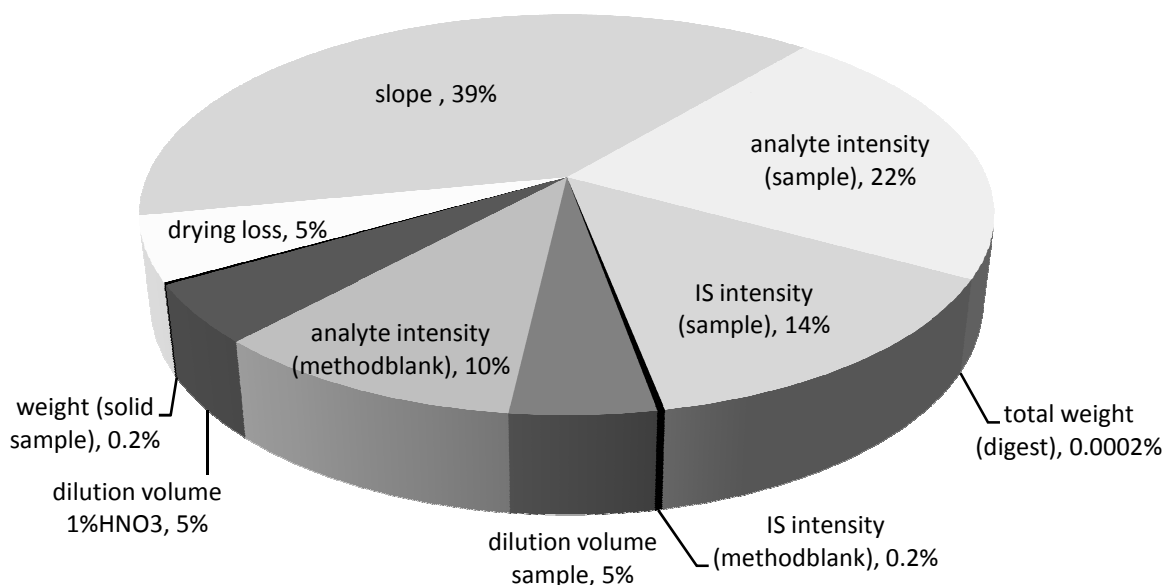

Fig. 9 Contributions to total combined uncertainty for multi-element measurement of wood digests

Relative uncertainties of solutions from leaching of prehistoric wood resembled those of digests, of course depending on analyte intensities again. RSU (k=2) were roughly between 6% and 20% for most elements above LoQ.

III.2.2 Digests of recent wood drill cores

Most elements could be determined in digests of recent wood via the applied method. U and Al were below the LoD. The results with expanded total combined uncertainties are shown in Tab. 28 and Tab. 29 in the appendix. The main purpose of these measurements was an insight into typical concentration values for wood samples from the mine's proximity. Furthermore, the influence of bedrock and species was investigated.

Fig. 10 shows the logarithmic plots of average values for drill cores of bedrock and tree species. In case values were below the LoD (grey area), the LoD value was plotted in order to receive continuous lines allowing pattern recognition and comparability. Elements were sorted according to chemical similarity. The logarithmic plots do not allow the identification of small differences but reveal, that patterns are in general very similar.

Although no general discrimination between the bedrocks seems possible on the basis of these multi-element patterns, some elements or element ratios can be identified which show differences. Ba, Sr and Rb or any ratio of two of them could be useful, as well as Co, Ni, Cu and Zn.
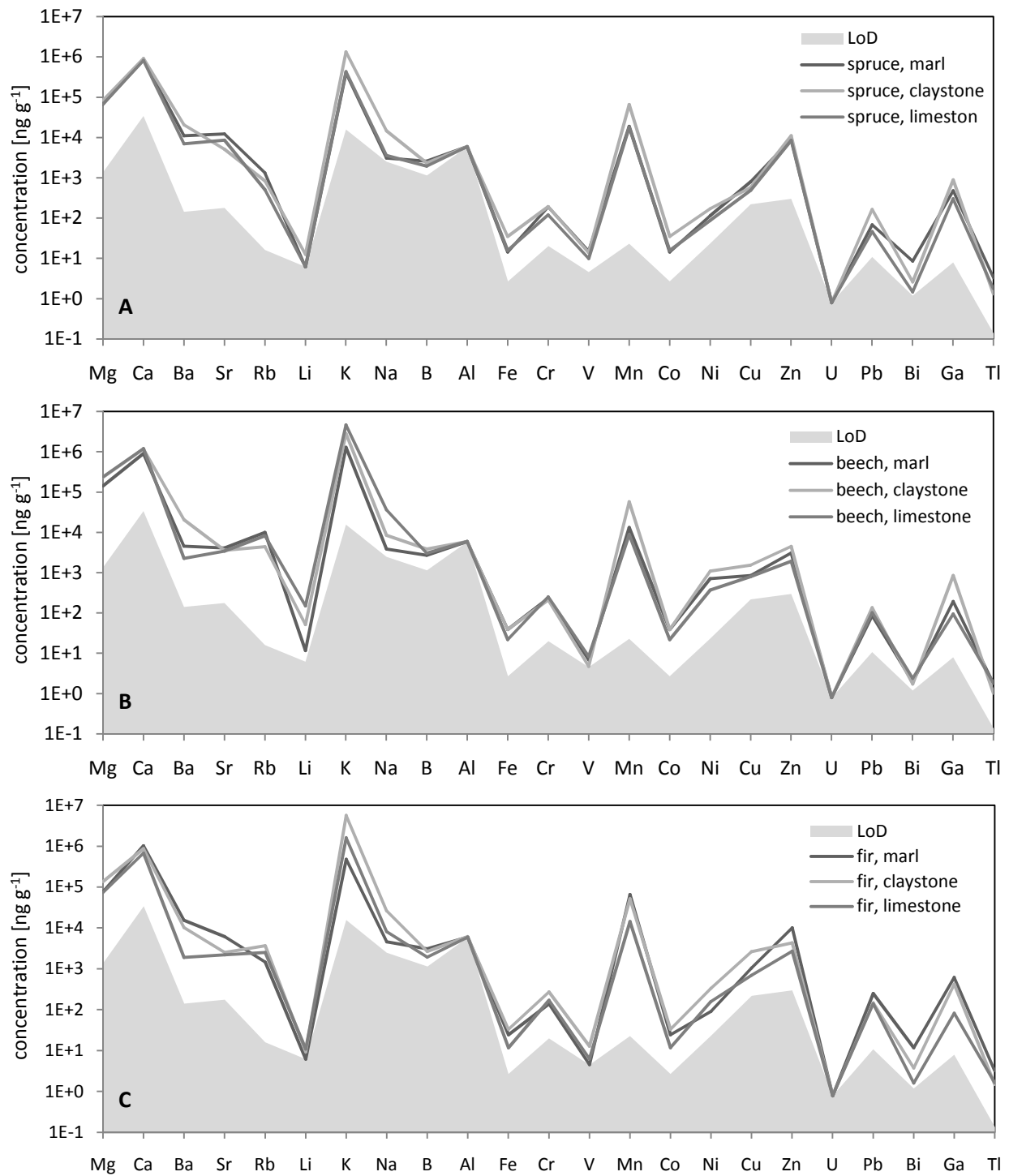

Fig. 10 Multi element patterns for recent trees (A – spruce, B – beech, C – fir) averaged for each bedrock

III.2.3 Extracts of mine material

Ammonium nitrate extracts of mine material were surveyed in order to get an insight into the possible elemental composition of contaminating salts. Extracts were first measured in 1:25 dilution, then in 1:100 dilution. Na was again separately measured in 1:10000 dilution to allow quantification of Na. Blank levels for macro elements were elevated in NH_4NO_3 blanks (> 10 ng g^{-1} for Na and K, > 100 ng g^{-1} for Ca and > 1 µg g^{-1} for Mg), but low compared to the sample contents of these elements. Result agreed for most elements between different dilution factors, recoveries were usually between 70 and 130%. Leached element concentrations relative to mass of solid material used for extraction are plotted on a logarithmic scale in Fig. 11. The grey area represents the range between minimum and maximum determined value for eleven extracts. Additionally the two lines represent results for total leached element fraction in five steps out of two prehistoric wood samples (see chapter III.2.4). Differences are observable, but in general agreement is quite good. This means, that the leaching procedure for wood is suitable to remove present contaminations (provided that the extraction procedure applied for mine material is suitable to reflect the mobile fraction of minerals in the mine environment).
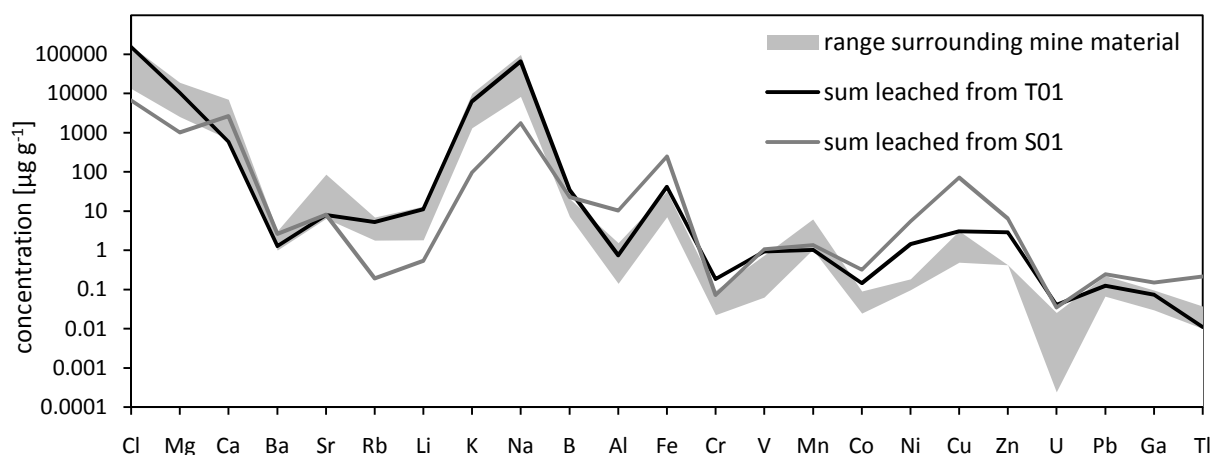
Fig. 11 Results of multi-element analysis for Heidengebirge extracts compared to leaching of prehistoric wood

III.2.4 Leaching solutions of prehistoric wood samples

Leaching solutions which were used to remove the probably diagenetic ions from the prehistoric samples were screened for their elemental contents as well. Solutions were diluted 1:10 and 1:40. Measurement of Na was compromised due to very high contents causing a

detector overload and shut down. Concentrations of bulk elements like Na, Mg and K were often far beyond the working range of the applied calibration, so values given represent estimates even though the linear dynamic range covers several orders of magnitude.

Chlorine intensity was surveyed as well. As it was not contained in the calibration standards, NaCl solutions with known Cl concentration between 100 ng g^{-1} and 400 µg g^{-1} were measured in order to get an estimate of Cl sensitivity and consequently concentration in the sample. Measurement of Cl is difficult due to its very high first ionisation potential resulting in a low yield of Cl$^+$ in the plasma and consequently low sensitivities of ~100 cps (ng g^{-1})$^{-1}$ for the sum of both natural isotopes ^{35}Cl and ^{37}Cl. Instrumental LoDs of chlorine were approximately 20 ng g^{-1} for ^{35}Cl and 2 µg g^{-1} for ^{37}Cl. The measured solutions contained between 10 and 400 µg g^{-1} Cl.

Comprehensive results in units of leached µg analyte per g solid wood for all detectable elements can be found in the appendix in tables Tab. 24 – Tab. 27. An average RSU is also given for each analyte, as well as the method LoDs which were between <0.1 ng g^{-1} for U and >1µgg^{-1} for Ca, Mg and Cl. Furthermore the sum of leached analyte from one sample in all five leaching steps is quoted, as well as the sum of all analytes in each leaching step given in weight percent. The latter gives an estimate of total contamination removal in each step and from each sample.

Differences between elements can be observed concerning their leaching behaviour, which is strongly linked to water solubility. Most elements are more efficiently removed by extraction with diluted HNO$_3$ compared to pure water, which was applied in the first three extraction steps. Fig. 12 illustrates this claim on the example of Sr (earth alkaline) and Rb (alkaline) in tool handle sample S02. The total concentration in wood was calculated from the concentration in leaching solutions and the final digest. The resulting line shows the decrease in element content during the leaching procedure. About a third of the total Sr is removed in the first leaching step with water, while the following steps do not remove large amounts of further ions. The acid solution applied afterwards is able to leach more Sr; again the second step only has minor effect. In contrast, Rb content (shown on the secondary y axis) is reduced by almost 2/3 by water extraction, while additional steps with lower pH do not lead to the removal of more ions.
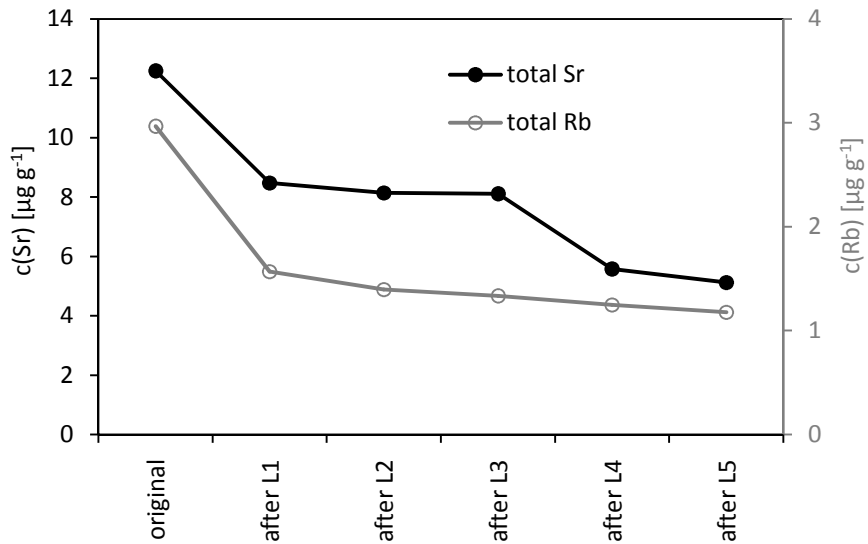
Fig. 12 Total concentration of Sr and Rb in wood sample S02 before and after five leaching steps

Furthermore, differences between samples concerning total removed elemental content and compositions can be observed. Fig. 13 compares the leaching of the major ions sodium and chloride to calcium for all investigated prehistoric samples. The two charts differ not only concerning the leaching steps (color of the column), in which the respective ions were dominantly contained. Additionally, the individual sample groups showed distinct differences. While timber samples in general released much higher amounts of NaCl compared to the other samples, more calcium was extracted from most tool handles and illumination chips.
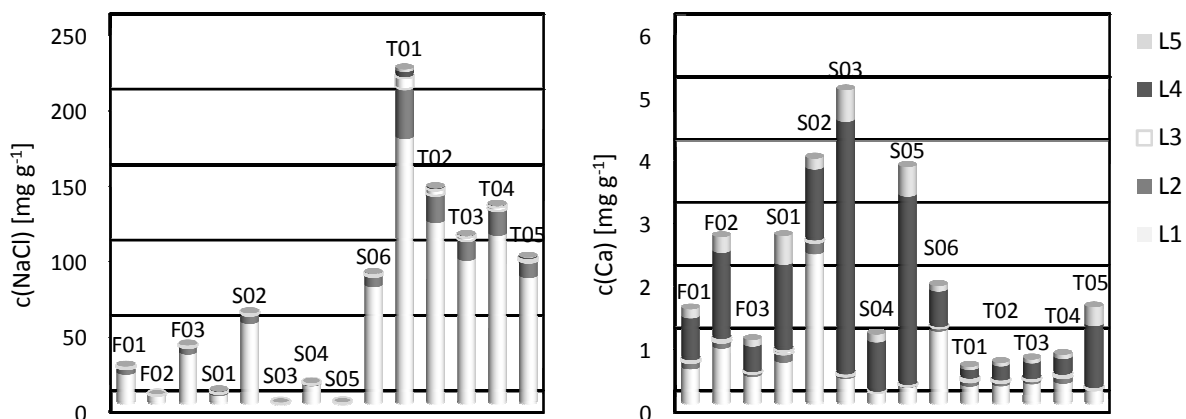

Fig. 13 Leached fraction relative to wood mass of NaCl (left) and Ca (right) with each leaching step

III.2.5 Digests of prehistoric wood samples

After five leaching steps the dried wood splinters were digested assuming that all or most secondary ions had been removed. Comparison of element contents of prehistoric and recent wood digests reveal whether and for which elements this can be true and which elements could not be removed. Comprehensive data with expanded total combined uncertainties are given in Tab. 30 in the appendix. Sample S01 was divided into two aliquots after leaching. While the first digestion of an aliquot visibly did not yield full digestion and dissolution, the second one (S01_II) with a smaller sample weight delivered a digest with only minor diffusion. All digests and blanks of this type were consequently filtered. As expected, multi-element data show increased element contents in the second digest. The material, which remained undigested in the first run is interpreted as sparingly soluble mine contamination, e.g. clays.

Recent and prehistoric samples of each tree species are compared in Fig. 14. Average values from all recent trees of one species and of all stated prehistoric sample types are plotted with a logarithmic scale. The grey area refers to the method LoD for prehistoric samples. The obtained picture is similar for all three wood types (oak and beech were subsumed as the deciduous tree group). If the line for the leached sample should be about equal or below the line for the recent tree, the leaching was successful. This is true for most alkaline and earth alkaline elements like Mg, Ca, Sr, Rb and K. Sodium was often still present in slightly elevated levels in spite of its good water solubility and enormous mass fractions determined in the leaching solutions. Heavy metals were in general removed less efficiently. Transition metals with the exception of Mn and Zn were elevated compared to contents found in modern wood. Elements with the highest accumulation in spite of leaching are U and Al, both present around (minimum) hundredfold enriched, while they were below LoD in recent wood. Al may be an indicator of contaminating silicates [Benson et al., 2006].
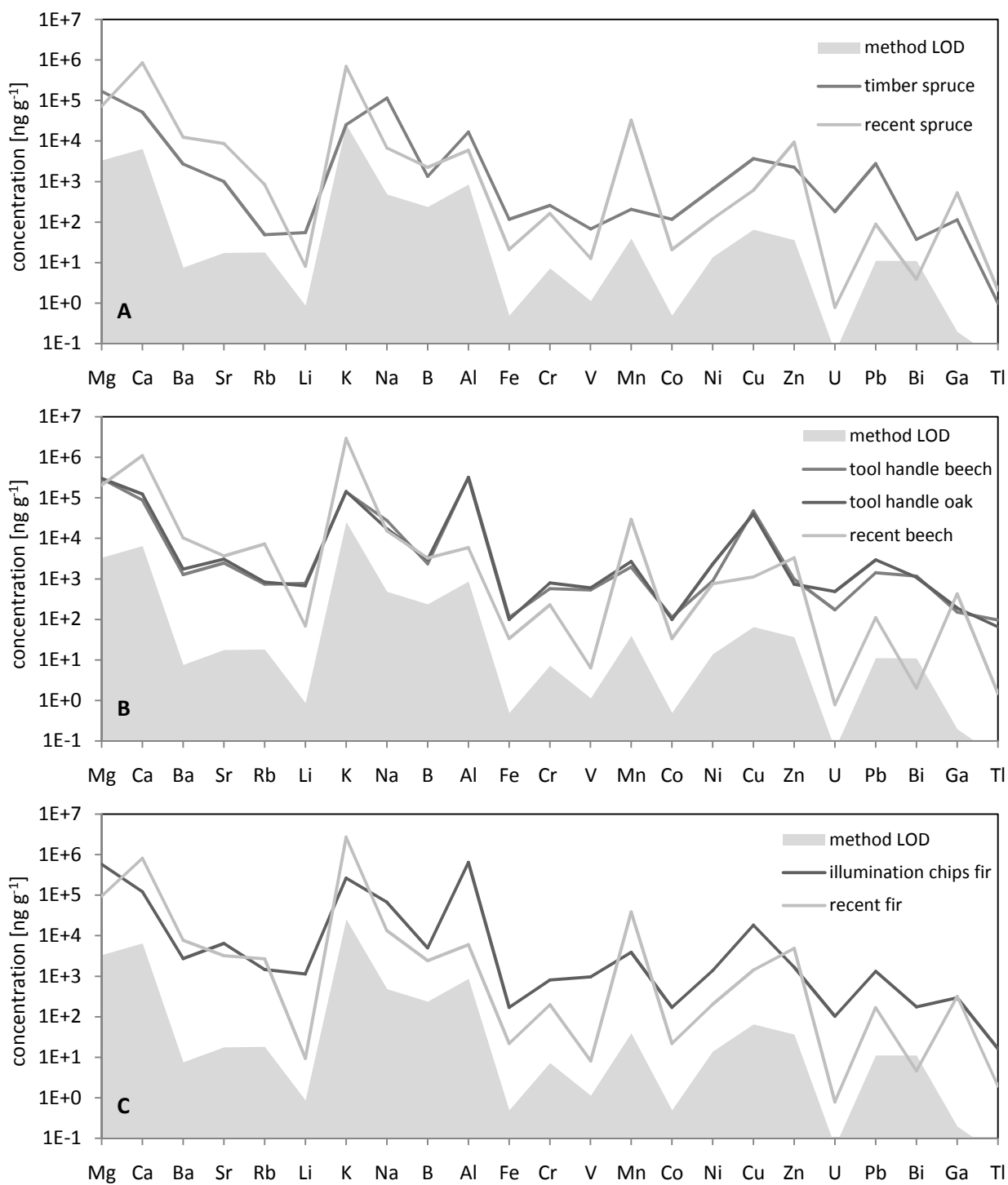
Fig. 14 Comparison of multi-element measurement results of prehistoric and recent wood (A – spruce, B – oak and beech, C – fir)

III.3 Measurement of rare earth elements

III.3.1 Measurement performance

Working range theoretically covered concentrations between 0.001 and 1 ng g^{-1} in the measured solution corresponding to 0.3 to 300 ng g^{-1} in solid wood and to ~0.03 to 30 ng g^{-1} extracted from surrounding material, but in many cases the method's LoD increased the lower working range limit. LoDs for the measured elements in wood digests are reported in Tab. 32 with the results for wood. Measurement of some isotopes in high resolution gave backgrounds of 0 cps in method blanks hindering the determination of a detection limit. Linearity of the external calibration was very good with R^2 values > 0.999 (R = Pearson product moment correlation coefficient). Sensitivities were between 10^5 and 10^6 cps·(ng·g^{-1})$^{-1}$ in low resolution and between 10^3 and 10^4 in medium and high resolution, calculated as intensity for each measured isotope relative to ng·g^{-1} of the respective element.

III.3.2 Quality control

The accuracy of the calibration was tested during each sequence by repeated measurements of two geological reference materials, certified for their REE content. The isotopes ^{89}Y, ^{139}La, ^{140}Ce, ^{141}Pr, ^{147}Sm, ^{149}Sm, ^{143}Nd, ^{165}Ho, ^{169}Tm, and ^{232}Th could be measured in low resolution and their concentrations with estimated total combined uncertainties of 15% overlapped with the recommended values from the certificate. ^{151}Eu and ^{153}Eu delivered too high values, probably caused by Ba derived polyatomic interferences. Their separation would require a resolution higher than 10000. No quantitative values can be reported here for Eu.

The three measured Yb isotopes (masses 171, 172, 173) interestingly gave too low concentrations for one RM, while the other, which had lower contents, showed slightly better agreement. Probably an overcorrection of interferences via instrumental equations occurred. A calculation of concentrations without corrections gave rather too high values, however. The reason might be Ba-Cl as well as Gd-O interferences, which occur on all three masses. Ba-Cl can be separated using medium resolution, while removal of the Gd-O interference requires high resolution. Unfortunately, count rates were very low in high resolution resulting in a loss of precision. Total combined uncertainties were therefore very high and the concentration values scattered.

[155]Gd concentrations were overestimated by about a factor two when measured in low resolution in BCR-2, while the values from BHVO-2 were shifted to higher values, too, but less pronounced. The responsible interferences may be Ba-O-H or La-O, both of which would require resolutions above 10000. Therefore, another isotope ([157]Gd) was measured in high resolution, where its Pr-O interference can be separated.

[175]Lu suffers from Ba derived polyatomic interferences as well as Tb-O. Here again, the instrument seems to correct inadequately resulting in negative concentration values. Uncorrected calculation gave better agreement with the certificate, but values tended to be too high. Monoisotopic [159]Tb gave generally about 20% too high concentration values, but high resolution could solve the problem going along with a decrease in precision by factor 10. Both Lu and Tb were therefore included in the evaluation with reservations and marked unreliable (italic letters). The same was applied for Er and Dy because both RMs are not certified for their Er and Dy concentration. Two isotopes of each element were measured in high and low resolution leading to comparable results.

Barium intensities in one reference material were about 100 times higher than in standards and blanks, as well as intensities in prehistoric wood samples, giving evidence that the interference did not affect quantification. Intensities in recent wood were much higher, though.

III.3.3 Wood samples

Full quantitative results (with the restrictions explained above) with total combined uncertainties can be found in the appendix (Tab. 31, Tab. 32). Plotting the obtained concentration values on a logarithmic scale against the elements sorted by their atomic numbers gives characteristic patterns for the lanthanoids with higher values for even and lower values for odd atomic numbers reflecting their natural abundances. The patterns for prehistoric and recent wood samples are shown in Fig. 15 Three were selected for each type for clarity reasons. The border of the grey area signifies the limit of detection. It should be noted, that no values for Pm and Eu (atomic number 61 and 63) could be obtained.

REE contents in prehistoric wood samples were shown to be by about a factor 100 higher than in recent samples. In fact, many elements could not be quantified (<LoQ) in recent wood, some

were even below LoD, especially those measured in high resolution. The value of the LoD was plotted in this case, the same was applied for statistical evaluation.

An obvious explanation might be, that the leaching procedure was not optimized for this kind of elements but for light elements with good water solubility. Solubility of REE is strongly dependent on pH, but also on dissolved organic matter because of the REE's high tendency toward complexation [Tyler, 2004]. Furthermore, not only thermodynamics might play a role, but also the kinetics of dissolution. This consideration is derived from the fact, that in timber from the salt mine lower contents were found compared to smaller wood parts like tool handles and illumination chips. While the same leaching procedure was applied for all samples, the pre-treatment for stability reasons, performed in the course of excavation, involved a longer water leaching period for timber than for smaller artefacts.
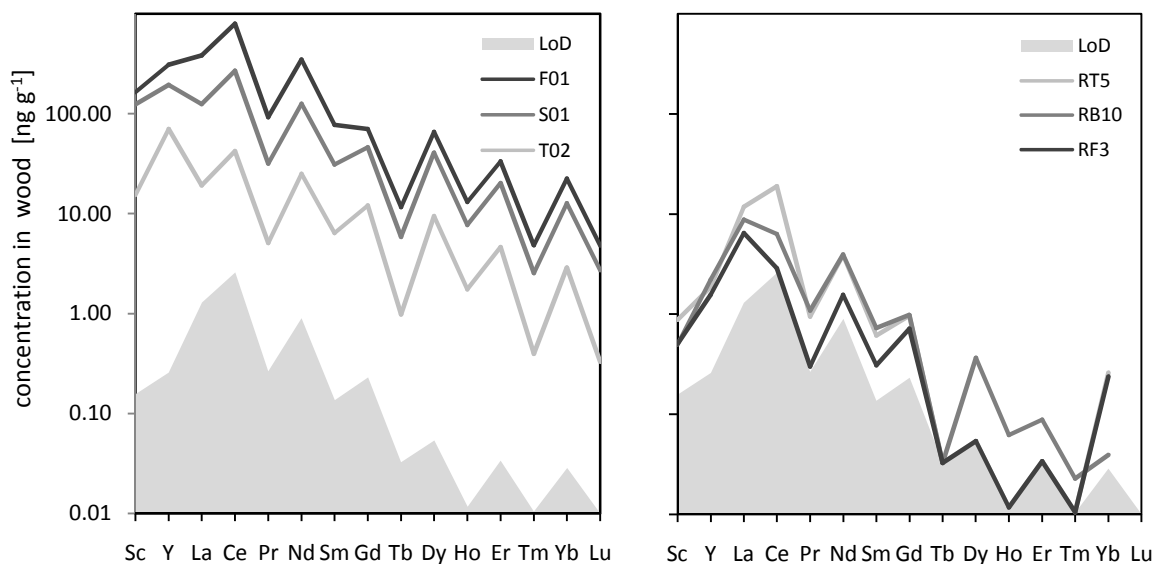
Fig. 15 REE pattern in some prehistoric (left) and recent (right) wood samples

In a study on aerosol contamination on plant surfaces, Wyttenbach and Tobler highlight the importance to consider potential deposited material, especially in the course of REE determination. Furthermore, they present a method of calculating correlations between element concentrations in order to reveal the exogenous origin of often unusually high contents measured in plant samples and plant CRMs. They suggest to use log transformed element concentrations and to relate them to Sc. The better the correlation the higher the probability, that exogenous material reflecting the earth's crust abundances dominates measured element concentrations hindering sensible conclusions on plant physiology and REE

uptake. [Wyttenbach and Tobler, 2002] Applying the suggested calculations to our data, scandium proved to show worst correlation of all determined REEs, though. Better correlation was achieved by relating element concentrations to Y, Sm, Dy, Er or Yb. Fig. 16 shows a log/log plot of Dy vs. Y concentrations for all prehistoric wood samples visualising the good correlation. In this case R^2 was 0.996.
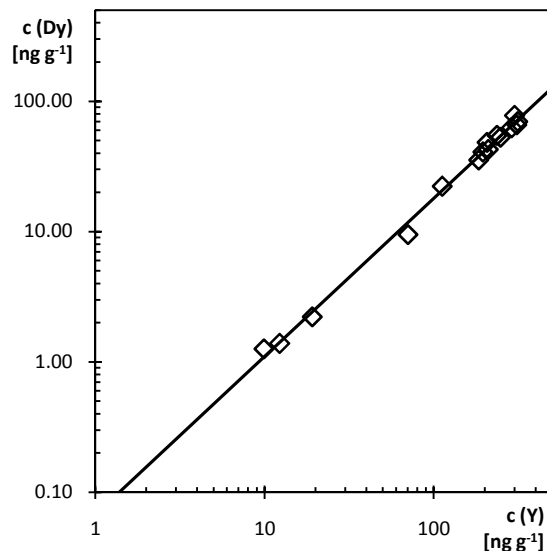

Fig. 16 Correlation of log (c_{Dy}) and log (c_Y) for prehistoric wood samples

III.3.3.1 Chondrite patterns

In order to facilitate interpretation of the data, normalization against a reference is often applied. One possible reference are chondrites, e.g. the carbonaceous Ivuna (CI) chondrite. Values for recommended average CI composition were taken from [McDonough and Sun, 1995]. The logarithmic plot of the normalized values against the elements sorted by increasing atomic numbers shows a slightly decreasing trend for the lanthanoids, while Sc and Y lie much lower. Only Gd shows an anomaly. Applying the normalization to literature earth's crust mean values taken from [Greenwood and Earnshaw, 1990] reveals, that the unexpectedly high Gd in comparison to CI carbonaceous chondrite is obviously true for the earth crust in general, as well as lower Sc and Y values. Furthermore, Sm breaks ranks in the earth's crust, but not in the measured wood samples. Fig. 17 shows the plots of three prehistoric and recent wood samples, respectively, as well as earth's crust values (shifted for visibility reasons by multiplying with 500) and normalized LoDs.
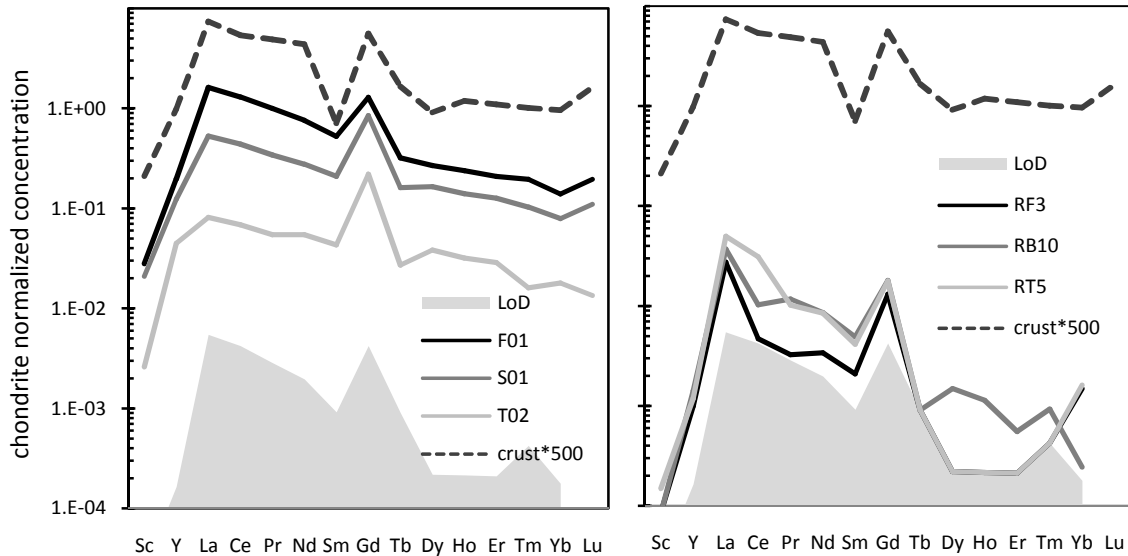
Fig. 17 Chondrite normalized REE concentration in prehistoric (left) and recent (right) wood samples

These results suggest the normalization with earth's crust abundances instead of chondrites. The resulting logarithmic plots show similar values for all REEs with variations within half an order of magnitude. Deviations increase with decreasing REE content in wood. This may be the results of two effects: on the one hand the measurement of concentrations close to the LoD may produce artificial variations. On the other hand the scattering might reflect comparably higher variation in the endogenous patterns in wood than of the contamination in the mine. As expected from the chondrite patterns, Sm shows a positive anomaly relative to the earth's crust mean contents.
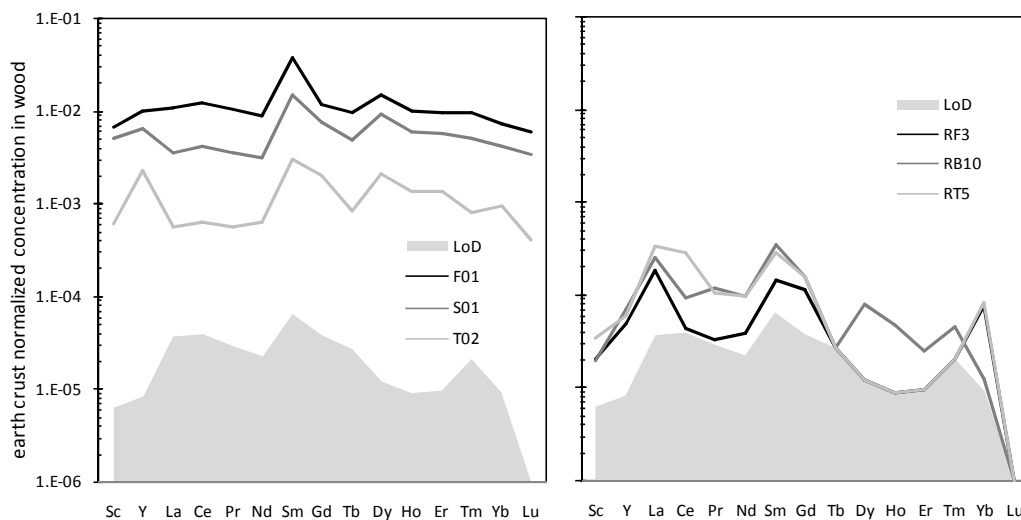

Fig. 18 Earth crust normalized REE concentrations in 3 prehistoric (left) and 3 recent (right) wood samples

Only Sc and Y average values from 11 samples were above the LoQ determined from the extraction blank. La, Ce, Nd and Gd were in average detectable, but below the LoQ, while all other elements were below the detection limit.

III.3.3.2 Results from statistical evaluation

Factor analysis with principal component extraction was calculated using SPSS 16. Thus a reduction of the dataset can be achieved. 10 REE concentrations for all 29 recent wood samples were used as input parameters. Correlation matrices were used, so concentration data were normalized first.
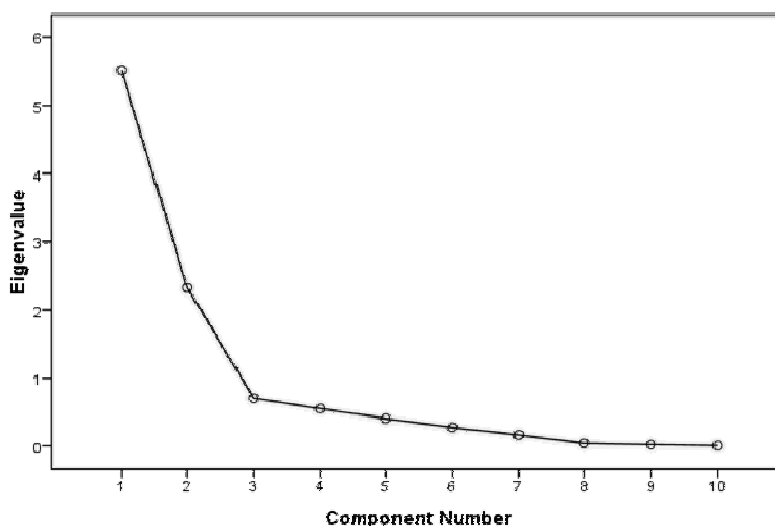
Fig. 19 Scree plot for principal component extraction

The Scree plot shows, that an extraction of two factors is a minimum requirement. Thus 78% of the total variance are explained. The first factor accounts for 55% of the total variance.

A plot of factor score 2 versus factor score 1 gives insight into similarities between samples. Group membership concerning bedrock is no input parameter here. It was only used in the plot to clarify whether data points cluster according to their bedrock, as shown in Fig. 20 Factor analysis (principal component extraction) for recent wood samples, factor 1 vs factor 2Fig. 20. It is obvious, however, that grouping rather reflects tree species than bedrock, but not strictly. PCA does not seem to be a suitable tool for bedrock discrimination based on REE data.
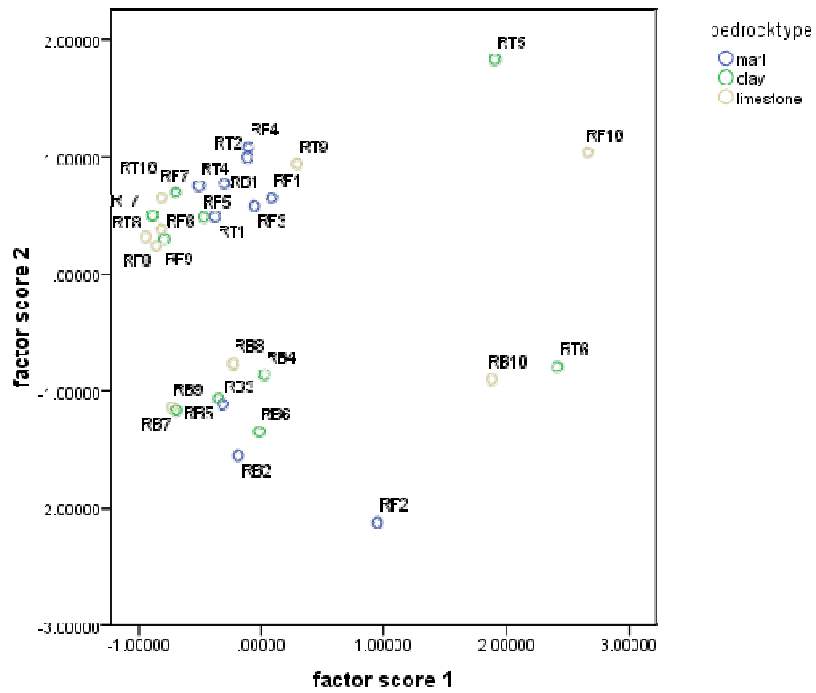
Fig. 20 Factor analysis (principal component extraction) for recent wood samples, factor 1 vs factor 2

Therefore, a discriminant technique was applied. In this case, the group membership is an input parameter for the calculation additionally to 15 (semi-)quantitative REE concentrations. The total variance of the data is expressed in two functions, where the first accounts for about 90%.
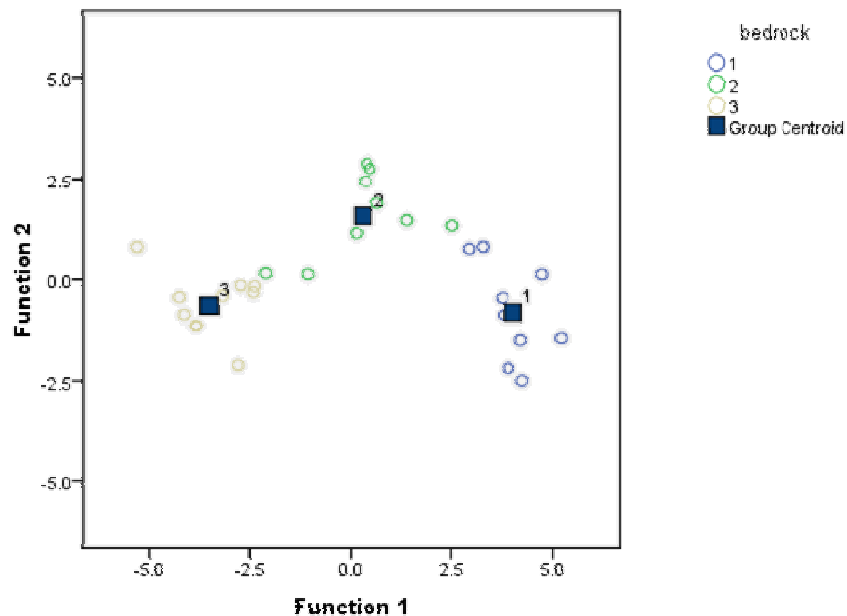
Fig. 21 Canonical discriminant functions for recent wood samples – discrimination between bedrocks: 1 marl, 2 claystone, 3 limestone

Classification was correct in 97% of original grouped cases, but only in 69% when cross validated. Although these data have to be treated cautiously, it seems that there is potential in bedrock discrimination using rare earth element concentrations.

The same calculation but with groups according tree species reveals that discrimination is possible, too, especially between the deciduous tree beech and the two conifer species, which overlap.
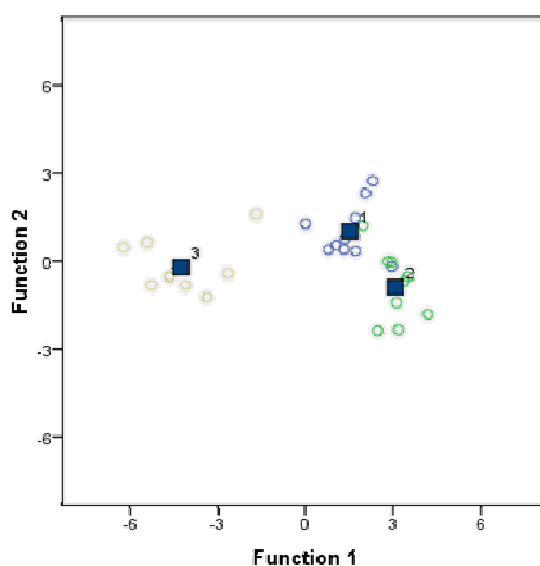
Fig. 22 Canonical discriminant functions for recent wood samples – discrimination between species: 1 spruce, 2 fir, 3 beech

III.3.4 Surrounding mine material

In order to confirm or refute the hypothesis of REE contamination from the mine, the extracts of the surrounding mine material ('Heidengebirge') were analysed as well. The measurement of NH_4NO_3 extracts of mine material was compromised, however, probably due to high salt contents. A sudden decrease in internal standard intensity during the measurement of the extracts in the sequence by about 50% may indicate either partial clogging of cone orifices, decreased nebulization efficiency and/or ionization efficiency. A higher dilution did not deliver improved results because of the very low REE contents in the extract. Therefore, optimization of the extraction procedure by using another extracting agent is suggested.

Detections limits were determined from two measurements of the extraction blank from two different days. Thus they were probably overestimated. Blank concentrations were in most

cases in the range of those of digestion blanks from the same day, but differences and in measurement conditions and the mentioned problems had more effect on the extraction blanks resulting in quite a large difference between the two days of measurement and consequently very high LoDs (Tab. 33).

Only Sc and Y average values from 11 samples were above the LoQ determined from the extraction blank. La, Ce, Nd and Gd were in average detectable, but below the LoQ, while all other elements were below the detection limit. Tab. 33 shows average, minimum and maximum values of the 11 SM samples regardless of whether they lie below the determined LoD. Only those were excluded and marked '<LoD*', which were even below a theoretical LoD derived from digestion blanks (taking into account the extraction weights and dilution of the SM samples). These LoD* and respective LoQ* are given in the table as well as the average REE content of 6 tool handle samples from the mine. These values show, that only a minor fraction of total REE content could be extracted from the surrounding material and/or wood samples strongly accumulated REE during storage.
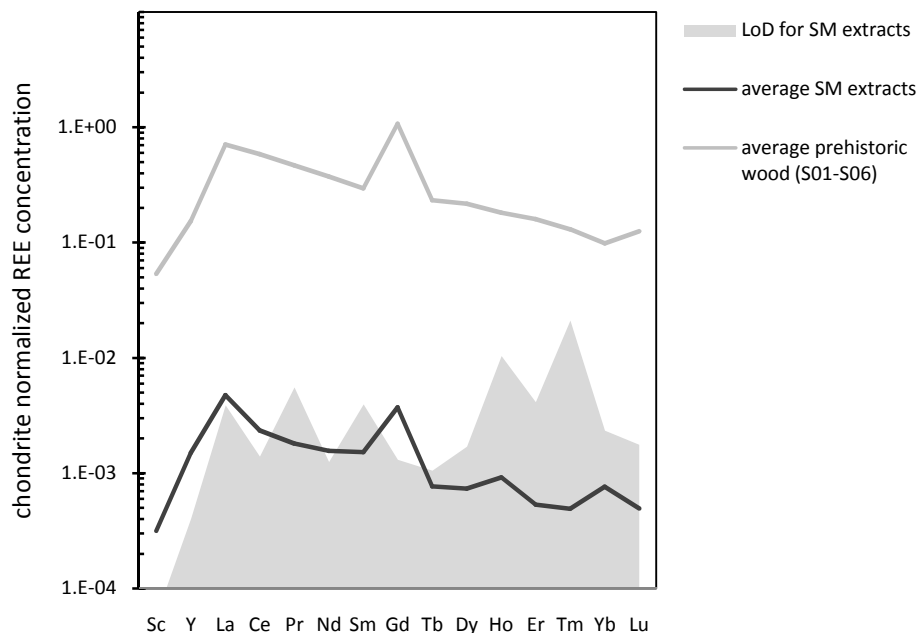
Fig. 23 Chondrite normalized REE contents for extracts of surrounding material (SM) and prehistoric wood

Due to a lack of reliability of the data, the comparison of patterns with mine material is compromised. Nonetheless, a plot of chondrite patterns (Fig. 23) shows strong similarities between prehistoric tool handles and surrounding material (SM) extracts. In this case, values below the determined LoD were plotted anyhow, assuming it was overestimated, as can be

seen in the chart. It shows the average of all measured Heidengebirge extracts compared to the average of the 6 tool handle digests.

III.4 Spike experiment

The possibility to discriminate between endogenous and contaminating Sr should be confirmed by a spike experiment using modern wood. A first trial with the spike solution as obtained resulted in observations that the spiking process was accompanied by strong leaching due to the low pH of the spike solution. Furthermore modification of wood structure could not be excluded. A yellow colouring of the solution was visible for one wood sample (oak). Eventually a large fraction between 10 and 50% of secondary Sr remained in the wood after leaching applying the first leaching procedure with water only.

Consequently, the spike experiment was repeated by using neutralized spike solution. Furthermore three blanks were created by subjecting a splinter of each tested wood species to a similar solution without [84]Sr. So the accompanying leaching of natural Sr could be monitored. Fig. 24 shows the obtained results with quantification restrictions explained in II.2.2.1. Three lines were ablated for each sample and the mean value was plotted. RSDs were increasing strongly with decreasing analyte concentration – up to >100% in one case. Most RSDs were around 30%.

The left part of each chart (Fig. 24) shows the spiked sample: an aliquot was kept before spiking, then one after spiking and drying and one after the optimized leaching procedure was applied. The right part of each chart shows the same three steps, but without spike in the solution, representing the blank for each species. The behaviour of the natural isotope [88]Sr seems unaffected by the presence of secondary Sr as the comparison between spike and blank shows. The plotted numbers only give rough estimates, so the approximately uniform [88]Sr signals for the oak blank in all three stages may be the result of high uncertainties.

Furthermore a high enrichment in the spike isotope can be observed, independent of the original sample Sr concentration. In contrast to the mine environment, Sr is the only contamination that the wood is exposed to, so Sr ions can take the spots of all ions, also those which are leached by the spike solution itself. Unfortunately it is finally not removed completely from the samples after the leaching procedure. It is decreased by ~90, 95 and 98% of the

content after spiking, however. The natural Sr decreases still, but by minor fractions (~60, 70 and <90%, respectively).
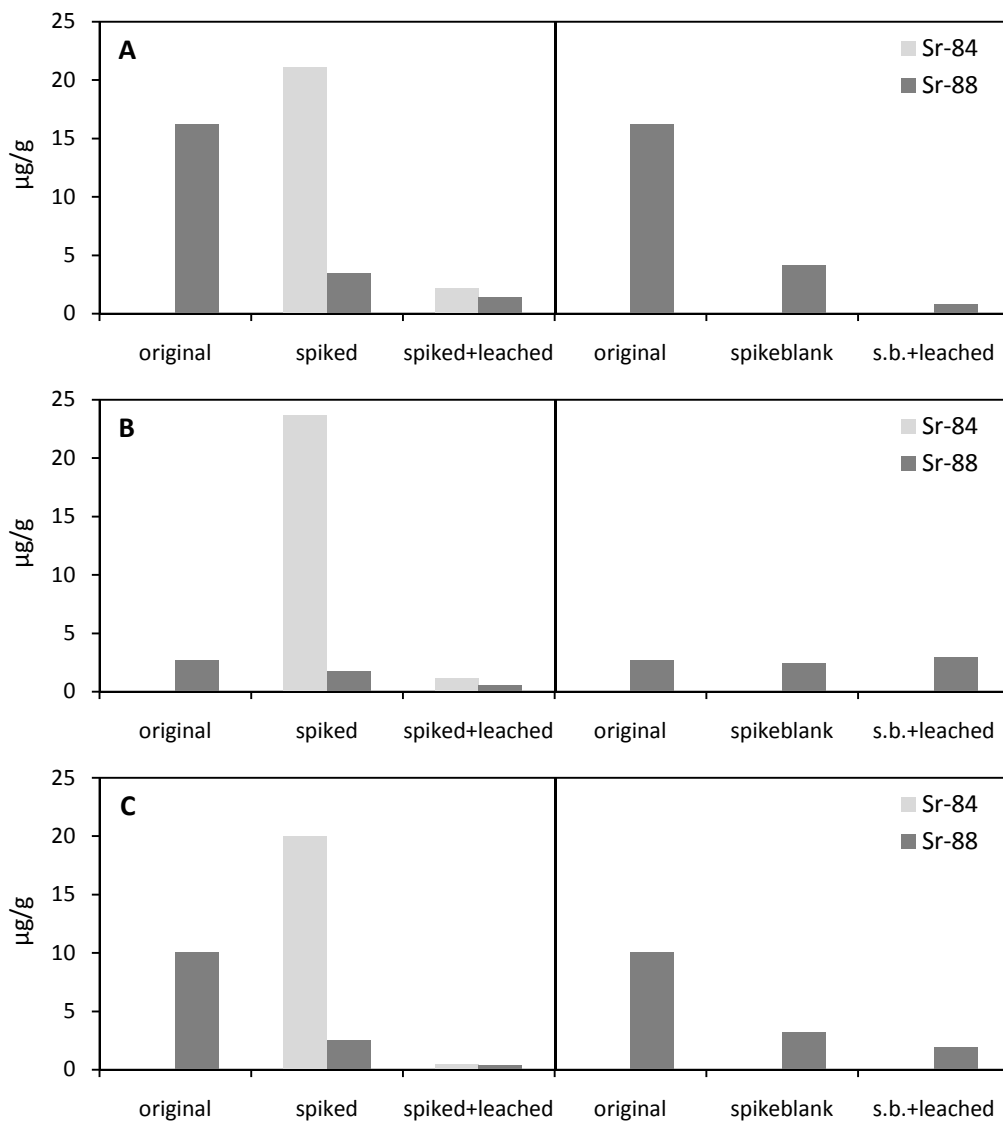
Fig. 24 Results of the spike experiment for A spruce, B oak, C beech

The spike experiment is a powerful tool to observe the processes taking place during exposure to contamination and the suggested removal procedures. Conclusions are compromised here, however. The assumption seems likely, that the chosen exposure situation strongly overestimated the influence in the mine, especially concerning the presence of liquid solution. Further improvements of this simulation are suggested in order to receive more reliable information on the processes. Understandably, a time period of 3000 years is hard to integrate, though.

III.5 Determination of Sr isotope ratios

III.5.1 Sr/Rb screening

Samples were screened via ICP-QMS for their Sr and Rb content after separation using the Sr specific resin. On the one hand separation efficiency was controlled to monitor the Rb separation efficiency. On the other hand, the actual Sr concentration needs to be known in order to select an appropriate dilution to obtain optimum signal intensities for MC-ICP-MS measurement.

The recovery of Sr after separation was calculated. Wood digests and leaching solutions containing between 20 and 500 ng g^{-1} Sr exhibited recoveries mostly in the range between 10 and 50%. Ammonium nitrate extracts with Sr concentrations between 2 and 50 µg g^{-1} yielded similar recoveries of separation (15-30%). Rb concentrations were always close to the blank level except one, so reliable quantification was not possible.

III.5.2 Instrument performance and validation

III.5.2.1 Sensitivity

Sensitivities were usually around 300 V (µg g^{-1} Sr), while in one measurement a five times higher sensitivity was achieved although no high performance cones were used.

III.5.2.2 Quality control

Fig. 25 shows the results of the measurement of the certified reference material SRM 987 in order to control the accuracy of the measurement, especially with respect to mass bias correction. Roman numerals signify sequences (days of measurement), while Arabic numbers number the standard measurements during each sequence consecutively. Error bars give total combined uncertainties (k=2). The continuous line indicates the certified value for SRM 987, the dashed lines margin the certified range (^{87}Sr/^{86}Sr = 0.71034 ± 0.00026). Clearly, all CRM measurements delivered values within this range: all determined mean values deviated by less than 0.017% from the certified value. Thus the result's SU range always included the certificate's mean value. RSUs were between 0.016 and 0.035% for SRM 987. The accepted value in literature is 0.71026, though. [Balcaen et al., 2005]
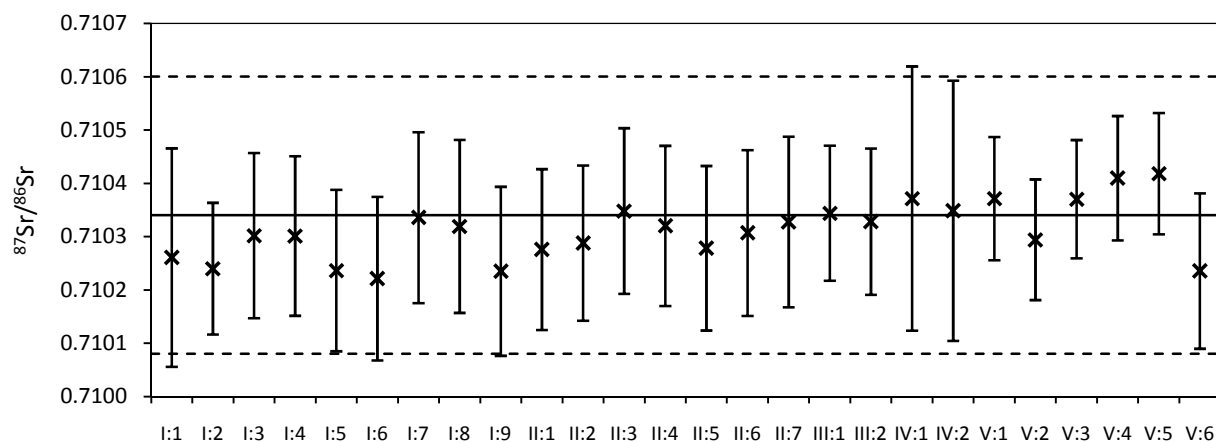
Fig. 25 Sr isotope ratio data for SRM 987

III.5.2.3 Measurement uncertainty

The calculation of the total combined uncertainty for Sr isotope ratio covered contributions of the blank correction, measurement precision, the applied mass bias correction and Rb correction. Measurement precision and mass bias correction were combined and gave the smallest contribution, as precision was good (RSDs of measured ratio ^{87}Sr/^{86}Sr around 0.001% for signals of 5V and higher, but increased strongly with lower signals).

The uncertainty contribution of the blank is a major part of the resulting combined uncertainty (in average ~70%). It roughly increases proportionally to the reciprocal measured voltage for Sr. So signals of minimum 1 V are crucial to guarantee results with satisfyingly low uncertainties. Blank standard deviations were calculated from six blank measurements during a sequence while blank correction uses always the last measured blank value, but the applied method ('measure-zero') only gave a single value output. Consequently, blank contributions might be overestimated by the determined blank signal RSDs between 0.5 and 20% on different masses.

Rb content effects accuracy of measurement results as it contributes to uncertainty as well. Rb was measured on mass 85 and its proportion was calculated as signal for ^{85}Rb relative to the total signal for all Sr isotopes. These ratios were not always optimum values below 0.1% - partly due to low Sr contents in the samples preventing dilution after separation. The median Rb/Sr fraction was 0.07%, but values up to 0.3% were frequent resulting in consequently higher uncertainties.

Average uncertainty contributions of the three mentioned influences are shown in Fig. 26. Furthermore sample specific contribution values are given in Tab. 37 with the isotope ratio results for recent wood digests.

U_{blk}
66%

U_{Rb}
33%

$U_{mb/meas}$
1%
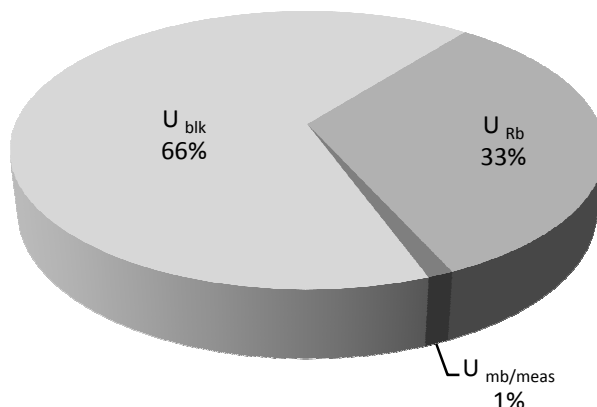
Fig. 26 Average uncertainty contributions to Sr isotope ratio results

Results are given with expanded uncertainties with coverage factor 2.

III.5.2.4 Method blanks

Method blanks from digestion or filtration of samples were not included in the calculation of results. Nonetheless, the procedures were surveyed by conducting all sample preparation steps with the corresponding blanks, too. Additionally, blanks from the separation procedure only were made for comparison reasons. All these blanks were then measured in the end of a sequence in order to control and trace back possible contamination and consequently distortion of results. Fig. 27 shows the measured voltages for Sr for 9 digestion blanks and 3 blanks derived from the separation procedure only. Voltages show a decreasing trend in the beginning and are relatively high. The highest blank exhibits a signal of about 4% of the average sample signal. Isotope ratios were calculated from the voltages applying Rb (voltages were about 1% of Sr) and mass bias correction. The resulting ratios are plotted in the chart on the secondary axis. A calculated theoretical contribution of the worst blank to an average sample applying the determined ratios and voltages would lead to a bias of 0.04% in the final ratio, so roughly in the range of typical expanded total combined uncertainties.
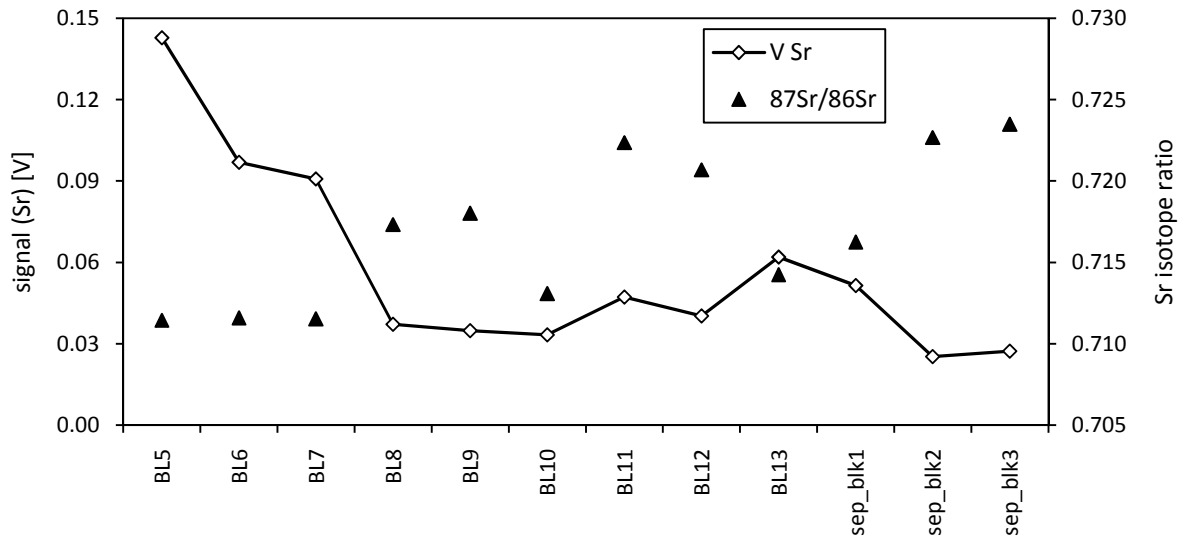
Fig. 27 Method blank Sr signals and Sr isotope ratios

III.5.3 Local background in the salt mine

In order to assess the applicability of the procedures with respect to the determination of endogenous Sr isotope ratios after removal of diagenetic Sr, it is necessary to know the isotopic composition of the contamination. Therefore, extracts of the mine material were analysed. The results are presented in Fig. 28 (below) and Tab. 34 (appendix). The arithmetic mean of eleven independent extracts was calculated (dashed line; $^{87}Sr/^{86}Sr$ = 0.7079 ± 0.0005 (2 SD)) and the local range was defined by adding/subtracting the doubled standard deviation (shaded area). On a scale of possible geological Sr isotope ratios, this represents a narrow range.
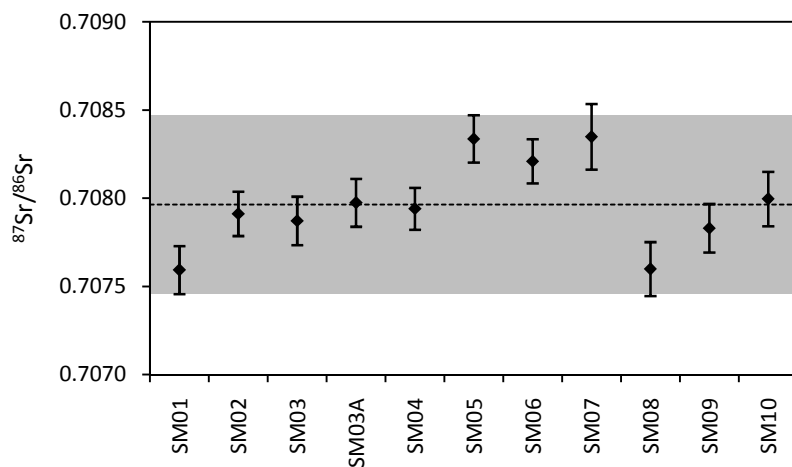
Fig. 28 Sr isotope ratio results for surrounding mine material with SU (k=2)

These values are partly consistent with values from literature: Spötl and Pak report five values for Haselgebirge evaporites and Lower Triassic evaporites (anhydrite and gypsum) from Hallstatt [Spötl and Pak, 1996], two of which lie within the range established in this work. One is slightly below the range, two others are significantly higher. (Fig. 29, Tab. 35) This may have the reason, that we investigated only a small detail compared to the total geological surroundings. However, it was the most relevant detail for our purpose: the material directly bordering the investigated wood samples during storage in the mine.
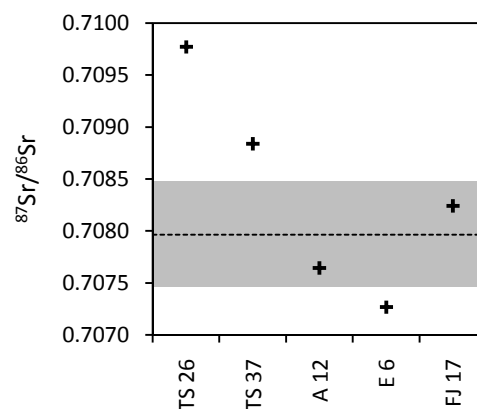
Fig. 29 Hallstatt literature Sr isotope ratio values, data from Spötl and Pak [1996]. Grey bar: range determined for mine material in this study

It should be considered, however, that the applied leaching procedure probably only dissolved minerals with good solubility at slightly acidic pH values, but not silicates (clays), which require HF for dissolution. Gypsum and other Ca containing minerals are expected to be the major Sr source of contaminations, but the Sr content in silicates [Benson et al., 2010] should not be neglected but investigated, too. In case of expansion of clays, ion exchange processes may occur. [Benson et al., 2008] The potentially released Sr should be removed from wood by leaching, however.

III.5.4 Local signal in recent trees

As a broader diversity of Sr isotope ratio values was to be expected in the Northern Limestone Alps for the reasons mentioned above, the local range for endogenous Sr isotopic composition in wood had to be established by sampling of trees in the proximity of the mine taking into account the different bedrocks present (II.1.3.2). The results from these determinations are presented in Fig. 30, grouped by bedrock type and sorted by vicinity of sampling spots. The different tree species investigated are denoted by different symbols (circles for spruce, squares

for beech and triangles for fir). The grey area indicates the range of mine material as shown in III.5.3. Only the results of two samples overlap with this range. This fact highlights the importance of analysing trees (or other plants) in order to interpret the isotopic composition of wooden findings because different Sr sources result in a wider distribution of isotope ratios as the investigation of a few Heidengebirge extracts would suggest. All measurement results can be found in the appendix in Tab. 37.
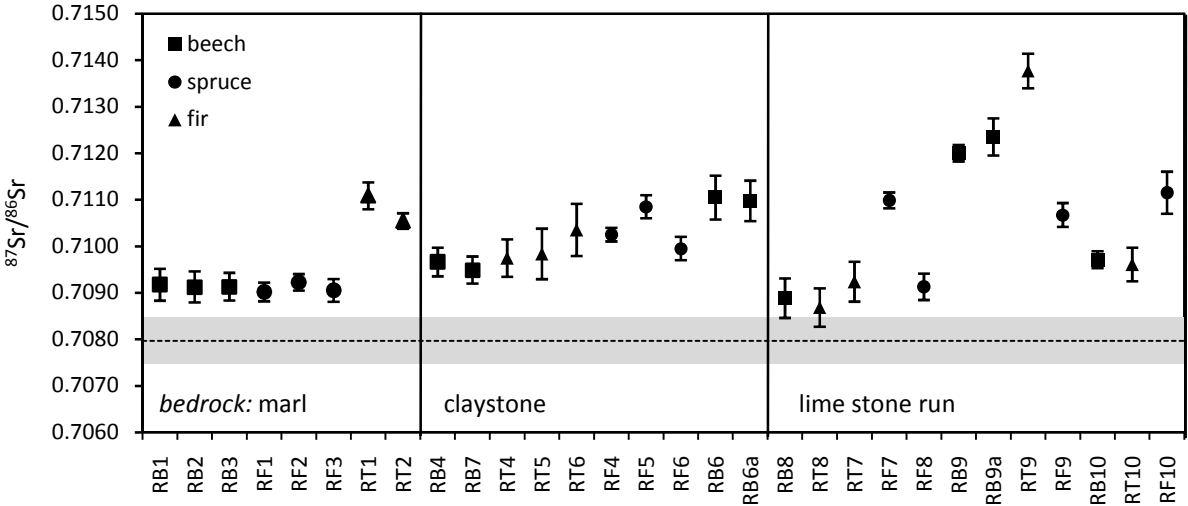
Fig. 30 Sr isotope ratio results for recent trees growing in the proximity of the mine

On a first glance, no clear distinction between the three bedrocks is possible. Trees growing on all three geological locations seem to exhibit scattered isotopic composition. When taking a closer look at the distinct sampling spots, a few more conclusions are possible. In the case of marl, samples were taken along the path to the mountain 'Hohe Sieg' (Fig. 31). Trees RB1-3 and RF1-3 were growing below the walkway in an area of about 7 m diameter and RT1 and 2 were growing about 10 m apart on the other side of the path. Interestingly, these two groups can be clearly distinguished.

Fig. 31 Sampling site 'Hohe Sieg', marl

Most samples from salt-bearing claystone bedrock were taken on an area with a diameter of about 50 m alongside the path to 'Dammwiese', on the same slope. Their isotope ratios are distributed more widely and shifted slightly to higher values compared to the uniform first marl group. The beech named RB6 was situated slightly apart; and so was RB5, which was growing in a rift at a watercourse. The latter's $^{87}Sr/^{86}Sr$ value of 0.71786 ± 0.00035 was classified as an outlier when observing all recent trees as a group and is missing in the chart for clarity reasons. It was suspected to be an analytical artefact and the determination was therefore repeated, delivering an even higher value. The second measurement was compromised, though, by unsatisfying Rb separation efficiency. RB6 and RB6a both refer to the same drill core, again to two independent determinations from digestion to measurement on two different days. They coincide perfectly.
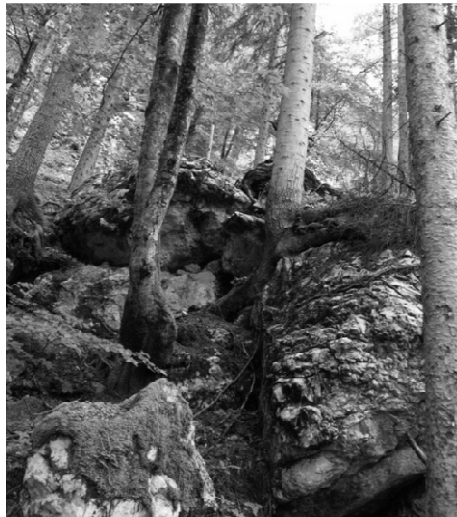
Fig. 32 Lime stone run behind 'Alte Schmiede'

Trees growing on large limestone blocks with hardly any soil along steep hillsides (

Fig. 32) delivered the widest range of Sr isotope ratios. Some wood samples showed very low ratios, two even overlapped with the determined local mine material range. With the exception of RF8, these trees can be attributed to pairs concerning sampling spots (compare Fig. 6). They are sorted accordingly in Fig. 30. The pairing is not reflected in the isotopic composition, though. RB9 and RB9a again refer to one drill core and prove the repeatability of the procedure.

Being aware that the number of samples was very small, especially in comparison to the geological variety in the Hallstatt hanging valley, any interpretation can only be assembled

cautiously from a few single values. Anyway, this investigation could at least give a first insight into how the Hallstatt geological variety is reflected in different trees of different species in different spots. A significant species influence could not be observed here, variations seemed to be rather dominated by growing spots, even within one bedrock type.

III.5.5 Leachates and digests of prehistoric wood

Fig. 33 shows the results for leached prehistoric wood samples from the salt mine as well as for the investigated leaching solutions (L1 – L5) of two samples (timber T01 and tool handle S01).
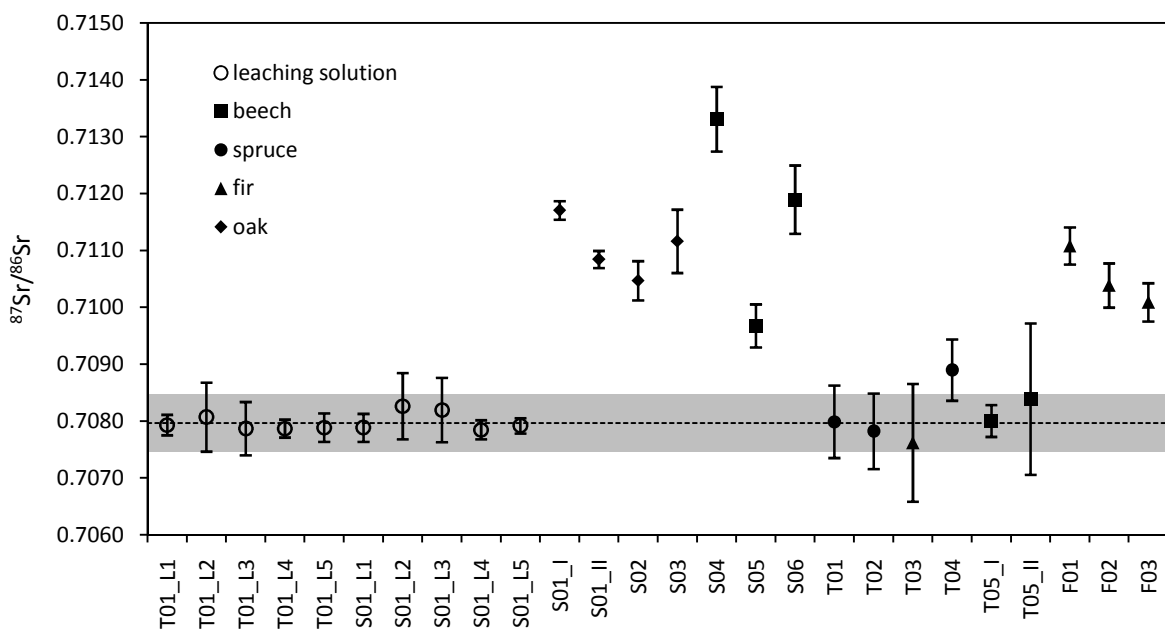
Fig. 33 Sr isotope ratio results for prehistoric wood digests and wood leaching solutions with SU (k=2)

The dashed line and grey area indicate the mean value and the 2 SD range of surrounding material inside the salt mine as explained in (III.5.3), i.e. the range of probably secondary Sr contaminating the wood samples. The means of all five leaching solutions for each of the two wood samples (open circles) lie inside this range. This fact approves the conclusion, that the Sr fraction removed during the leaching procedure is virtually exclusively composed of secondary material from the mine. All tool handle (S01 – S06) and illumination chip (F01 – F03) samples exhibit distinctly higher Sr isotope ratio values. Apparently, the separation of endogenous and exogenous Sr is possible – at least to some extent. In case of complete exchange between natural and diagenetic Sr we would experience uniform isotope ratios in the local range of the mine, as secondary Sr is available in great excess. Timber samples (T01 – T05) do lie within the

predefined mine range, however. The mean value of sample T04 lies above the range, but its uncertainty overlaps with it, so no distinction is possible. T05_I and T05_II refer to the same timber sample, but to two independent leachings and digestions. The first leaching was definitely incomplete. One possible interpretation might be that in case of timber samples more (maybe even exhaustive) exchange occurs for unknown reason. This can be supported additionally by the fact that a very low Sr fraction remains in these samples after leaching (causing also larger uncertainties due to lower measured voltages). Another obvious explanation derives from comparison to the measurement of recent wood samples (0): the timber trees may have grown in spots where Sr sources were comparable to the Heidengebirge material inside the mine, like recent samples RB8 and RT8, for example.

Tool handle sample S01 was leached once, but digested twice due to incomplete digestion in the first place. Two significantly different Sr isotope ratios are the result, which can be explained by a fraction of secondary Sr, that had not been extracted in the course of the leaching procedure and was not digested in the first run either. The second digestion (S01_II) with more acid could dissolve more material resulting in an isotope ratio shifted to a lower value compared to S01_I.

III.5.6 Comparison of recent and prehistoric wood

Measured Sr isotope ratios, sorted by value in ascending order, for recent (grey symbols) and prehistoric (black symbols) wood are compared in Fig. 34.
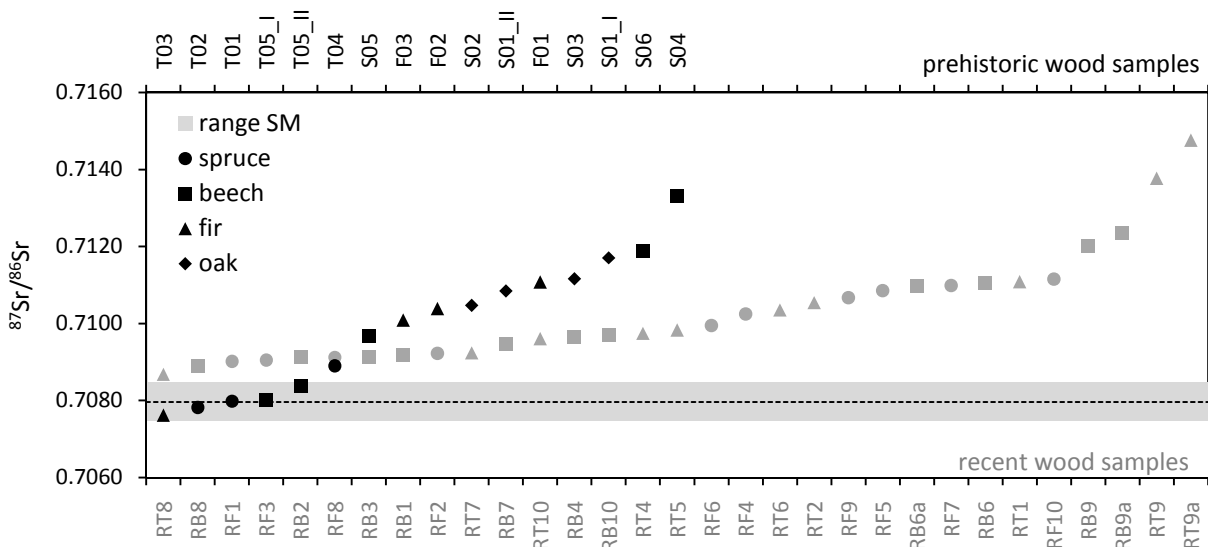
Fig. 34 Comparison of Sr isotope ratios of prehistoric and recent wood samples

All values were pooled, disregarding species, sample type or bedrock type. At the first sight, both groups show similar distribution, but this is better illustrated in Fig. 35. Comparison is compromised due to the very small number of samples for prehistoric wood. Median values for both sample groups are not significantly different, although prehistoric samples can be seen to be shifted to lower values in the charts. They also exhibit higher isotopic ratios with increased frequency compared to the medium ratios, which are most frequent for recent samples. These observations require verification by increasing the sample number, though.
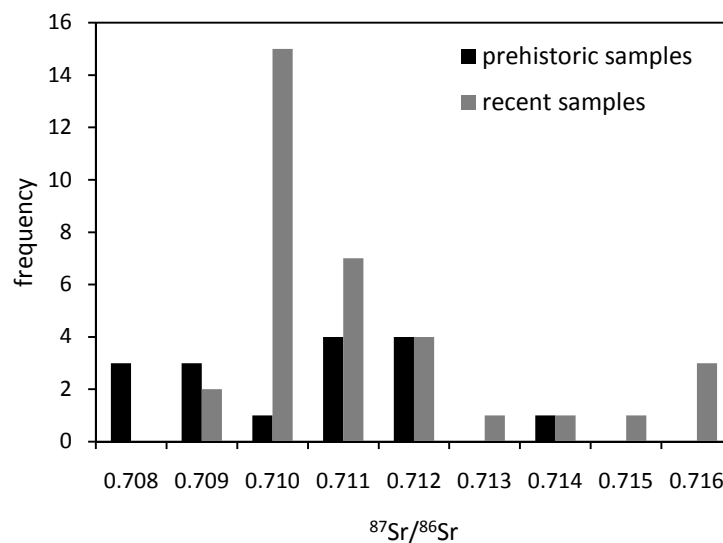
Fig. 35 Frequency distribution of Sr isotope ratios in prehistoric and recent wood samples

III.5.7 Sr isotope ratio vs. Sr concentration

The plot of Sr isotope ratio against the determined Sr concentration is a powerful tool to show clustering of groups or give insight into probable contamination. All investigated wood samples are displayed in Fig. 36.

Although a few subgroups of only one tree species (denoted by symbol geometry) and bedrock (denoted by symbol colour) seem to cluster, no general discrimination between bedrocks or species is possible. Furthermore, most prehistoric samples (open symbols) match the picture in general, but none can clearly be assigned to a group of the same species.
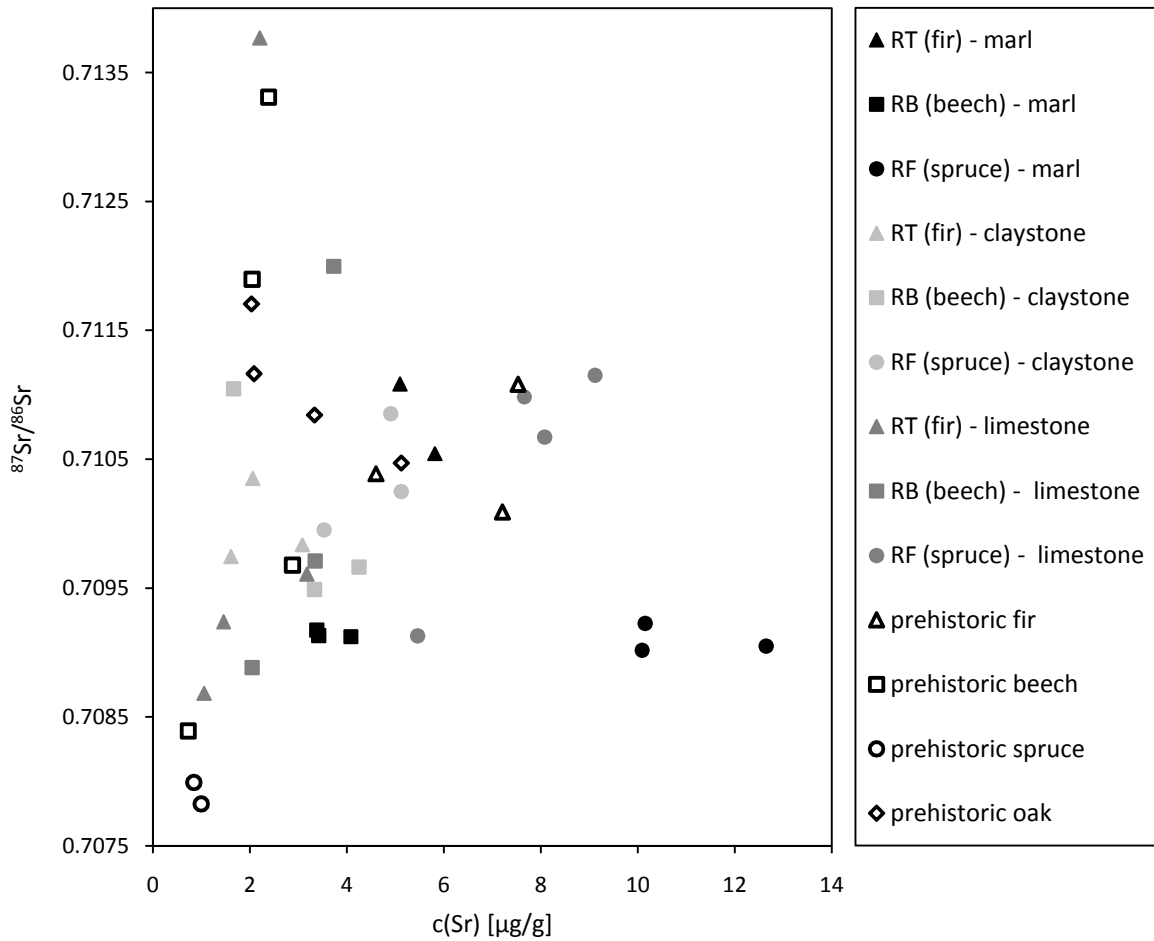
Fig. 36 Sr isotope ratio vs. concentration plot for prehistoric and recent wood samples

III.5.8 Educing the natural Sr signal in prehistoric samples

The above considerations have left one question open, so far: Is the measured Sr isotope ratio for leached prehistoric wood samples identical to the endogenous signal? This cannot be taken for granted from the investigations carried out, but some conclusions are possible as follows:

- Leaching solutions contain dominantly (or even exclusively) secondary material (III.5.5). Although comparative leaching experiments with recent wood pieces have shown, that metal ions are released from not contaminated wood, too (III.1.4), we hypothesize that the leachable fraction of the original wood has already been extracted and/or replaced by diagenetic ions from the mine storage during thousands of years of storage. Thus it is favourable to remove the leachable fraction as quantitatively as possible.

- Recent trees from the mine proximity show generally higher Sr isotopic values. Consequently, a fractionated leaching procedure with digestion of aliquots in-between

is expected to result in isotope ratios which increase linearly with decreasing relative diagenetic Sr content in the digests.

- The endpoint of this 'mixing line', where all diagenetic material has been removed, represents the endogenous Sr isotope ratio. It is characterized by the natural (non-leachable) Sr concentration. A range for natural Sr content in wood can be concluded from multi-element measurements of recent wood.

- The other endpoint of the mixing line is defined by the sum of leached and remaining Sr content and an isotope ratio derived from additive 'mixture' of these two Sr fractions with known values.

- As a consequence, even if we do not analyse exclusively endogenous Sr, our measurement result is one point on the mixing line. The line itself, however, can be derived in principle from these two latter values (measured digest and calculated endpoint 'wooden finding untreated'), but only if a concise natural Sr content for each sample is defined or the relative residual contamination is known.

Theoretical mixing lines for a ^{87}Sr/^{86}Sr of the contamination of 0.70796 and a natural ^{87}Sr/^{86}Sr of 0.713 in a sample with natural Sr concentration of $2\,\mu\mathrm{g\,g}^{-1}$ and increasing content of contamination are shown in Fig. 37.
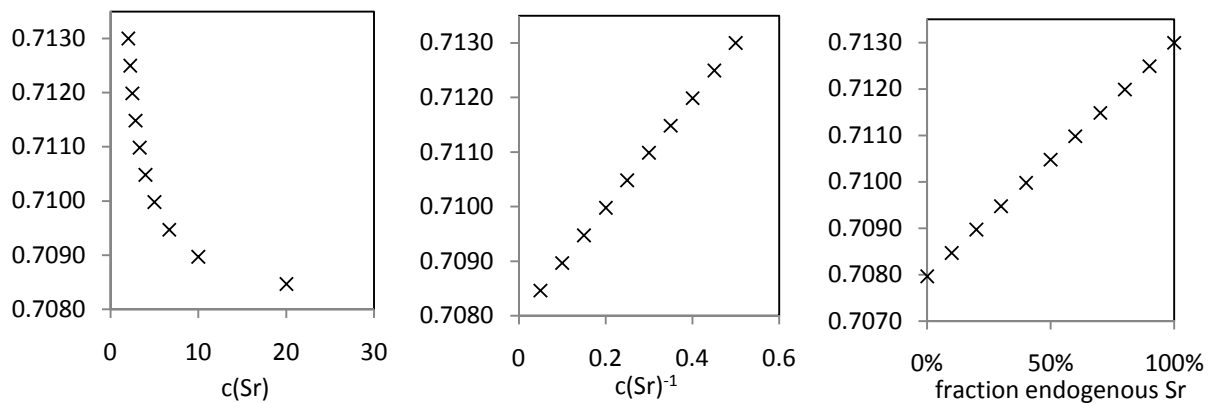
Fig. 37 Theoretical mixing lines for a hypothetical natural Sr isotope ratio

Consequently a plot of measured Sr isotope ratio against the reciprocal Sr concentration gives a linear mixing line, as shown in Fig. 38. The endpoint of this line would represent the natural Sr concentration and therefore the desired isotope ratio. Multiplication of the x-axis values with the natural Sr concentration would result in a chart with the fraction of endogenous Sr from 0-

100% as shown above in Fig. 37 (right chart), out of which the ratio for 100% could easily be read.
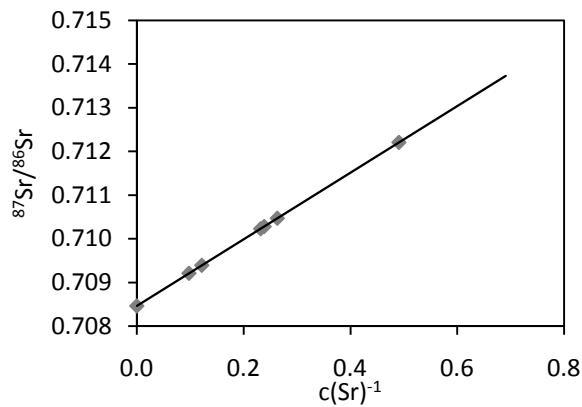
Fig. 38 Mixing line for wood with different contamination content for sample S01

Unfortunately we do not know the percentage of endogenous Sr in our digest of leached wood. Assuming it is 100% renders the mixing lines unnecessary. Cautious assumptions like 'between 0 and 30% remaining contamination' result in ranges of possible natural Sr ratios which are shown in Fig. 39. The lower end of each bar reflects the measured isotope ratio after leaching, corresponding to assumed zero remaining contamination. The upper limit of the range corresponds to an assumed remaining content of 30% diagenetic Sr relative to total Sr. The different widths of ranges for different samples are caused by different slopes of calculated mixing lines. Two determinations of the same sample S01 and S01_II show an overlap in ranges, which suggests, that the possible range for this sample could be reduced to this intersection. Multiple or at least double determination could thus improve the data. It should be noted, that measurement uncertainties as plotted before in Fig. 33 are not shown to ease the display.
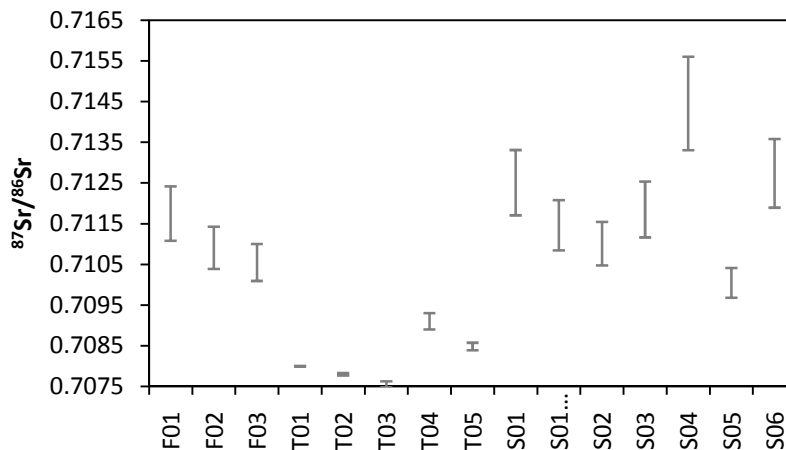
Fig. 39 Ranges of possible natural Sr isotope ratios in prehistoric samples calculated from mixing lines

The above considerations do not take into account known ranges for natural Sr concentration, but rely on assumptions only. Comparing Sr contents of recent wood samples from Hallstatt, which were not leached, to decontaminated prehistoric samples reveals, that the contents of the latter are often lower. Consequently, an assessment of the non-leachable Sr fraction in recent wood is suggested.

Another option to extract the estimated natural isotope ratio using the present data is an estimation of the non-leachable Sr fraction from comparison of leached prehistoric samples of the same species. The lowest remaining Sr concentration of each species was taken as the baseline, with remaining cautiously estimated 0-10% contamination. The other samples of the same species were expressed relative to the 90% natural Sr value and the other limit was chosen 100% (on the safe side because of possible variations in concentration). The following isotope ratio ranges result from these considerations (Fig. 40). An exception was made for the illumination chip samples F01-F03, which were not compared to fir timber sample T03, but only internally. The lower end of each bar represents the measured isotope ratio.
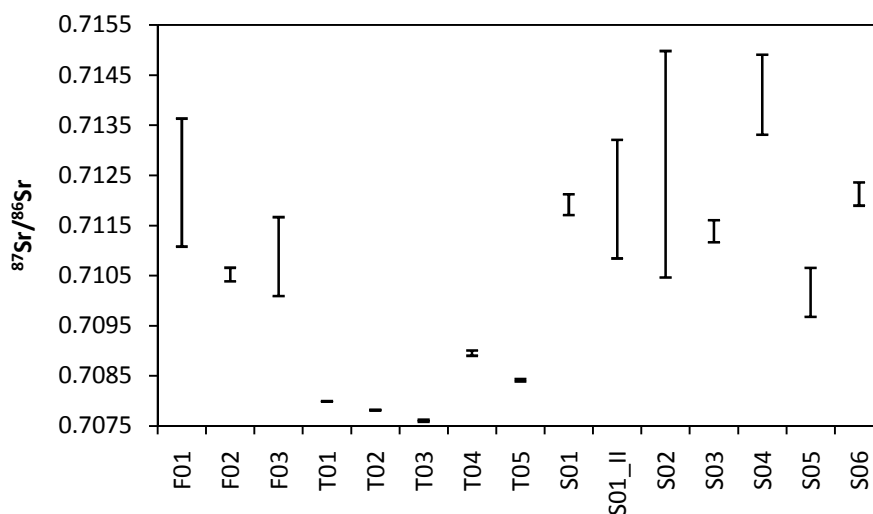
Fig. 40 Calculated ranges for natural Sr ratios from Sr concentration comparison between prehistoric samples

Another option is taking into account the known ranges for Sr concentrations from modern Hallstatt trees. The approach was as follows: the Sr isotope ratio and concentration of the original sample before leaching was calculated from the measured digest and leaching solutions. The resulting concentration was then compared to the value of the same wood species (except for oak, which was compared to beech) and the relative natural Sr content was calculated. The ratio obtained by weighted addition was then plotted against the relative

natural Sr concentration. The ratio of the surrounding material was charted at zero relative natural Sr and a mixing lined can be drawn. Fig. 41 shows this approach on the example of sample S01, for which the isotope ratios of the leaching solutions were measured. The horizontal error bars are calculated from the RSD of the natural beech Sr concentration from ten samples. The vertical error bars relate to the measurement of Sr isotope ratio, but neglecting the Sr concentration uncertainties which also contribute to the calculated value. The measurement of this value instead of its calculation is suggested to achieve this precision. The intersections of the grey lines with the right border of the chart area (corresponding to 100% natural strontium) describe the resulting possible natural Sr isotope ratio range.
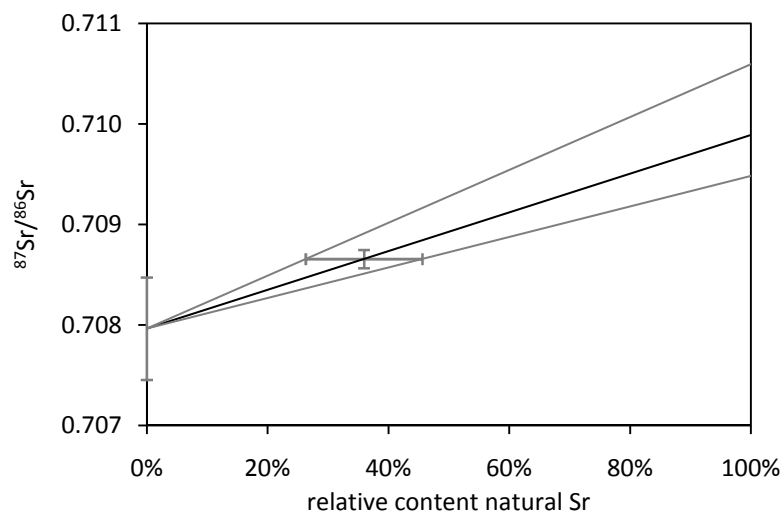
Fig. 41 Extraction of the natural Sr ratio for sample S01 using modern wood Sr concentration as reference value

Accordingly, calculations were carried out for all prehistoric samples. Results are shown in Fig. 42.
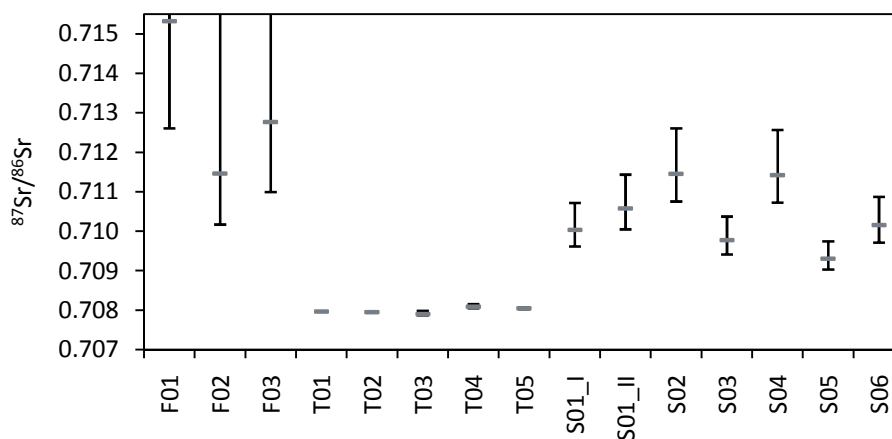
Fig. 42 Calculated natural Sr isotope ratios of all prehistoric samples using modern wood reference Sr concentrations

A few limitations of these calculation trials are obvious. In the latter attempt, timber samples showed relative contents of natural Sr up to 98%, which can hardly be true. Thus, an assessment of the non-leachable fraction of natural Sr is of crucial importance for more reliable estimations. In general, variations between natural Sr content are quite large; RSDs for 10 modern samples were between 25 and 58% which causes the wide ranges observable above. Fir samples F01-F03 showed high remaining Sr concentration maybe due to incomplete decontamination, while modern fir had the lowest Sr content of the three tree species. The measured ratios did not suggest contamination, however. These samples require further experimental examination.

The latter isotope ratio extraction method is based on two assumptions, which should be verified before adopting the obtained values. Oak samples could not be compared to modern oak as none is growing in Hallstatt. Therefore, the equivalency of concentration ranges for oak and beech needs to be tested. Furthermore, only the leaching solutions of samples T01 and S01 were analysed for their Sr isotope ratios. Ratios in the range of the surrounding material were found and assumed for all other prehistoric samples. This should be verified for more samples, e.g. fir illumination chips.

IV Summary and Outlook

IV.1 Achievements

The main goal of this study was to assess the applicability of geochemical tracing methods (i.e. isotopic and elemental fingerprinting) to samples stored in a salt mine environment for 3000 years. After full penetration of contaminating salts was detected (which was expectable), it involved two main problems: (1) It had to be clarified, if the natural signatures had survived or full exchange against diagenetic ions had taken place. If this prerequisite was fulfilled, (2) a way towards removal of secondary salts masking this signal had to be found.

A leaching procedure was developed and surveyed using multi-element analyses via laser ablation and liquid analysis of leaching solutions and of wood after microwave digestion. Quantitative determination using laser ablation is challenging, but order of magnitude estimates could be obtained by a simple one-point-calibration approach applying a reference material with a matrix similar to wood. Laser ablation represents a good screening tool, allowing repeated measurements on virtually the same material. This advantage was utilised in a spike experiment, too. It was carried out in order to test and hopefully confirm the applicability of the approach with regard to possible separation of natural and secondary strontium in principle and the capability of the developed leaching procedure to achieve this goal. The interpretation of the obtained data is not trivial, as soaking in a spike solution results in spiking and simultaneous leaching processes. Secondary cations could be removed to a large extent by the developed leaching procedure, yet not quantitatively. The behaviour of the natural strontium seemed unaffected by the presence of contaminating ^{84}Sr in the solution, though.

The first question stated above could not be answered until strontium isotope ratio measurement of leaching solutions, digests of residual wood and Heidengebirge extracts had been carried out. The obtained data revealed differences between leached and remaining strontium, so full exchange and homogenisation can be excluded. The first prerequisite for the application of isotopic provenancing could thus be confirmed. The remaining problem was, whether full quantitative removal of diagenetic strontium could be achieved. A mixing theory

approach was applied, which allows the reconstruction of a range for the possible natural isotope ratio. Some parameters are still unknown, however, hindering the reliable extraction of the distinct signature of the original tree.

Furthermore, the determination of origin requires reference values for possible regions of provenance. Obviously, the first step towards identification of sources is defining the local signal and attempting to differentiate between local and non-local origin of samples. First steps towards establishing a small-range local strontium map for the immediate surroundings of the mine in the Hallstatt hanging valley were accomplished. The local geological diversity as well as different tree species were taken into account. In comparison to material from inside the mine, which surrounded the prehistoric samples during storage, modern trees growing in the proximity of the mine exhibited a wider range of strontium ratios, which were shifted to higher values. Isotope ratios between 0.709 and 0.711 dominate the distribution, but the number of samples did not appear sufficiently large to reliably represent the total local range.

Multi-element patterns, with special consideration of rare earth elements, were also taken into account as possible tracing fingerprints. Rare earth element measurement presented a challenge in modern wood, though, due to low contents. Chemometric evaluation using discriminant analysis indicates a certain potential to differentiate between bedrocks and consequently origins. The application to prehistoric samples is challenged by non-stoichometric removal in case of multi-element content. In contrast to different isotopes of an element different elements show variable chemical behaviour such as solubility in water or acid, or affinity to wood. Rare earth elements stand out due to their very similar chemistry, but they are characterised by low water solubility and high affinity to lignocellulosic material. Consequently the developed leaching procedure was not suitable for these elements and requires adaptation, e.g. by using chelating agents.

IV.2 Open and newly emerged questions

The influence of storage conditions inside the mine were only considered by simulating elements with high mobility. The ion exchange properties of wood may enhance the accumulation of elements with low water solubility and consequently mobility, however. An adopted leaching procedure or full quantitative analysis after digestion may provide further

insights into composition, maybe also regarding strontium isotope ratios because fractions of Sr might be incorporated into hardly soluble minerals such as silicates, which are not accessible by mild ammonium nitrate extraction. This would result in better understanding of diagenetic processes during storage.

Furthermore, the decontamination method regarding strontium requires confirmation. The quantitative removal of secondary strontium has to be guaranteed, or at least the degree of remaining contamination needs to be assessed quantitatively, which would allow the calculation of the natural isotope ratio via mixing equations. Reproducibility is an important parameter in this context, which needs to be tested.

Another residual question mark concerns the geochemical signatures of possible other regions of origin. Strontium isotope ratio measurements of modern wood samples from these regions will show, if distinct signatures can be defined and consequently if they are distinguishable between sites. Geological diversity is high in the Northern Calcareous Alps, even on a small scale. In case of unsatisfying inter-site variability, the combination with other methods, such as REE fingerprints, may enhance discrimination power.

IV.3 Prospect

The first major task of a continued effort towards provenancing of prehistoric wood will be the proof of principle with regard to decontamination prior to Sr isotope ratio measurement. The reproducibility of the leaching procedure needs to be investigated and guaranteed. An assessment of non-leachable natural strontium content will enable the application of a mixing theory. Furthermore, these mixing lines should be confirmed by determination of more points on the line and an approach towards exhaustive leaching, while residual Sr isotope ratios are surveyed. While decreasing concentrations during removal of contamination are accompanied by a strong increase in isotope ratios (in case the diagenetic ratio is lower than the natural ratio), the residual strontium should exhibit a constant ratio, after all secondary material has been removed.

Furthermore, an optimized spike experiment based on thorough investigation of storage conditions and according simulation, especially with regard to elemental composition, may

provide further insight into incorporation and decontamination mechanisms and support the objected proof of principle.

Another important step is the mapping of strontium isotope signatures for the possible trading area in prehistoric times. Basically the Alpine region around Hallstatt as well as the lowlands to the North and to the South are of interest. A defined number of potential origins needs to be selected taking into account geological conditions and tree growth areas for the species of interest. A sufficient number of samples shall be taken in these regions and the Sr isotope ratios will be determined applying established methods.

Development in the analytical chemical context should involve reduction of required sample amount, especially on behalf of the uniqueness and consequently value of archaeological findings. Sample introduction via laser ablation presents a promising tool for this requirement. Small splinters of wood could be ablated after decontamination and returned, virtually not destroyed. The technique presents a few obstacles, however. Reference material with known isotopic composition is required, but not available so far. It has to be produced in-house, e.g. by spiking an exhaustively leached wood with a solution of known isotopic composition. Interferences, especially from Rb, are another obstacle, which requires the development of accurate correction techniques. Additionally, Sr concentration in wood is rather low (low µg/g range) and ratios may thus be difficult to measure using the standard multi-collector arrangement. Instead of Faraday cups, ion counters may be required presenting additional method development tasks.

If these challenges can be mastered, the door will be open for expansion to other sample material found in the mine, such as fur, animal skin or ropes. These finds are present in much smaller amounts and require again method development or adaptation, especially concerning decontamination strategies.

Furthermore, the range of methods in order to fulfil the task of provenancing can be expanded from strontium isotope ratios not only maybe towards REE patterns, but also to different scientific methods covering other than geochemical processes. Light stable isotopes are one obvious option, as well as dendrological investigations. The combination of independent methods can provide valuable clues to the answers archaeologists seek. This pilot study was consequently one first step toward the integration of analytical inorganic chemistry in an

interdisciplinary approach in order to decipher the unique information source of organic findings preserved in a salt mine for 3000 years. Eventually, this approach shall deliver insights into economic and social structures in prehistoric times.

V   Literature

Åberg G., BIOGEOMON, International Symposium on Ecosystem Behavior and the Evaluation of Integrated Monitoring of Small Catchments, Prague, Czech Republic, 1993.

Aggarwal J., Habicht-Mauche J. and Juarez C.: Application of heavy stable isotopes in forensic isotope geochemistry: A review. *Applied Geochemistry*, 2008, **23**, 2658-2666.

Albarede F., Telouk P., Blichert-Toft J., Boyet M., Agranier A. and Nelson B.: Precise and accurate isotopic measurements using multiple-collector ICPMS. *Geochimica Et Cosmochimica Acta*, 2004, **68**, 2725-2744.

Balcaen L., Schrijver I. D., Moens L. and Vanhaecke F.: Determination of the 87Sr/86Sr isotope ratio in USGS silicate reference materials by multi-collector ICP-mass spectrometry. *International Journal of Mass Spectrometry*, 2005, **242**, 251-255.

Balter V., Telouk P., Reynard B., Braga J., Thackeray F. and Albarede F.: Analysis of coupled Sr/Ca and Sr-87/Sr-86 variations in enamel using laser-ablation tandem quadrupole-multicollector ICPMS. *Geochimica Et Cosmochimica Acta*, 2008, **72**, 3980-3990.

Barrelet T., Ulrich A., Rennenberg H. and Krahenbuhl U.: Seasonal profiles of sulphur, phosphorus, and potassium in Norway spruce wood. *Plant Biology*, 2006, **8**, 462-469.

Barrelet T., Ulrich A., Rennenberg H., Zwicky C. N. and Krahenbuhl U.: Assessing the suitability of Norway spruce wood as an environmental archive for sulphur. *Environmental Pollution*, 2008, **156**, 1007-1014.

Barth F. E.: The uniqueness of Hallstatt, in: *Kingdom of Salt - 7000 years of Hallstatt*, eds. Kern A., Kowarik K., Rausch A. W. and Reschreiter H., Natural History Museum, Vienna, 2009.

Bea F., Montero P., Stroh A. and Baasner J.: Microanalysis of minerals by an Excimer UV-LA-ICP-MS system. *Chemical Geology*, 1996, **133**, 145-156.

Benson L., Cordell L., Vincent K., Taylor H., Stein J., Farmer G. L. and Futa K.: Ancient maize from Chacoan great houses: Where was it grown? *Proceedings of the National Academy of Sciences of the United States of America*, 2003, **100**, 13111-13115.

Benson L. V., Hattori E. M., Taylor H. E., Poulson S. R. and Jolie E. A.: Isotope sourcing of prehistoric willow and tule textiles recovered from western Great Basin rock shelters and caves - proof of concept. *Journal of Archaeological Science*, 2006, **33**, 1588-1599.

Benson L. V., Taylor H. E., Peterson K. A., Shattuck B. D., Ramotnik C. A. and Stein J. R.: Development and evaluation of geochemical methods for the sourcing of archaeological maize. *Journal of Archaeological Science*, 2008, **35**, 912-921.

Benson L. V., Taylor H. E., Plowman T. I., Roth D. A. and Antweiler R. C.: The cleaning of burned and contaminated archaeological maize prior to 87Sr/86Sr analysis. *Journal of Archaeological Science*, 2010, **37**, 84-91.

Bentley R. A.: Strontium isotopes from the earth to the archaeological skeleton: A review. *Journal of Archaeological Method and Theory*, 2006, **13**, 135-187.

Berger T. W., Swoboda S., Prohaska T. and Glatzel G.: The role of calcium uptake from deep soils for spruce (Picea abies) and beech (Fagus sylvatica). *Forest Ecology and Management*, 2006, **229**, 234-246.

Bernabei M., Bontadi J. and Rognoni G. R.: A dendrochronological investigation of stringed instruments from the collection of the Cherubini Conservatory in Florence, Italy. *Journal of Archaeological Science*, 2010, **37**, 192-200.

Boulyga S. F. and Heumann K. G.: Direct determination of halogens in powdered geological and environmental samples using isotope dilution laser ablation ICP-MS. *International Journal of Mass Spectrometry*, 2005, **242**, 291-296.

Brunner M., Eugster R., Trenka E. and BerganminStrotz L.: FT-NIR spectroscopy and wood identification. *Holzforschung*, 1996, **50**, 130-134.

Burnett A., Kurtz A. C., Brabander D. and Shailer M.: Dendrochemical record of historical lead contamination sources, wells G&H superfund site, Woburn, Massachusetts. *Journal of Environmental Quality*, 2007, **36**, 1488-1494.

Capo R. C., Stewart B. W. and Chadwick O. A.: Strontium isotopes as tracers of ecosystem processes: theory and methods. *Geoderma*, 1998, **82**, 197-225.

Chan G. C. Y., Chan W.-T., Mao X. and Russo R. E.: Investigation of matrix effects in inductively coupled plasma-atomic emission spectroscopy using laser ablation and solution nebulization -- effect of second ionization potential. *Spectrochimica Acta Part B: Atomic Spectroscopy*, 2001, **56**, 77-92.

Deguilloux M. F., Pemonge M. H., Bertel L., Kremer A. and Petit R. J.: Checking the geographical origin of oak wood: molecular and statistical tools. *Molecular Ecology*, 2003, **12**, 1629-1636.

Delmdahl R. and von Oldershausen G.: Quantitative solid sample analysis by ArF excimer laser ablation. *Journal of Molecular Structure*, 2005, **744-747**, 255-258.

Djingova R., Ivanova J., Wagner G., Korhammer S. and Markert B.: Distribution of lanthanoids, Be, Bi, Ga, Te, Tl, Th and U on the territory of Bulgaria using Populus nigra 'Italica' as an indicator. *The Science of The Total Environment*, 2001, **280**, 85-91.

Durand S. R., Shelley P. H., Antweiler R. C. and Taylor H. E.: Trees, chemistry, and prehistory in the American Southwest. *Journal of Archaeological Science*, 1999, **26**, 185-203.

Ehleringer J. R., Casale J. F., Lott M. J. and Ford V. L.: Tracing the geographical origin of cocaine: Cocaine carries a chemical fingerprint from the region where the coca was grown. *Nature*, 2000, **408**, 311-312.

Ehret D.: *Geotechnische Untersuchungen und GIS-gestützte Erfassung der Massenbewegungen zwischen Hallstatt und Plassen (UNESCO-Welterberegion Hallstatt-Dachstein, Österreich)*, Diploma Thesis (unpublished), Universität (TH) Karlsruhe, 2002.

Ehret D.: The great catastrophe, in: *Kingdom of Salt - 7000 years of Hallstatt*, eds. Kern A., Kowarik K., Rausch A. W. and Reschreiter H., Natural History Museum, Vienna, 2009.

English N. B., Betancourt J. L., Dean J. S. and Quade J.: Strontium isotopes reveal distant sources of architectural timber in Chaco Canyon, New Mexico. *Proceedings of the National Academy of Sciences of the United States of America*, 2001, **98**, 11891-11896.

EURACHEM, *The Fitness for Purpose of Analytical Methods*: *A Laboratory Guide to Method Validation and Related Topics*, LGC (Teddington) Ltd, 1998.

Feldmann J., Kindness A. and Ek P.: Laser ablation of soft tissue using a cryogenically cooled ablation cell. *Journal of Analytical Atomic Spectrometry*, 2002, **17**, 813-818.

Fengel D. and Wegener G., *Wood. Chemistry, Ultrastructure, Reactions*, Walter de Gruyter, Berlin, New York, 1989.

Finkeldey R., Leinemann L. and Gailing O.: Molecular genetic tools to infer the origin of forest plants and wood. *Applied Microbiology and Biotechnology*, **85**, 1251-1258.

Frei K. M., Frei R., Mannering U., Gleba M., Nosch M. L. and Lyngstrom H.: Provenance of Ancient Textiles-a Pilot Study Evaluating the Strontium Isotope System in Wool. *Archaeometry*, 2009a, **51**, 252-276.

Frei K. M., Skals I., Gleba M. and Lyngstrom H.: The Huldremose Iron Age textiles, Denmark: an attempt to define their provenance applying the strontium isotope system. *Journal of Archaeological Science*, 2009b, **36**, 1965-1971.

Freydier R., Candaudap F., Poitrasson F., Arbouet A., Chatel B. and Dupre B.: Evaluation of infrared femtosecond laser ablation for the analysis of geomaterials by ICP-MS. *Journal of Analytical Atomic Spectrometry*, 2008, **23**, 702-710.

Fu F., Akagi T., Yabuki S. and Iwaki M.: The variation of REE (rare earth elements) patterns in soil-grown plants: A new proxy for the source of rare earth elements and silicon in plants. *Plant and Soil*, 2001, **235**, 53-64.

Grabner M., Klein A., Geihofer D., Reschreiter H., Barth F. E., Sormaz T. and Wimmer R.: Bronze age dating of timber from the salt-mine at Hallstatt, Austria. *Dendrochronologia*, 2007, **24**, 61-68.

Greenwood N. N. and Earnshaw A., *Chemie der Elemente*, VCH Verlagsgesellschaft mbH, Weinheim, Germany, 1990.

Guillong M., Horn I. and Günther D.: A comparison of 266 nm, 213 nm and 193 nm produced from a single solid state Nd : YAG laser for laser ablation ICP-MS. *Journal of Analytical Atomic Spectrometry*, 2003, **18**, 1224-1230.

Haneca K., Katarina C. and Beeckman H.: Oaks, tree-rings and wooden cultural heritage: a review of the main characteristics and applications of oak dendrochronology in Europe. *Journal of Archaeological Science*, 2009, **36**, 1-11.

Haneca K., Wazny T., Van Acker J. and Beeckman H.: Provenancing Baltic timber from art historical objects: success and limitations. *Journal of Archaeological Science*, 2005, **32**, 261-271.

Heier A., Evans J. A. and Montgomery J.: The potential of carbonized grain to preserve biogenic [87]SR/[86]Sr signatures within the burial environment. *Archaeometry*, 2009, **51**, 277-291.

Henrion R. and Henrion G., *Multivariate Datenanalyse*, Springer Verlag, Berlin, Heidelberg, New York, London, Paris, Tokyo, Hong Kong, Barcelona, Budapest, 1995.

Heumann K. G., Gallus S. M., Radlinger G. and Vogl J.: Precision and accuracy in isotope ratio measurements by plasma source mass spectrometry. *Journal of Analytical Atomic Spectrometry*, 1998, **13**, 1001-1008.

Hoffmann E., Ludke C. and Scholze H.: Is laser-ablation-ICP-MS an alternative to solution analysis of solid samples? *Fresenius Journal of Analytical Chemistry*, 1997, **359**, 394-398.

Horacek M., Jakusch M. and Krehan H.: Control of origin of larch wood: discrimination between European (Austrian) and Siberian origin by stable isotope analysis. *Rapid Communications in Mass Spectrometry*, 2009, **23**, 3688-3692.

Horn I., Rudnick R. L. and McDonough W. F.: Precise elemental and isotope ratio determination by simultaneous solution nebulization and laser ablation-ICP-MS: application to U-Pb geochronology. *Chemical Geology*, 2000, **164**, 281-301.

Horstwood M. S. A.: Magnetic sector field instruments - Multi-collector devices, in: *Inductively Coupled Plasma Mass Spectrometry Handbook*, ed. Nelms S., Blackwell Publishing Ltd, Oxford, UK, 2005.

IUPAC, *Nomenclature of Inorganic Chemistry*: *IUPAC Recommendations 2005 (Red Book)*, RSC Publishing, Cambridge, UK, 2005.

Ivanova J., Korhammer S., Djingova R., Heidenreich H. and Markert B.: Determination of lanthanoids and some heavy and toxic elements in plant certified reference materials by inductively coupled plasma mass spectrometry. *Spectrochimica Acta Part B: Atomic Spectroscopy*, 2001, **56**, 3-12.

Jochum K. P., Stoll B., Weis U., Kuzmin D. V. and Sobolev A. V.: In situ Sr isotopic analysis of low Sr silicates using LA-ICP-MS. *Journal of Analytical Atomic Spectrometry*, 2009, **24**, 1237-1243.

Joosten I., van Bommel M. R., Keijzer R. H. D. and Reschreiter H.: Micro analysis on Hallstatt textiles: Colour and condition. *Microchimica Acta*, 2006, **155**, 169-174.

Keppler F. and Hamilton J.: Tracing the geographical origin of early potato tubers using stable hydrogen isotope ratios of methoxyl groups. *Isotopes in environmental and health studies*, 2008, **44**, 337-347.

Kerstel E. and Gianfrani L.: Advances in laser-based isotope ratio measurements: selected applications. *Applied Physics B-Lasers and Optics*, 2008, **92**, 439-449.

Klein A.: *Bronzezeitliche Holznutzung in Hallstatt (unpublished)*, Diploma Thesis, University of Natural Resources and Applied Life Sciences, 2006.

Koch J., Feldmann I., Hattendorf B., Günther D., Engel U., Jakubowski N., Bolshov M., Niemax K. and Hergenröder R.: Trace element analysis of synthetic mono- and poly-crystalline CaF2 by ultraviolet laser ablation inductively coupled plasma mass spectrometry at 266 and 193 nm. *Spectrochimica Acta Part B: Atomic Spectroscopy*, 2002, **57**, 1057-1070.

Komarek M., Ettler V., Chrastny V. and Mihaljevic M.: Lead isotopes in environmental sciences: A review. *Environment International*, 2008, **34**, 562-577.

Kowarik K.: Aus nah und fern. Gedanken zu den Versorgungsstrukturen des bronzezeitlichen Salzbergbaus in Hallstatt. *Mitteilungen der Anthropologischen Gesellschaft in Wien*, 2009, **139**, 105-113.

Krachler M., Mohl C., Emons H. and Shotyk W.: Two thousand years of atmospheric rare earth element (REE) deposition as revealed by an ombrotrophic peat bog profile, Jura Mountains, Switzerland. *Journal of Environmental Monitoring*, 2003, **5**, 111-121.

Kratzert M., 2000: http://www.chemie.fu-berlin.de/chemistry/kunststoffe/bilder/cellulose.gif, Didaktik der Chemie, FU Berlin, access date: 2010-03-30.

Kylander M. E., Weiss D. J., Jeffries T. E., Kober B., Dolgopolova A., Garcia-Sanchez R. and Coles B. J.: A rapid and reliable method for Pb isotopic analysis of peat and lichens by laser ablation-quadrupole-inductively coupled plasma-mass spectrometry for biomonitoring and sample screening. *Analytica Chimica Acta*, 2007, **582**, 116-124.

Lee-Thorp J. A.: On isotopes and old bones. *Archaeometry*, 2008, **50**, 925-950.

Lee Y.-L., Chang C.-C. and Jiang S.-J.: Laser ablation inductively coupled plasma mass spectrometry for the determination of trace elements in soil. *Spectrochimica Acta Part B: Atomic Spectroscopy*, 2003, **58**, 523-530.

Liang T., Ding S., Song W., Chong Z., Zhang C. and Li H.: A review of fractionations of rare earth elements in plants. *Journal of Rare Earths*, 2008, **26**, 7-15.

Loader N. J., Santillo P. M., Woodman-Ralph J. P., Rolfe J. E., Hall M. A., Gagen M., Robertson I., Wilson R., Froyd C. A. and McCarroll D.: Multiple stable isotopes from oak trees in southwestern Scotland and the potential for stable isotope dendroclimatology in maritime climatic regions. *Chemical Geology*, 2008, **252**, 62-71.

Martínez del Rio C., Wolf N., Carleton S. A. and Gannes L. Z.: Isotopic ecology ten years after a call for more laboratory experiments. *Biological Reviews*, 2009, **84**, 91-111.

McDonough W. F. and Sun S. s.: The composition of the Earth. *Chemical Geology*, 1995, **120**, 223-253.

Meija J., Yang L., Sturgeon R. and Mester Z. n.: Mass Bias Fractionation Laws for Multi-Collector ICPMS: Assumptions and Their Experimental Verification. *Analytical Chemistry*, 2009, **81**, 6774-6778.

Monticelli D., Di Iorio A., Ciceri E., Castelletti A. and Dossi C.: Tree ring microanalysis by LA-ICP-MS for environmental monitoring: validation or refutation? Two case histories. *Microchimica Acta*, 2009, **164**, 139-148.

Müller W.: Strengthening the link between geochronology, textures and petrology. *Earth and Planetary Science Letters*, 2003, **206**, 237-251.

Myburg A. A. and Sederoff R. R.: Xylem Structure and Function in: *ENCYCLOPEDIA OF LIFE SCIENCES,* 2001, John Wiley & Sons, Ltd., www.els.net.

N.N., 2009: http://en.wikipedia.org/wiki/File:Xylan.svg, access date: 2010-03-31.

Nakatsuka T., Ohnishi K., Hara T., Sumida A., Mitsuishi D., Kurita N. and Uemura S.: Oxygen and carbon isotopic ratios of tree-ring cellulose in a conifer-hardwood mixed forest in northern Japan. *Geochemical Journal*, 2004, **38**, 77-88.

New Wave Research: *UP 193 Solid State Laser Operator's Manual*, New Wave Research, Inc, Fremont, USA, 2005.

Niu H. and Houk R. S.: Fundamental aspects of ion extraction in inductively coupled plasma mass spectrometry. *Spectrochimica Acta Part B-Atomic Spectroscopy*, 1996, **51**, 779-815.

Nu Instruments: *Nu Plasma Manual*, Nu Instruments Ltd., Wrexham, UK, 2007.

Pearson C., Manning S. W., Coleman M. and Jarvis K.: Can tree-ring chemistry reveal absolute dates for past volcanic eruptions? *Journal of Archaeological Science*, 2005, **32**, 1265-1274.

Pearson C. L., Dale D. S., Brewer P. W., Kuniholm P. I., Lipton J. and Manning S. W.: Dendrochemical analysis of a tree-ring growth anomaly associated with the Late Bronze Age eruption of Thera. *Journal of Archaeological Science*, 2009, **36**, 1206-1214.

Pickhardt C. and Becker J. S.: Trace analysis of high-purity graphite by LA–ICP–MS. *Fresenius' Journal of Analytical Chemistry*, 2001, **370**, 534-540.

Pickhardt C., Dietze H.-J. and Becker J. S.: Laser ablation inductively coupled plasma mass spectrometry for direct isotope ratio measurements on solid samples. *International Journal of Mass Spectrometry*, 2005, **242**, 273-280.

Pisonero J., Fernandez B. and Gunther D.: Critical revision of GD-MS, LA-ICP-MS and SIMS as inorganic mass spectrometric techniques for direct solid analysis. *Journal of Analytical Atomic Spectrometry*, 2009, **24**, 1145-1160.

Poszwa A., Ferry B., Dambrine E., Pollier B., Wickman T., Loubet M. and Bishop K.: Variations of bioavailable Sr concentration and Sr-87/Sr-86 ratio in boreal forest ecosystems - Role of biocycling, mineral weathering and depth of root uptake. *Biogeochemistry*, 2004, **67**, 1-20.

Prohaska T.: Magnetic sector field instruments - Single collector instruments, in: *Inductively Coupled Plasma Mass Spectrometry Handbook*, ed. Nelms S., Blackwell Publishing Ltd, Oxford, UK, 2005.

Prohaska T., Latkoczy C., Schultheis G., Teschler-Nicola M. and Stingeder G.: Investigation of Sr isotope ratios in prehistoric human bones and teeth using laser ablation ICP-MS and ICP-MS after Rb/Sr separation. *Journal of Analytical Atomic Spectrometry*, 2002, **17**, 887-891.

Prohaska T., Stadlbauer C., Wimmer R., Stingeder G., Latkoczy C., Hoffmann E. and Stephanowitz H.: Investigation of element variability in tree rings of young Norway spruce by laser-ablation-ICPMS. *Science of the Total Environment*, 1998, **219**, 29-39.

Prohaska T., Wenzel W. W. and Stingeder G.: ICP-MS-based tracing of metal sources and mobility in a soil depth profile via the isotopic variation of Sr and Pb. *International Journal of Mass Spectrometry*, 2005, **242**, 243-250.

Rana R., Mueller G., Naumann A. and Polle A.: FTIR spectroscopy in combination with principal component analysis or cluster analysis as a tool to distinguish beech (Fagus sylvatica L.) trees grown at different sites. *Holzforschung*, 2008, **62**, 530-538.

Rehkämper M., Schönbächler M. and Stirling C. H.: Multiple Collector ICP-MS: Introduction to Instrumentation, Measurement Techniques and Analytical Capabilities. *Geostandards and Geoanalytical Research*, 2001, **25**, 23-40.

Resano M., Garcia-Ruiz E. and Vanhaecke F.: Laser ablation-inductively coupled plasma mass spectrometry in archaeometric research. *Mass Spectrometry Reviews*, 2010, **29**, 55-78.

Reschreiter H. and Kowarik K.: A different kind of archaeology, in: *Kingdom of Salt - 7000 years of Hallstatt*, eds. Kern A., Kowarik K., Rausch A. W. and Reschreiter H., Natural History Museum, Vienna, 2009a.

Reschreiter H. and Kowarik K.: A start of salt-mining, in: *Kingdom of Salt - 7000 years of Hallstatt*, eds. Kern A., Kowarik K., Rausch A. W. and Reschreiter H., Natural History Museum, Vienna, 2009b.

Reschreiter H., Kowarik K. and Pany D.: The Hallstatt culture: the golden age, in: *Kingdom of Salt - 7000 years of Hallstatt*, eds. Kern A., Kowarik K., Rausch A. W. and Reschreiter H., Natural History Museum, Vienna, 2009.

Reynolds A. C., Betancourt J. L., Quade J., Jonathan Patchett P., Dean J. S. and Stein J.: 87Sr/86Sr sourcing of ponderosa pine used in Anasazi great house construction at Chaco Canyon, New Mexico. *Journal of Archaeological Science*, 2005, **32**, 1061-1075.

Rohn J., Ehret D., Moser M. and Czurda K.: Prehistoric and recent mass movements of the World Cultural Heritage Site Hallstatt, Austria. *Environmental Geology*, 2005, **47**, 702-714.

Rom W., Golser R., Kutschera W., Priller A., Steier P. and Wild E. M.: AMS C-14 dating of equipment from the Iceman and of spruce logs from the prehistoric salt mines of Hallstatt. *Radiocarbon*, 1999, **41**, 183-197.

Romagnoli M., Sarlatto M., Terranova F., Bizzarri E. and Cesetti S.: Wood identification in the Cappella Palatina ceiling (12th century) in Palermo (Sicily, Italy). *Iawa Journal*, 2007, **28**, 109-123.

Rosman K. J. R. and Taylor P. D. P.: Isotopic compositions of the elements 1997. *Pure and Applied Chemistry*, 1998, **70**, 217-235.

Russo R. E., Mao X., Liu H., Gonzalez J. and Mao S. S.: Laser ablation in analytical chemistry--a review. *Talanta*, 2002, **57**, 425-451.

Schultheis G., Prohaska T., Stingeder G., Dietrich K., Jembrih-Simburger D. and Schreiner M.: Characterisation of ancient and art nouveau glass samples by Pb isotopic analysis using laser ablation coupled to a magnetic sector field inductively coupled plasma mass spectrometer (LA-ICP-SF-MS). *Journal of Analytical Atomic Spectrometry*, 2004, **19**, 838-843.

Seelmann-Eggebert W., Pfennig G., Münzel H. and Klewe-Nebenius H.: *Karlsruher Nuklidkarte*, Kernforschungszentrum Karlsruhe GmbH, 1981.

Sjöström E., *Wood Chemistry. Fundamentals and Applications*, Academic Press, Inc., 1981.

Spalla S., Baffi C., Barbante C., Turretta C., Cozzi G., Beone G. M. and Bettinelli M.: Determination of rare earth elements in tomato plants by inductively coupled plasma mass spectrometry techniques. *Rapid Communications in Mass Spectrometry*, 2009, **23**, 3285-3292.

Spötl C. and Pak E.: A strontium and sulfur isotopic study of Permo-Triassic evaporites in the Northern Calcareous Alps, Austria. *Chemical Geology*, 1996, **131**, 219-234.

Steen C., 2010: http://www.uni-duesseldorf.de/MathNat/Biologie/Didaktik/Holz/bilder_f/molek/lig_2.gif, access date: 2010-03-30.

Steiger R. H. and Jäger E.: Subcommission on geochronology: Convention on the use of decay constants in geo- and cosmochronology. *Earth and Planetary Science Letters*, 1977, **36**, 359-362.

Steinhoefel G., Horn I. and von Blanckenburg F.: Matrix-independent Fe isotope ratio determination in silicates using UV femtosecond laser ablation. *Chemical Geology*, 2009, **268**, 67-73.

Stern B., Clelland S. J., Nordby C. C. and Urem-Kotsou D.: Bulk stable light isotopic ratios in archaeological birch bark tars. *Applied Geochemistry*, 2006, **21**, 1668-1673.

Stewart B. W., Capo R. C. and Chadwick O. A.: Quantitative strontium isotope models for weathering, pedogenesis and biogeochemical cycling. *Geoderma*, 1998, **82**, 173-195.

Sulzman E. W.: Stable isotope chemistry and measurement: a primer, in: *Stable Isotopes in Ecology and Environmental Science*, eds. R M. and K L., Blackwell Publishing, 2007.

Swoboda S.: *Elemental and Isotopic Fingerprinting by (LA)-ICP-MS (Laser Ablation Inductively Coupled Plasma Mass Spectrometry) – Development and Applications*, PhD-Thesis, University of Natural Resources and Applied Life Sciences, Vienna, 2008.

Swoboda S., Brunner M., Boulyga S. F., Galler P., Horacek M. and Prohaska T.: Identification of Marchfeld asparagus using Sr isotope ratio measurements by MC-ICP-MS. *Analytical and Bioanalytical Chemistry*, 2008, **390**, 487-494.

Sylvester P. J.: LA-(MC)-ICP-MS Trends in 2006 and 2007 with Particular Emphasis on Measurement Uncertainties. *Geostandards and Geoanalytical Research*, 2008, **32**, 469-488.

Telouk P., Rose-Koga E. F. and Albarede F.: Preliminary Results from a New 157 nm Laser Ablation ICP-MS Instrument: New Opportunities in the Analysis of Solid Samples. *Geostandards and Geoanalytical Research*, 2003, **27**, 5-11.

Thomas R.: A Beginner's Guide to ICP-MS - Part II: The sample introduction system. *Spectroscopy*, 2001a, **16**, 56-60.

Thomas R.: A Beginner's Guide to ICP-MS - Part III: The plasma source. *Spectroscopy*, 2001b, **16**, 26-30.

Thomas R.: A Beginner's Guide to ICP-MS - Part IX: Mass analyzers: collision/reaction cell technology. *Spectroscopy*, 2001c, **17**, 42-48.

Thomas R.: A Beginner's Guide to ICP-MS - Part X: Detectors. *Spectroscopy*, 2001d, **17**, 34-39.

Thomas R.: Beginner's guide to ICP-MS - Part XIII - Sampling accessories. *Spectroscopy*, 2002, **17**, 26-33.

Thomas R.: Beginner's guide to ICP-MS - Part XIV - Sampling accessories, Part II. *Spectroscopy*, 2003, **18**, 42-54.

Tnah L. H., Lee S. L., Ng K. K. S., Tani N., Bhassu S. and Othman R. Y.: Geographical traceability of an important tropical timber (Neobalanocarpus heimii) inferred from chloroplast DNA. *Forest Ecology and Management*, 2009, **258**, 1918-1923.

Tyler G.: Rare earth elements in soil and plant systems - A review. *Plant and Soil*, 2004, **267**, 191-206.

Uzunoglu-Obenaus W., Hörweg C., Sattmann H., Picher O., Aspöck H., Popa G., Grömer K., Mautendorfer H., Hofmann-de Keijzer R. and van Bommel M. R.: Transdisciplinary research, in: *Kingdom of Salt - 7000 years*

of Hallstatt, eds. Kern A., Kowarik K., Rausch A. W. and Reschreiter H., Natural History Museum, Vienna, 2009.

Vanhaecke F., Balcaen L. and Malinovsky D.: Use of single-collector and multi-collector ICP-mass spectrometry for isotopic analysis. *Journal of Analytical Atomic Spectrometry*, 2009, **24**, 863-886.

von Carnap-Bornheim C., Nosch M. L., Grupe G., Mekota A. M. and Schweissing M. M.: Stable strontium isotopic ratios from archaeological organic remains from the Thorsberg peat bog. *Rapid Communications in Mass Spectrometry*, 2007, **21**, 1541-1545.

Wanner B., Moor C., Richner P., Bronnimann R. and Magyar B.: Laser ablation inductively coupled plasma mass spectrometry (LA-ICP-MS) for spatially resolved trace element determination of solids using an autofocus system. *Spectrochimica Acta Part B-Atomic Spectroscopy*, 1999, **54**, 289-298.

Ward N. I., Durrant S. F. and Gray A. L.: Analysis of biological standard reference materials by laser ablation inductively coupled plasma mass-spectrometry. *Journal of Analytical Atomic Spectrometry*, 1992, **7**, 1139-1146.

Watling R. J.: Sourcing the provenance of cannabis crops using inter-element association patterns 'fingerprinting' and laser ablation inductively coupled plasma mass spectrometry. *Journal of Analytical Atomic Spectrometry*, 1998, **13**, 917-926.

Watmough S. A., Hutchinson T. C. and Evans R. D.: Application of laser ablation inductively coupled plasma-mass spectrometry in dendrochemical analysis. *Environmental Science & Technology*, 1997, **31**, 114-118.

Wyttenbach A., Furrer V., Schleppi P. and Tobler L.: Rare earth elements in soil and in soil-grown plants. *Plant and Soil*, 1998a, **199**, 267-273.

Wyttenbach A. and Tobler L.: Soil contamination in plant samples and in botanical reference materials: Signature, quantification and consequences. *Journal of Radioanalytical and Nuclear Chemistry*, 2002, **254**, 165-174.

Wyttenbach A., Tobler L., Schleppi P. and Furrer V.: Variation of the rare earth element concentrations in the soil, soil extract and in individual plants from the same site. *Journal of Radioanalytical and Nuclear Chemistry*, 1998b, **231**, 101-106.

Xiao H., Zhang Z., Li F. and Chai Z.: Study on contents and distribution characteristics of REE in fern by NAA. *Nuclear Techniques*, 2003, **26**, 420-424.

Xu X. K., Zhu W. Z., Wang Z. J. and Witkamp G. J.: Accumulation of rare earth elements in maize plants (Zea mays L.) after application of mixtures of rare earth elements and lanthanum. *Plant and Soil*, 2003, **252**, 267-277.

Yang L.: Accurate and precise determination of isotopic ratios by MC-ICP-MS: a review. *Mass Spectrometry Reviews*, 2009, **28**, 990-1011.

Zhong R. and Ye Z.-H.: Secondary Cell Walls in: *ENCYCLOPEDIA OF LIFE SCIENCES,* 2009, John Wiley & Sons, Ltd., www.els.net.

VI Appendix

VI.1 Certificates of Analysis

VI.1.1 TM-28.3

Environment Canada / Environnement Canada
Certified Reference Material
TM-28.3
A trace element fortified calibration standard

NWRI certified reference waters for trace elements are made in filtered and diluted Lake Ontario water and preserved with 0.2% nitric acid. TM-28.3 has concentrations in the low m g/L range and can be used to verify accuracy. The certified values and statistics for this CRM are derived from interlaboratory proficiency testing (PT) studies 85, 87 & 89 dated Dec. '04, Dec. '05 and Dec. '06 respectively. Trace element CRMs are noted for their integrity and consistency, and are monitored in additional PT studies. "For Information" values are given for elements where insufficient data exists for certification or for elements which may have long-term instability. These values are given to help characterize the sample and may be certified as more data becomes available. A more detailed report on the methods used in our PT studies for specific parameters (measurands) is available upon request. Expiry dates are indicated on each individual bottle and are not indicative of sample stability, but rather of sample transport, handling and storage. We strongly recommend that the CRM be tightly capped and refrigerated immediately after use.

Measurand	Value[a] in µg/L	2 σ[b]	C.I.[c]	Studies/Results
Aluminum	81.3	5.57	0.572	3 / 93
Antimony	5.38	0.667	0.0738	3 / 80
Arsenic	6.12	0.848	0.0871	3 / 93
Barium	15.5	1.42	0.141	3 / 101
Beryllium	3.34	0.434	0.0469	3 / 92
Bismuth	2.53	1.10	0.171	3 / 41
Boron	16.4	3.31	0.429	3 / 60
Cadmium	1.91	0.230	0.0226	3 / 108
Chromium	4.83	0.768	0.0745	3 / 104
Cobalt	3.53	0.519	0.0539	3 / 91
Copper	8.15	0.863	0.0872	3 / 96
Iron	16.5	3.71	0.418	3 / 77
Lead	5.97	0.567	0.0602	3 / 87
Lithium	4.12	0.417	0.0678	3 / 44
Manganese	6.90	0.521	0.0529	3 / 95
Molybdenum	3.82	0.463	0.0568	3 / 65
Nickel	9.80	1.16	0.117	3 / 97
Selenium	4.31	0.916	0.106	3 / 73
Silver	3.78	0.436	0.0516	3 / 76
Strontium	69.7	5.53	0.547	3 / 100
Thallium	3.89	0.328	0.0434	3 / 87
Tin	3.83	0.529	0.0771	3 / 47
Titanium	8.10	1.08	0.122	3 / 76
Uranium	6.06	0.455	0.0572	3 / 62
Vanadium	3.07	0.394	0.0444	3 / 77
Zinc	27.5	3.37	0.338	3 / 103

[a] Or in units. Outliers of > 3 standard deviations excluded.
[b] 2-sigma limit for an individual measurement.
[c] 95% Confidence Interval for the population mean (σ ÷ (1.96 √ N)).

For Information:

Rubidium	0.42	24 results

Certificate Date: April 2007, Lot 407

Ing. Hatzl – Beta Analytik
Sportplatzgasse 6
A-2104 Spillern
Austria

Tel.   02266/80872-0
Fax 02266/80872-3
e-mail: beta-analytik@aon.at
Internet: www.betavertrieb.at

National Institute of Standards & Technology

Certificate of Analysis

Standard Reference Material® 987

Strontium Carbonate
(Isotopic Standard)

This Standard Reference Material (SRM) is certified for use as an isotopic reference material for the calibration of mass spectrometers. The material consists of highly purified strontium carbonate of high homogeneity. A unit of SRM 987 consists of 1 g of powder.

Certified Values: The certified values for the absolute strontium isotopic abundance ratios and the atom fractions of ^{88}Sr, ^{87}Sr, ^{86}Sr and ^{84}Sr are listed in Table 1. A NIST-certified value is a value for which NIST has the highest confidence in its accuracy, in that all known or suspected sources of bias have been investigated or accounted for by NIST. A certified value is the present best estimate of the true value based on the results of analyses performed at NIST and cooperating laboratories. Value assignment categories are based on the definition of terms and modes used at NIST for chemical reference materials [1]. The uncertainties listed with the values are expanded uncertainties (95 % confidence interval) and are calculated according to the methods in the ISO and NIST Guides [2].

Table 1. Certified Values for SRM 987 Strontium Carbonate

Absolute Abundance Ratios	
	$^{88}Sr/^{86}Sr = 8.378\,61 \pm 0.003\,25$
	$^{87}Sr/^{86}Sr = 0.710\,34 \pm 0.000\,26$
	$^{84}Sr/^{86}Sr = 0.056\,55 \pm 0.000\,14$
that yield atom percents of:	
	$^{88}Sr = 82.584\,5 \pm 0.006\,6$
	$^{87}Sr = 7.001\,5 \pm 0.002\,6$
	$^{86}Sr = 9.856\,6 \pm 0.003\,4$
	$^{84}Sr = 0.557\,4 \pm 0.001\,5$

This material was used as the reference sample in a determination of the absolute abundance ratios and atomic weight of strontium [3]. The atomic weight of strontium calculated from the absolute abundance ratios is $87.616\,81 \pm 0.000\,12$.

Expiration of Certification: The certification of this SRM is deemed to be indefinite within the stated uncertainties. However, certification is nullified if the SRM is contaminated or otherwise altered.

Maintenance of Certified Values: NIST will monitor this SRM and, if substantive changes occur in the certified values, NIST will notify the purchaser. Registration (see attached sheet) will facilitate notification.

Stephen A. Wise, Chief
Analytical Chemistry Division

Gaithersburg, MD 20899
Certificate Issue Date: 19 June 2007
See Certificate Revision History on Last Page

Robert L. Watters, Jr., Chief
Measurement Services Division

The overall direction and coordination of the technical measurements leading to the certification of this SRM were performed under the chairmanship of I.L. Barnes and W.R. Shields of the NIST Analytical Chemistry Division.

The characterization of this SRM was performed by G. Marinenko, E.E. Etz, D.G. Friend, I.L. Barnes, L.J. Moore, T.C. Rains, T.A. Rush, L.A. Machlan, T.J. Murphy, and P.J. Paulsen, all of the NIST Analytical Chemistry Division.

The support aspects involved in the preparation of this SRM were coordinated through the NIST Measurement Services Division. The current revised certificate was coordinated by Robert D. Vocke, Jr. of the Analytical Chemistry Division.

Storage and Handling: There are no special storage or handling instructions. While strontium carbonate is slightly hygroscopic (absorbing approximately 0.02 % moisture at 90 % humidity), this has no effect on the isotopic abundances.

The strontium carbonate used for this SRM was obtained from Spex Industries, Inc[1]. of Metuchen, NJ. The material, when received, was of high purity in relation to cationic impurities but assayed only 99.0 % due to moisture and other volatile impurities. The impurities reported in the strontium carbonate material are lithium, 4 mg/kg; sodium, 6 mg/kg; potassium, < 1 mg/kg; magnesium, < 2 mg/kg; calcium, 5 mg/kg; barium, < 15 mg/kg; copper, < 3 mg/kg; iron, < 3 mg/kg; aluminum, < 1 mg/kg; and silicon, < 1 mg/kg.

REFERENCES

[1] May, W.E.; Parris, R.M.; Beck II, C.M.; Fassett, J.D.; Greenberg, R.R.; Guenther, F.R.; Kramer, G.W.; Wise; S.A.; Gills, T.E.; Colbert, J.C.; Gettings, R.J.; MacDonald, B.S.; *Definitions of Terms and Modes Used at NIST for Value-Assignment of Reference Materials for Chemical Measurements*; NIST Spec. Pub. 260-136, U.S. Government Printing Office: Washington, DC (2000).

[2] ISO; *Guide to the Expression of Uncertainty in Measurement*; ISBN 92-67-10188-9, 1st ed., International Organization for Standardization: Geneva, Switzerland (1993); see also Taylor, B.N.; Kuyatt, C.E.; *Guidelines for Evaluating and Expressing the Uncertainty of NIST Measurement Results*; NIST Technical Note 1297, U.S. Government Printing Office: Washington, DC (1994); available at http://physics.nist.gov/Pubs/.

[3] Moore, L.J.; Murphy, T.J.; Barnes, I.L.; Paulsen, P.J.; *Absolute Isotopic Abundance Ratios and Atomic Weight of a Reference Sample of Strontium*, J. of Res. (NBS) Vol. 87, No. 1, pp. 1–8 (1982).

Users of this SRM should ensure that the certificate in their possession is current. This can be accomplished by contacting the SRM Program at: telephone (301) 975-6776; fax (301) 926-4751; e-mail srminfo@nist.gov; or via the Internet at http://www.nist.gov/srm.

[1]Certain commercial equipment, instrumentation, or materials are identified in this certificate to specify adequately the experimental procedure. Such identification does not imply recommendation or endorsement by the NIST, nor does it imply that the materials or equipment identified are necessarily the best available for the purpose.

VI.2 Measurement Results

VI.2.1 Laser Ablation screening (LA-ICP-QMS)

sample name	approximate median concentration [µg g^{-1}]					
	Na	Cl	Ca	Sr	Pb	S
T01-i	30000	50000	600	5	0.5	5000
T01-ii	20000	50000	400	3	0.4	8000
T01-iii	20000	60000	400	3	0.5	10000
T01-iv	20000	60000	400	4	0.3	6000
T01-v	20000	40000	500	6	0.7	8000
T02-i	30000	60000	800	9	3	7000
T02-ii	20000	50000	1000	8	2	4000
T02-iii	20000	50000	800	6	1	8000
T02-iv	30000	70000	800	10	0.2	7000
T03-i	50000	100000	1000	20	1	7000
T03-ii	30000	80000	1000	10	1	4000
T03-iii	40000	90000	1000	10	2	5000
T03-iv	40000	90000	1000	10	2	4000
T03-v	40000	90000	1000	10	2	4000
T04-i	20000	70000	1000	10	2	9000
T04-ii	20000	60000	1000	10	2	9000
T05-i	20000	50000	800	10	0.2	3000
T05-ii	20000	60000	700	10	0.2	3000

Tab. 22 LA results for individual sections of each timber sample prior to leaching

sample type	sample name	concentration [µg g^{-1}]		concentration [ng g^{-1}]	
		Na	Ca	Sr	Pb
leaching water	T02ii L1	2000	220	2100	24
	T02ii L2	800	89	330	1.6
	T02ii L3	660	220	690	1.8
	T02ii L4	15	23	42	0.82
	spruce L1	70	160	360	37
	spruce L2	3.8	51	61	1.3
	spruce L3	< LoD	380	300	5.8
	spruce L4	< LoD	43	44	0.23
	T05i L1	1600	310	2500	18
	T05i L2	390	77	430	1.2
	T05i L3	600	420	1800	0.71
	T05i L4	730	43	49	0.74
	beech L1	47	46	130	35
	beech L2	3.5	38	88	5.2
	beech L3	< LoD	230	130	5.5
	beech L4	< LoD	130	37	1.7
digest	T02ii	68	4400	13000	310
	spruce	5.6	7000	8600	340
	T05i	2300	1400	6000	180
	beech	5.8	1500	4500	270
	leaching LOD	0.65	1.0	1.6	0.14

Tab. 23 Results from liquid measurement of leaching water and digest from first leaching experiment

VI.2.2 Multi-element measurements

sample	sum [w/w]	concentration [µg g^{-1}]										
		Cl	*Mg*	*Ca*	Ba	Sr	Rb	Li	*K*	*Na*	B	Al
F01_L1	2.28%	10000	*2000*	*600*	0.1	4	0.4	1	*700*	*9000*	10	0.1
F01_L2	0.44%	2000	*400*	*100*	0.04	0.7	0.09	0.3	*200*	*2000*	4	0.4
F01_L3	0.12%	500	*80*	*30*	0.02	0.2	0.04	0.08	*70*	*500*	2	3
F01_L4	0.25%	200	*1000*	*700*	0.6	5	0.06	0.07	*80*	*500*	2	8
F01_L5	0.06%	50	*200*	*100*	0.2	1	0.04	0.04	*< LoD*	*90*	0.7	7
sum F01	3.20%	10000	*4000*	*2000*	0.9	10	0.6	2	*1000*	*10000*	20	20
F02_L1	0.69%	3000	*800*	*900*	0.2	6	0.1	0.4	*200*	*2000*	8	0.2
F02_L2	0.07%	200	*90*	*100*	0.03	0.7	0.02	0.05	*< LoD*	*300*	2	2
F02_L3	0.02%	30	*30*	*40*	< LoD	0.2	0.01	0.02	*< LoD*	*80*	0.8	3
F02_L4	0.22%	< LoD	*600*	*1000*	1	9	0.02	0.02	*< LoD*	*80*	1	5
F02_L5	0.05%	< LoD	*100*	*300*	0.2	2	0.03	0.02	*< LoD*	*10*	0.6	6
sum F02	1.06%	3000	*2000*	*3000*	1	20	0.2	0.5	*400*	*3000*	10	20
F03_L1	3.73%	20000	*3000*	*400*	0.4	20	0.7	2	*1000*	*20000*	10	0.1
F03_L2	0.52%	2000	*400*	*50*	0.07	2	0.1	0.4	*200*	*2000*	4	0.3
F03_L3	0.10%	400	*50*	*6*	0.02	0.2	0.04	0.09	*70*	*500*	2	7
F03_L4	0.23%	100	*1000*	*400*	0.9	10	0.05	0.07	*90*	*500*	2	5
F03_L5	0.06%	30	*300*	*100*	0.4	4	0.04	0.03	*< LoD*	*100*	0.9	6
sum F03	4.06%	20000	*5000*	*1000*	2	30	0.9	3	*2000*	*10000*	20	20
T01_L1	18.85%	100000	*7000*	*300*	0.2	3	4	9	*5000*	*50000*	20	0.3
T01_L2	3.59%	20000	*2000*	*80*	0.05	0.9	0.8	2	*900*	*10000*	7	0.06
T01_L3	0.81%	5000	*500*	*30*	0.03	0.4	0.2	0.4	*200*	*3000*	3	0.05
T01_L4	0.51%	3000	*800*	*200*	0.5	3	0.09	0.2	*100*	*1000*	3	0.2
T01_L5	0.21%	1000	*200*	*50*	0.5	1	0.03	0.05	*< LoD*	*300*	1	0.2
sum T01	19.87%	200000	*10000*	*600*	1	8	5	10	*6000*	*30000*	30	0.7
T02_L1	13.80%	80000	*10000*	*300*	0.3	3	3	10	*6000*	*40000*	30	0.2
T02_L2	2.08%	9000	*2000*	*60*	0.06	0.8	0.4	1	*900*	*9000*	6	< LoD
T02_L3	0.42%	2000	*400*	*20*	0.04	0.3	0.1	0.3	*200*	*2000*	2	< LoD
T02_L4	0.30%	500	*1000*	*200*	1	4	0.06	0.1	*100*	*800*	2	0.8
T02_L5	0.07%	90	*300*	*50*	0.7	1	0.01	0.02	*50*	*200*	0.7	0.6
sum T02	13.52%	90000	*10000*	*700*	2	10	4	10	*8000*	*20000*	40	2
T03_L1	11.04%	60000	*10000*	*300*	0.2	3	3	8	*5000*	*30000*	30	0.2
T03_L2	1.51%	7000	*1000*	*50*	0.06	0.4	0.4	1.0	*700*	*6000*	10	0.05
T03_L3	0.27%	1000	*200*	*10*	0.02	0.08	0.08	0.2	*200*	*1000*	4	< LoD
T03_L4	0.28%	300	*1000*	*300*	1	2	0.06	0.09	*100*	*600*	4	3
T03_L5	0.06%	40	*300*	*60*	0.5	0.8	0.01	0.02	*< LoD*	*100*	1	2
sum T03	11.29%	70000	*10000*	*700*	2	7	3	9	*6000*	*20000*	50	5
T04_L1	13.46%	80000	*20000*	*300*	0.9	6	5	10	*5000*	*40000*	70	0.08
T04_L2	2.00%	9000	*3000*	*90*	0.3	2	0.6	2	*700*	*8000*	10	0.06
T04_L3	0.31%	1000	*500*	*40*	0.2	0.5	0.1	0.3	*200*	*1000*	4	0.08
T04_L4	0.29%	400	*2000*	*300*	4	6	0.07	0.1	*100*	*500*	3	2
T04_L5	0.06%	70	*400*	*60*	2	2	0.02	0.03	*< LoD*	*100*	1	1
sum T04	13.78%	90000	*20000*	*800*	8	20	6	20	*6000*	*20000*	90	3
T05_L1	9.43%	50000	*7000*	*200*	0.07	2	2	5	*3000*	*30000*	60	0.1
T05_L2	1.13%	5000	*400*	*20*	< LoD	0.1	0.2	0.6	*400*	*5000*	10	< LoD
T05_L3	0.17%	700	*40*	*20*	0.02	< LoD	0.05	0.1	*100*	*800*	6	< LoD
T05_L4	0.52%	200	*3000*	*1000*	2	5	0.09	0.1	*200*	*1000*	10	0.1
T05_L5	0.11%	20	*400*	*300*	0.6	1	0.02	0.02	*60*	*200*	2	0.2
sum T05	9.90%	60000	*10000*	*2000*	2	7	2	6	*4000*	*20000*	100	0.4
LoD [µg g^{-1}]		6	*1*	*3*	0.01	0.02	0.003	0.001	*50*	*0.04*	0.04	0.04
RSU (k=2)		n.d.	*21%*	*18%*	21%	28%	6%	7%	*46%*	*8%*	8%	14%

Tab. 24 Multi-element data for leaching solutions of prehistoric illumination chips and timber

sample	concentration [µg g^{-1}]											
	Fe	Cr	V	Mn	Co	Ni	Cu	Zn	U	Pb	Ga	Tl
F01_L1	*2*	< LoD	0.1	0.5	0.04	0.2	0.5	0.3	0.0002	< LoD	0.005	0.02
F01_L2	*< LoD*	< LoD	0.10	0.1	0.010	0.08	0.4	0.04	0.0002	< LoD	0.002	0.005
F01_L3	*2*	< LoD	0.07	0.04	0.005	0.05	0.4	0.06	0.0006	< LoD	0.002	0.002
F01_L4	*70*	< LoD	0.2	1	0.3	2	20	5	0.003	0.4	0.03	0.01
F01_L5	*40*	< LoD	0.1	0.7	0.06	0.7	7	1	0.003	0.4	0.009	0.004
sum F01	*100*	< LoD	0.6	3	0.4	3	20	6	0.007	0.8	0.04	0.04
F02_L1	*3*	< LoD	0.06	0.5	0.03	0.1	0.3	0.8	0.0001	< LoD	0.007	0.009
F02_L2	*0.6*	< LoD	0.05	0.07	0.007	0.05	0.1	0.1	0.0002	< LoD	0.002	0.002
F02_L3	*1*	< LoD	0.04	0.03	0.004	0.04	0.1	0.07	0.0002	< LoD	0.001	0.0008
F02_L4	*60*	< LoD	0.1	1	0.2	2	6	6	0.001	0.1	0.05	0.005
F02_L5	*50*	< LoD	0.09	0.5	0.04	0.6	3	1	0.001	0.4	0.010	0.002
sum F02	*100*	< LoD	0.4	2	0.3	3	9	8	0.003	0.5	0.07	0.02
F03_L1	*2*	0.006	0.1	0.5	0.06	0.3	3	0.6	0.0003	< LoD	0.02	0.08
F03_L2	*< LoD*	< LoD	0.03	0.09	0.01	0.08	1	0.1	0.0002	< LoD	0.003	0.02
F03_L3	*3*	< LoD	0.03	0.03	0.004	0.04	0.7	0.04	0.0008	< LoD	0.003	0.004
F03_L4	*50*	< LoD	0.1	0.8	0.2	2	40	4	0.005	0.2	0.04	0.03
F03_L5	*50*	< LoD	0.08	0.6	0.06	0.7	20	1	0.004	0.6	0.02	0.009
sum F03	*100*	< LoD	0.4	2	0.3	3	70	6	0.01	0.8	0.08	0.1
T01_L1	*4*	0.09	0.7	0.6	0.03	0.1	2	0.4	0.002	0.04	0.01	0.009
T01_L2	*2*	0.04	0.2	0.1	0.009	0.04	0.1	0.06	0.0007	< LoD	0.004	0.001
T01_L3	*1*	0.02	0.05	0.04	0.004	0.03	< LoD	< LoD	0.0005	< LoD	0.002	0.0002
T01_L4	*20*	0.02	0.04	0.2	0.07	0.8	0.6	2	0.02	0.03	0.03	0.0007
T01_L5	*20*	0.02	0.03	0.08	0.03	0.4	0.5	0.6	0.02	0.05	0.03	< LoD
sum T01	*40*	0.2	0.9	1	0.1	1	3	3	0.04	0.1	0.07	0.01
T02_L1	*10*	0.1	0.5	2	0.6	0.2	1	1	0.0005	0.1	0.009	0.01
T02_L2	*< LoD*	0.007	0.06	0.2	0.1	0.08	0.3	0.2	0.0002	< LoD	0.002	0.002
T02_L3	*< LoD*	< LoD	0.01	0.06	0.03	0.06	0.1	0.08	0.0002	< LoD	0.002	0.0006
T02_L4	*60*	0.08	0.05	0.5	0.6	1	5	4	0.01	4	0.06	0.002
T02_L5	*50*	0.09	0.04	0.1	0.2	0.4	2	3	0.01	3	0.03	0.0005
sum T02	*100*	0.3	0.7	3	2	2	9	9	0.02	8	0.1	0.02
T03_L1	*10*	0.2	0.5	0.8	0.2	0.05	0.7	0.6	0.0003	0.10	0.007	0.003
T03_L2	*0.8*	0.01	0.1	0.09	0.03	0.05	< LoD	0.1	0.0003	< LoD	0.002	0.0006
T03_L3	*0.6*	0.01	0.05	0.02	0.01	0.03	< LoD	< LoD	0.0002	< LoD	0.0008	0.0001
T03_L4	*60*	0.08	0.1	0.5	0.6	2	0.4	5	0.006	0.02	0.06	0.0009
T03_L5	*50*	0.07	0.08	0.1	0.2	0.8	0.3	1	0.006	0.08	0.02	0.0003
sum T03	*100*	0.3	0.9	1	1	3	1	7	0.01	0.2	0.09	0.005
T04_L1	*10*	0.2	0.7	0.7	0.1	0.3	2	3	0.002	0.03	0.03	0.06
T04_L2	*1.0*	0.01	0.09	0.1	0.02	0.09	0.3	0.4	0.0009	< LoD	0.01	0.009
T04_L3	*< LoD*	0.006	0.02	0.02	0.005	0.05	0.1	0.1	0.0007	< LoD	0.008	0.002
T04_L4	*20*	0.006	0.04	0.2	0.1	2	8	6	0.03	0.2	0.2	0.004
T04_L5	*20*	< LoD	0.03	0.07	0.04	0.7	5	2	0.03	0.3	0.09	0.001
sum T04	*60*	0.2	0.9	1	0.3	3	10	10	0.07	0.5	0.3	0.07
T05_L1	*20*	0.2	0.5	1.0	0.006	< LoD	0.6	< LoD	0.001	< LoD	0.002	0.002
T05_L2	*2*	0.009	0.04	0.07	0.001	0.01	< LoD	0.1	0.001	< LoD	0.0005	0.0003
T05_L3	*3*	0.007	0.009	0.02	0.0009	0.02	< LoD	0.1	0.002	< LoD	0.0007	0.00004
T05_L4	*100*	< LoD	0.007	6	0.03	0.6	0.2	2	0.01	< LoD	0.08	0.002
T05_L5	*60*	< LoD	0.009	2	0.006	0.2	0.2	0.6	0.01	< LoD	0.03	0.0005
sum T05	*200*	0.2	0.5	9	0.04	0.8	1	3	0.03	< LoD	0.1	0.004
LoD [µg g^{-1}]	*0.5*	0.006	0.004	0.0007	0.0003	0.008	0.07	0.04	0.00005	0.01	0.0005	0.00003
RSU (k=2)	*10%*	76%	10%	5%	7%	9%	7%	18%	16%	15%	10%	8%

Tab. 25 Multi-element data for leaching solutions of prehistoric illumination chips and timber (continued)

sample	sum [w/w]	concentration [µg g^{-1}]										
		Cl	*Mg*	*Ca*	Ba	Sr	Rb	Li	*K*	*Na*	B	Al
S01_L1	0.64%	4000	*300*	*700*	0.4	2	0.1	0.4	*60*	*1000*	10	1
S01_L2	0.19%	1000	*100*	*100*	0.1	0.4	0.03	0.1	*< LoD*	*300*	4	0.7
S01_L3	0.07%	500	*30*	*50*	0.04	0.1	0.01	0.04	*< LoD*	*100*	2	0.7
S01_L4	0.29%	900	*400*	*1000*	1	4	0.02	0.03	*< LoD*	*100*	2	4
S01_L5	0.08%	< LoD	*200*	*500*	0.9	2	0.02	0.02	*< LoD*	*40*	2	4
sum S01	1.27%	7000	*1000*	*3000*	3	8	0.2	0.5	*< LoD*	*2000*	20	10
S02_L1	6.52%	30000	*8000*	*2000*	0.3	4	1	4	*2000*	*20000*	20	0.4
S02_L2	0.66%	3000	*600*	*200*	0.08	0.3	0.2	0.5	*200*	*3000*	4	2
S02_L3	0.10%	400	*70*	*20*	0.04	0.04	0.06	0.1	*70*	*500*	2	10
S02_L4	0.38%	100	*2000*	*1000*	2	3	0.09	0.09	*90*	*500*	3	10
S02_L5	0.08%	7	*300*	*200*	0.7	0.4	0.07	0.06	*< LoD*	*80*	0.9	20
sum S02	6.88%	40000	*10000*	*4000*	3	7	2	5	*2000*	*10000*	30	50
S03_L1	0.07%	200	*50*	*400*	0.08	0.3	0.03	0.03	*< LoD*	*30*	20	6
S03_L2	0.01%	10	*10*	*40*	0.02	0.04	0.02	0.02	*< LoD*	*5*	2	9
S03_L3	0.01%	< LoD	*10*	*20*	0.03	< LoD	0.03	0.02	*< LoD*	*2*	0.9	20
S03_L4	0.47%	< LoD	*300*	*4000*	1	3	0.03	0.009	*< LoD*	*4*	3	20
S03_L5	0.07%	< LoD	*60*	*500*	0.4	0.5	0.02	0.01	*< LoD*	*1*	0.7	7
sum S03	0.63%	200	*400*	*5000*	2	4	0.1	0.09	*< LoD*	*40*	20	50
S04_L1	1.34%	6000	*1000*	*200*	0.1	1	0.4	1	*500*	*5000*	30	1
S04_L2	0.14%	600	*50*	*6*	0.02	0.06	0.08	0.2	*90*	*600*	5	10
S04_L3	0.03%	80	*10*	*4*	0.02	< LoD	0.05	0.06	*< LoD*	*100*	2	20
S04_L4	0.34%	10	*2000*	*800*	1	7	0.10	0.10	*90*	*500*	3	20
S04_L5	0.06%	< LoD	*300*	*100*	0.3	1	0.05	0.04	*< LoD*	*80*	0.8	10
sum S04	1.91%	7000	*3000*	*1000*	2	9	0.7	2	*800*	*7000*	40	50
S05_L1	0.08%	200	*200*	*300*	0.07	0.5	0.02	0.06	*< LoD*	*100*	10	2
S05_L2	0.01%	< LoD	*20*	*30*	0.02	0.06	0.02	0.02	*< LoD*	*20*	2	8
S05_L3	0.00%	< LoD	*10*	*10*	0.03	< LoD	0.01	0.01	*< LoD*	*10*	0.9	5
S05_L4	0.44%	< LoD	*1000*	*3000*	1	6	0.01	0.009	*< LoD*	*20*	3	10
S05_L5	0.07%	< LoD	*200*	*500*	0.2	1	0.01	0.007	*< LoD*	*3*	0.7	5
sum S05	0.61%	200	*1000*	*4000*	2	8	0.08	0.1	*< LoD*	*200*	20	30
S06_L1	9.07%	50000	*9000*	*1000*	0.3	9	2	6	*3000*	*30000*	20	0.3
S06_L2	0.78%	4000	*500*	*50*	0.03	0.4	0.2	0.6	*300*	*3000*	4	2
S06_L3	0.11%	400	*30*	*4*	< LoD	< LoD	0.05	0.1	*70*	*500*	1	6
S06_L4	0.34%	90	*2000*	*600*	0.7	6	0.08	0.10	*100*	*700*	3	10
S06_L5	0.06%	< LoD	*300*	*90*	0.1	0.9	0.03	0.03	*50*	*100*	0.7	6
sum S06	8.70%	60000	*10000*	*2000*	1	20	2	6	*4000*	*10000*	30	20
LoD [µg g^{-1}]		6	*1*	*3*	0.01	0.02	0.003	0.001	*50*	*0.04*	0.04	0.04
RSU (k=2)		n.d.	*21%*	*18%*	21%	28%	6%	7%	*46%*	*8%*	8%	14%

Tab. 26 Multi-element data for leaching solutions of prehistoric tool handle samples

sample	concentration [µg g⁻¹]											
	Fe	Cr	V	Mn	Co	Ni	Cu	Zn	U	Pb	Ga	Tl
S01_L1	*9*	0.02	0.2	0.2	0.04	0.3	2	0.5	0.0009	0.03	0.02	0.06
S01_L2	*3*	< LoD	0.1	0.06	0.01	0.1	1	0.1	0.0008	0.02	0.006	0.03
S01_L3	*3*	0.008	0.1	0.02	0.007	0.10	1	0.09	0.0004	0.01	0.002	0.01
S01_L4	*100*	0.01	0.4	0.5	0.2	3	40	4	0.01	0.01	0.07	0.08
S01_L5	*100*	0.03	0.3	0.5	0.07	2	30	2	0.02	0.2	0.05	0.04
sum S01	*300*	0.07	1	1	0.3	5	70	7	0.03	0.2	0.2	0.2
S02_L1	*10*	0.03	0.2	0.5	0.1	1	8	3	0.006	0.01	0.01	0.3
S02_L2	*3*	< LoD	0.05	0.07	0.02	0.2	2	0.2	0.003	< LoD	0.004	0.04
S02_L3	*9*	0.01	0.04	0.03	0.006	0.1	2	0.1	0.007	0.03	0.006	0.007
S02_L4	*200*	0.02	0.08	0.9	0.3	5	100	8	0.3	2	0.07	0.1
S02_L5	*100*	0.03	0.06	0.9	0.05	1	30	1	0.2	2	0.03	0.03
sum S02	*300*	0.09	0.5	2	0.5	8	100	10	0.5	5	0.1	0.5
S03_L1	*3*	< LoD	0.2	0.09	0.02	0.4	3	0.3	0.0007	< LoD	0.005	0.06
S03_L2	*4*	< LoD	0.2	0.03	0.005	0.10	1	0.1	0.0008	< LoD	0.004	0.02
S03_L3	*6*	< LoD	0.1	0.02	0.004	0.09	1	0.09	0.001	< LoD	0.006	0.009
S03_L4	*200*	0.02	0.6	1	0.3	7	200	8	0.07	0.7	0.06	0.1
S03_L5	*70*	0.008	0.2	0.5	0.04	1	40	1	0.03	0.9	0.02	0.03
sum S03	*300*	0.02	1	2	0.4	9	200	10	0.10	2	0.10	0.2
S04_L1	*3*	0.01	0.1	0.2	0.02	0.1	3	0.4	0.0004	< LoD	0.005	0.04
S04_L2	*6*	< LoD	0.09	0.07	0.004	0.05	0.9	0.08	0.0008	< LoD	0.004	0.007
S04_L3	*9*	< LoD	0.08	0.03	0.004	0.05	0.8	0.1	0.0010	< LoD	0.005	0.002
S04_L4	*200*	0.009	0.2	2	0.2	2	50	8	0.008	0.5	0.07	0.06
S04_L5	*60*	0.007	0.10	1	0.03	0.4	20	1	0.005	0.5	0.01	0.01
sum S04	*200*	0.03	0.6	3	0.2	2	70	10	0.02	1.0	0.10	0.1
S05_L1	*3*	< LoD	0.09	0.04	0.02	0.2	2	0.2	0.002	< LoD	0.004	0.07
S05_L2	*4*	< LoD	0.08	0.02	0.005	0.07	1	0.06	0.002	< LoD	0.003	0.02
S05_L3	*2*	< LoD	0.05	0.008	0.003	0.07	0.9	< LoD	0.002	< LoD	0.002	0.01
S05_L4	*200*	< LoD	0.2	0.7	0.3	3	90	6	0.06	0.8	0.06	0.2
S05_L5	*50*	< LoD	0.09	0.4	0.05	0.7	30	1	0.03	0.8	0.01	0.05
sum S05	*200*	< LoD	0.5	1	0.4	4	100	8	0.10	2	0.08	0.4
S06_L1	*7*	0.04	0.4	0.5	0.09	0.2	1	1	0.0008	< LoD	0.01	0.02
S06_L2	*2*	< LoD	0.1	0.06	0.01	0.07	0.3	0.1	0.0008	< LoD	0.002	0.003
S06_L3	*7*	< LoD	0.1	0.01	0.007	0.07	0.3	0.1	0.001	< LoD	0.002	0.0005
S06_L4	*200*	0.02	0.6	0.9	0.3	3	10	10	0.02	0.2	0.03	0.009
S06_L5	*80*	0.006	0.2	0.5	0.06	0.7	5	2	0.01	0.2	0.008	0.002
sum S06	*300*	0.05	1	2	0.5	4	20	10	0.04	0.3	0.06	0.03
LoD [µg g⁻¹]	*0.5*	0.006	0.004	0.0007	0.0003	0.008	0.07	0.04	0.00005	0.01	0.0005	0.00003
RSU (k=2)	*10%*	76%	10%	5%	7%	9%	7%	18%	16%	15%	10%	8%

Tab. 27 Multi-element data for leaching solutions of prehistoric tool handle samples (continued)

	concentration [µg g^{-1}]										
sample	*Mg*	Ca	Ba	Sr	Rb	K	Na	B	Mn	Cu	Zn
RF1	*56 ± 4*	*890 ± 110*	12 ± 1	11 ± 1	0.75 ± 0.09	*280 ± 50*	*<LoD*	3.0	17 ± 1	0.55	10 ± 2
RF2	*63 ± 4*	*810 ± 100*	12 ± 1	11 ± 1	1.7 ± 0.2	*380 ± 70*	*<LoD*	2.1	22 ± 1	1.2 ± 0.2	8.4 ± 1.2
RF3	*80 ± 5*	*850 ± 110*	9.5 ± 0.6	14 ± 1	1.5 ± 0.2	*550 ± 100*	*4.2*	2.6	17 ± 1	0.67	8.1 ± 1.2
RF4	*120 ± 10*	*1100 ± 100*	24 ± 1	5.8 ± 0.3	1.4 ± 0.2	*2600 ± 500*	*35 ± 2*	2.6	73 ± 3	0.58	10 ± 2
RF5	*75 ± 5*	*870 ± 110*	24 ± 1	5.5 ± 0.3	0.60 ± 0.07	*700 ± 120*	*6.3*	2.6	86 ± 4	0.70	14 ± 2
RF6	*57 ± 4*	*730 ± 90*	14 ± 1	4.0 ± 0.2	0.51 ± 0.06	*670 ± 120*	*<LoD*	1.8	36 ± 2	0.43	9.0 ± 1.3
RF7	*56 ± 4*	*930 ± 120*	7.0 ± 0.4	8.6 ± 0.5	0.53 ± 0.06	*340 ± 60*	*<LoD*	2.0	23 ± 1	0.37	6.8 ± 1.0
RF8	*62 ± 4*	*640 ± 80*	6.4 ± 0.4	6.1 ± 0.4	0.73 ± 0.09	*450 ± 80*	*<LoD*	1.9	18 ± 1	0.64	11 ± 2
RF9	*63 ± 4*	*840 ± 100*	6.2 ± 0.4	9.1 ± 0.5	0.43 ± 0.05	*510 ± 90*	*6.9*	2.2	13 ± 1	0.39	6.3 ± 0.9
RF10	*87 ± 6*	*850 ± 110*	8.4 ± 0.5	10 ± 1	0.34 ± 0.04	*410 ± 70*	*<LoD*	1.7	18 ± 1	0.54	9.5 ± 1.4
RB1	*92 ± 6*	*780 ± 100*	3.6 ± 0.2	3.8 ± 0.2	9.9 ± 1.2	*1100 ± 200*	*2.8*	2.7	5.2 ± 0.2	0.91 ± 0.13	2.3 ± 0.3
RB2	*170 ± 10*	*1200 ± 200*	5.8 ± 0.3	4.6 ± 0.3	15 ± 2	*1800 ± 300*	*6.3*	2.7	21 ± 1	0.64	4.2 ± 0.6
RB3	*160 ± 10*	*700 ± 90*	4.1 ± 0.2	3.8 ± 0.2	4.9 ± 0.6	*890 ± 160*	*<LoD*	2.7	14 ± 1	1.0 ± 0.1	2.8 ± 0.4
RB4	*240 ± 20*	*1200 ± 200*	16 ± 1	4.8 ± 0.3	5.7 ± 0.7	*2600 ± 500*	*6.1*	4.1 ± 0.6	29 ± 1	1.5 ± 0.2	2.7 ± 0.4
RB5	*300 ± 20*	*1400 ± 200*	40 ± 2	3.9 ± 0.2	3.6 ± 0.4	*1600 ± 300*	*16 ± 1*	3.9 ± 0.5	75 ± 3	1.2 ± 0.2	1.9 ± 0.3
RB6	*190 ± 10*	*1100 ± 100*	12 ± 1	1.9 ± 0.1	4.4 ± 0.5	*2000 ± 400*	*8.8 ± 0.5*	3.5	69 ± 3	1.4 ± 0.2	7.6 ± 1.1
RB7	*190 ± 10*	*910 ± 110*	14 ± 1	3.7 ± 0.2	3.9 ± 0.5	*5000 ± 900*	*3.4*	3.8 ± 0.5	54 ± 2	2.0 ± 0.3	5.6 ± 0.8
RB8	*220 ± 10*	*1100 ± 100*	2.8 ± 0.2	2.3 ± 0.1	12 ± 1	*3400 ± 600*	*53 ± 3*	2.9	9.2 ± 0.4	1.1 ± 0.2	2.1 ± 0.3
RB9	*86 ± 6*	*1100 ± 100*	3.4 ± 0.2	4.2 ± 0.2	2.8 ± 0.3	*860 ± 150*	*6.3*	2.9	15 ± 1	0.83 ± 0.12	1.4 ± 0.2
RB10	*400 ± 30*	*1400 ± 200*	0.49 ± 0.03	3.8 ± 0.2	9.9 ± 1.2	*9500 ± 1700*	*48 ± 3*	3.3	2.1 ± 0.1	0.49	2.3 ± 0.3
RT1	*68 ± 5*	*1000 ± 100*	12 ± 1	5.7 ± 0.3	0.73 ± 0.09	*270 ± 50*	*4.0*	3.3	77 ± 3	0.98 ± 0.14	9.7 ± 1.4
RT2	*84 ± 6*	*1000 ± 100*	19 ± 1	6.5 ± 0.4	2.2 ± 0.3	*690 ± 120*	*5.1*	2.9	53 ± 2	1.1 ± 0.2	10 ± 2
RT4	*100 ± 7*	*430 ± 50*	7.4 ± 0.4	1.8 ± 0.1	4.4 ± 0.5	*8800 ± 1500*	*19 ± 1*	2.8	12 ± 1	5.0 ± 0.7	2.5 ± 0.4
RT5	*170 ± 10*	*1200 ± 200*	16 ± 1	3.5 ± 0.2	2.1 ± 0.2	*3100 ± 500*	*13 ± 1*	2.6	78 ± 3	1.1 ± 0.2	6.3 ± 0.9
RT6	*140 ± 10*	*940 ± 120*	7.6 ± 0.4	2.3 ± 0.1	4.5 ± 0.5	*4900 ± 900*	*46 ± 3*	2.6	64 ± 3	1.8 ± 0.2	4.2 ± 0.6
RT7	*68 ± 5*	*440 ± 50*	2.3 ± 0.1	1.6 ± 0.1	3.4 ± 0.4	*2700 ± 500*	*22 ± 1*	2.1	7.3 ± 0.3	0.76 ± 0.11	2.8 ± 0.4
RT8	*73 ± 5*	*700 ± 90*	1.3 ± 0.1	1.2 ± 0.1	2.5 ± 0.3	*1100 ± 200*	*<LoD*	1.7	12 ± 1	0.69	4.3 ± 0.6
RT9	*67 ± 4*	*760 ± 90*	1.6 ± 0.1	2.5 ± 0.1	2.6 ± 0.3	*1400 ± 200*	*<LoD*	2.1	23 ± 1	0.61	1.6 ± 0.2
RT10	*89 ± 6*	*800 ± 100*	2.4 ± 0.1	3.6 ± 0.2	1.5 ± 0.2	*1200 ± 200*	*5.5*	1.8	15 ± 1	0.70	2.0 ± 0.3
LoD [µg g^{-1}]	1.4	34	0.14	0.18	0.016	16	2.5	1.1	0.023	0.22	0.30
LoQ [µg g^{-1}]	4.5	110	0.47	0.59	0.053	52	8.3	3.8	0.076	0.73	1.00

Italic values: with reservations; values without SU stated: <LoQ

Tab. 28 Results of multi-element measurement in recent wood digests, part I – concentrations in µg g^{-1} per dry mass wood, with SU (k=2)

sample	Li	*Fe*	Cr	V	Co	Ni	Pb	Bi	Ga	Tl
					concentration [ng g⁻¹]					
RF1	<LoD	*10 ± 1*	150 ± 10	16 ± 4	10 ± 1	180 ± 10	26	16 ± 4	*510 ± 50*	1.7 ± 0.5
RF2	<LoD	*22 ± 1*	180 ± 10	18 ± 4	22 ± 1	75	130 ± 20	3.5	*520 ± 50*	7.2 ± 2.2
RF3	<LoD	*11 ± 1*	240 ± 20	12	11 ± 1	87 ± 6	45 ± 6	5.6 ± 1.5	*400 ± 40*	1.1 ± 0.3
RF4	25 ± 7	*41 ± 2*	260 ± 20	21 ± 5	41 ± 2	320 ± 20	130 ± 20	3.7	*1000 ± 100*	0.90 ± 0.27
RF5	<LoD	*46 ± 3*	210 ± 20	11	46 ± 3	160 ± 10	310 ± 40	2.9	*1000 ± 100*	2.4 ± 0.7
RF6	<LoD	*17 ± 1*	110 ± 10	9.8	17 ± 1	32	48 ± 6	<LoD	*610 ± 60*	0.61 ± 0.19
RF7	<LoD	*15 ± 1*	130 ± 10	13	15 ± 1	95 ± 6	95 ± 12	1.3	*300 ± 30*	2.2 ± 0.7
RF8	<LoD	*3.3*	95 ± 8	9.8	3.3	38	15	1.6	*280 ± 30*	3.0 ± 0.9
RF9	<LoD	*17 ± 1*	150 ± 10	9.7	17 ± 1	130 ± 10	47 ± 6	1.7	*260 ± 20*	1.5 ± 0.4
RF10	<LoD	*27 ± 2*	100 ± 10	7.1	27 ± 2	88 ± 6	29	<LoD	*360 ± 30*	0.37
RB1	9.8	*28 ± 2*	220 ± 20	9.1	28 ± 2	470 ± 30	60 ± 7	<LoD	*150 ± 10*	1.6 ± 0.5
RB2	19	*55 ± 3*	210 ± 20	6.9	55 ± 3	780 ± 50	70 ± 9	3.4	*250 ± 20*	3.0 ± 0.9
RB3	<LoD	*33 ± 2*	250 ± 20	<LoD	33 ± 2	880 ± 60	120 ± 20	<LoD	*170 ± 20*	0.68 ± 0.20
RB4	18	*35 ± 2*	280 ± 20	5.3	35 ± 2	1900 ± 100	250 ± 30	<LoD	*660 ± 60*	1.3 ± 0.4
RB5	170 ± 50	*31 ± 2*	170 ± 10	<LoD	31 ± 2	800 ± 50	36 ± 5	1.8	*1700 ± 200*	0.75 ± 0.23
RB6	12	*72 ± 4*	210 ± 20	<LoD	72 ± 4	1100 ± 100	200 ± 30	2.8	*480 ± 50*	0.81 ± 0.25
RB7	<LoD	*18 ± 1*	180 ± 10	<LoD	18 ± 1	600 ± 40	52 ± 6	<LoD	*560 ± 50*	1.1 ± 0.3
RB8	16	*17 ± 1*	270 ± 20	12	17 ± 1	210 ± 10	100 ± 10	2.8	*120 ± 10*	3.6 ± 1.1
RB9	260 ± 70	*33 ± 2*	190 ± 20	<LoD	33 ± 2	530 ± 40	120 ± 20	<LoD	*140 ± 10*	0.65 ± 0.20
RB10	180 ± 50	*14 ± 1*	290 ± 20	8.3	14 ± 1	370 ± 20	81 ± 10	3.2	*22*	1.2 ± 0.4
RT1	<LoD	*26 ± 1*	110 ± 10	<LoD	26 ± 1	79 ± 5	390 ± 50	16 ± 4	*480 ± 50*	2.2 ± 0.7
RT2	<LoD	*23 ± 1*	160 ± 10	<LoD	23 ± 1	100 ± 10	110 ± 10	7.3 ± 2.0	*750 ± 70*	4.3 ± 1.3
RT4	9.0	*8.7*	210 ± 20	7.8	8.7	200 ± 10	210 ± 30	2.8	*300 ± 30*	1.2 ± 0.3
RT5	<LoD	*58 ± 3*	180 ± 10	8.4	58 ± 3	180 ± 10	160 ± 20	2.8	*650 ± 60*	1.2 ± 0.4
RT6	13	*33 ± 2*	430 ± 40	23 ± 5	33 ± 2	620 ± 40	76 ± 10	5.8 ± 1.6	*310 ± 30*	2.2 ± 0.7
RT7	10	*6.1*	140 ± 10	7.7	6.1	160 ± 10	36 ± 5	<LoD	*98 ± 9*	1.1 ± 0.3
RT8	<LoD	*4.3*	130 ± 10	<LoD	4.3	82 ± 5	33	<LoD	*58 ± 6*	2.1 ± 0.6
RT9	14	*20 ± 1*	170 ± 10	<LoD	20 ± 1	170 ± 10	460 ± 60	2.6	*68 ± 6*	0.68 ± 0.21
RT10	13	*16 ± 1*	250 ± 20	8.2	16 ± 1	220 ± 10	29	1.5	*110 ± 10*	2.6 ± 0.8
LoD [ng g⁻¹]	6.2	*2.7*	20	4.5	2.7	23	11	1.2	7.9	0.14
LoQ [ng g⁻¹]	21	*9.0*	67	15	9.0	78	36	4.0	26	0.45

Italic values: with reservations; values without SU stated: <LoQ

Tab. 29 Results of multi-element measurement in recent wood digests, part II – concentrations in ng g⁻¹ per dry mass wood, with SU (k=2)

	concentration [µg g-1]								
sample	*Mg*	*Ca*	Ba	Sr	K	*Na*	B	Al	Cu
F01	*740 ± 50*	*150 ± 10*	3.6 ± 0.2	7.5 ± 0.6	360 ± 30	*110 ± 10*	6.3 ± 0.5	900 ± 80	16 ± 2
F02	*340 ± 20*	*120 ± 10*	1.6 ± 0.1	4.6 ± 0.4	170 ± 10	*11 ± 1*	3.7 ± 0.3	420 ± 40	4.3 ± 0.6
F03	*650 ± 40*	*90 ± 8*	2.9 ± 0.2	7.2 ± 0.6	250 ± 20	*80 ± 5*	5.0 ± 0.4	600 ± 50	34 ± 5
T01	*140 ± 10*	*81 ± 7*	2.4 ± 0.1	0.85 ± 0.07	<LoD	*150 ± 10*	1.1 ± 0.1	2.7 ± 0.2	1.4 ± 0.2
T02	*180 ± 10*	*42 ± 4*	2.4 ± 0.1	1.00 ± 0.08	<LoD	*130 ± 10*	1.2 ± 0.1	6.7 ± 0.6	3.2 ± 0.4
T03	*130 ± 10*	*90 ± 8*	1.1 ± 0.1	0.59 ± 0.05	<LoD	*63 ± 4*	1.7 ± 0.1	8.9 ± 0.7	1.1 ± 0.1
T04	*180 ± 10*	*32 ± 3*	3.3 ± 0.2	1.1 ± 0.1	<LoD	*65 ± 4*	1.7 ± 0.1	41 ± 3	6.3 ± 0.8
T05	*150 ± 10*	*290 ± 30*	2.1 ± 0.1	0.72 ± 0.06	<LoD	*90 ± 6*	2.6 ± 0.2	<LoD	0.59 ± 0.08
S01_I	*190 ± 10*	*150 ± 10*	1.5 ± 0.1	2.0 ± 0.2	90 ± 8	*9.1 ± 0.6*	2.3 ± 0.2	210 ± 20	31 ± 4
S01_II	*300 ± 20*	*170 ± 20*	1.8 ± 0.1	3.3 ± 0.3	110 ± 10	*11 ± 1*	2.9 ± 0.2	260 ± 20	35 ± 5
S02	*480 ± 30*	*71 ± 6*	2.3 ± 0.1	5.1 ± 0.4	220 ± 20	*38 ± 3*	4.8 ± 0.4	470 ± 40	50 ± 7
S03	*230 ± 10*	*150 ± 10*	1.4 ± 0.1	2.1 ± 0.2	120 ± 10	*4.3 ± 0.3*	2.0 ± 0.2	250 ± 20	39 ± 5
S04	*420 ± 30*	*59 ± 5*	1.6 ± 0.1	2.4 ± 0.2	210 ± 20	*35 ± 2*	2.9 ± 0.2	490 ± 40	16 ± 2
S05	*180 ± 10*	*170 ± 20*	1.1 ± 0.1	2.9 ± 0.2	82 ± 7	*4.5 ± 0.3*	1.9 ± 0.1	190 ± 20	120 ± 20
S06	*280 ± 20*	*37 ± 3*	1.1 ± 0.1	2.0 ± 0.2	130 ± 10	*43 ± 3*	2.2 ± 0.2	290 ± 20	6.5 ± 0.9
LoD [µg g⁻¹]	*3.3*	*6.4*	0.0075	0.017	25	*0.48*	0.24	0.85	0.065

	concentration [ng g⁻¹]							
sample	Rb	Li	*Fe*	Cr	V	Mn	Co	Ni
F01	2000 ± 100	1400 ± 100	*230 ± 10*	1100 ± 100	1300 ± 100	5200 ± 300	230 ± 10	1900 ± 100
F02	960 ± 50	760 ± 50	*110 ± 10*	570 ± 40	640 ± 30	2300 ± 100	110 ± 10	860 ± 60
F03	1400 ± 100	1200 ± 100	*170 ± 10*	730 ± 50	920 ± 50	4200 ± 300	170 ± 10	1400 ± 100
T01	<LoD	25 ± 2	*61 ± 4*	150 ± 10	38 ± 2	120	61 ± 4	720 ± 50
T02	23	42 ± 3	*240 ± 20*	410 ± 30	81 ± 4	210 ± 10	240 ± 20	590 ± 40
T03	19	27 ± 2	*240 ± 20*	1100 ± 100	340 ± 20	170 ± 10	240 ± 20	1100 ± 100
T04	100 ± 10	98 ± 6	*45 ± 3*	210 ± 10	82 ± 4	280 ± 20	45 ± 3	650 ± 40
T05	<LoD	14 ± 1	*18 ± 1*	100 ± 10	9.1 ± 0.5	1300 ± 100	18 ± 1	210 ± 10
S01_I	700 ± 40	360 ± 20	*95 ± 6*	1100 ± 100	590 ± 30	3600 ± 200	95 ± 6	4700 ± 300
S01_II	870 ± 50	460 ± 30	*110 ± 10*	550 ± 40	730 ± 40	2400 ± 200	110 ± 10	2900 ± 200
S02	1200 ± 100	1100 ± 100	*110 ± 10*	690 ± 50	750 ± 40	2500 ± 200	110 ± 10	1200 ± 100
S03	590 ± 30	510 ± 30	*91 ± 6*	580 ± 40	450 ± 20	2000 ± 100	91 ± 6	1100 ± 100
S04	1100 ± 100	1100 ± 100	*140 ± 10*	710 ± 50	740 ± 40	3000 ± 200	140 ± 10	760 ± 50
S05	410 ± 20	400 ± 30	*59 ± 4*	390 ± 30	310 ± 20	1200 ± 100	59 ± 4	650 ± 40
S06	660 ± 40	760 ± 50	*140 ± 10*	610 ± 40	540 ± 30	1700 ± 100	140 ± 10	1200 ± 100
LoD [ng g⁻¹]	18	0.87	*0.49*	7.2	1.1	39	0.49	14

sample	*Zn*	*Ga*	Tl	U	Pb
F01	*2400 ± 200*	*400 ± 30*	19 ± 1	130 ± 10	1200 ± 200
F02	*1100 ± 100*	*190 ± 20*	7.2 ± 0.5	54 ± 3	790 ± 100
F03	*1500 ± 100*	*290 ± 20*	22 ± 2	120 ± 10	1900 ± 300
T01	*1000 ± 100*	*130 ± 10*	<LoD	150 ± 10	230 ± 30
T02	*3900 ± 300*	*83 ± 7*	1.4 ± 0.1	95 ± 5	7300 ± 1000
T03	*960 ± 80*	*41 ± 3*	0.26 ± 0.02	82 ± 4	330 ± 40
T04	*1800 ± 200*	*130 ± 10*	1.6 ± 0.1	290 ± 20	710 ± 90
T05	*430 ± 40*	*72 ± 6*	0.35 ± 0.02	220 ± 10	52 ± 7
S01_I	*490 ± 40*	*180 ± 10*	41 ± 3	140 ± 10	1300 ± 200
S01_II	*340 ± 30*	*210 ± 20*	44 ± 3	170 ± 10	1600 ± 200
S02	*910 ± 80*	*250 ± 20*	100 ± 10	1100 ± 100	5000 ± 700
S03	*810 ± 70*	*140 ± 10*	53 ± 4	220 ± 10	2500 ± 300
S04	*1300 ± 100*	*210 ± 20*	19 ± 1	72 ± 4	1100 ± 100
S05	*720 ± 60*	*99 ± 8*	270 ± 20	290 ± 20	2700 ± 300
S06	*890 ± 80*	*140 ± 10*	5.1 ± 0.4	150 ± 10	470 ± 60
LoD [ng g⁻¹]	*36*	*0.20*	0.040	0.062	11

Tab. 30 Results of multi-element measurement of leached prehistoric wood digests with SU (k=2)

VI.2.3 Measurement of rare earth elements

sample	concentration [ng g^{-1}]					
	Sc	Y	La	Ce	Pr	Nd
F01	160 ± 40	310 ± 20	380 ± 20	800 ± 40	93 ± 5	350 ± 20
F02	81 ± 20	210 ± 10	190 ± 10	410 ± 30	47 ± 3	190 ± 10
F03	120 ± 30	290 ± 10	270 ± 10	590 ± 30	72 ± 4	280 ± 20
S01	120 ± 30	190 ± 10	130 ± 10	270 ± 20	32 ± 2	130 ± 10
S01II	150 ± 40	250 ± 10	180 ± 10	390 ± 20	46 ± 2	180 ± 10
S02	290 ± 70	310 ± 80	230 ± 60	470 ± 120	57 ± 16	220 ± 60
S03	260 ± 60	300 ± 10	150 ± 10	330 ± 20	44 ± 2	190 ± 10
S04	150 ± 40	210 ± 10	230 ± 10	480 ± 20	56 ± 3	210 ± 10
S05	450 ± 110	240 ± 10	110 ± 10	260 ± 10	32 ± 1	130 ± 10
S06	790 ± 190	180 ± 10	150 ± 10	320 ± 20	36 ± 2	130 ± 10
T01	3.4 ± 0.9	12 ± 1	2.9	5.5	0.59	3.8 ± 0.6
T02	15 ± 4	70 ± 4	19 ± 1	42 ± 2	5.1 ± 0.3	25 ± 2
T03	7.1 ± 1.9	9.9 ± 0.6	75 ± 4	140 ± 10	1.1 ± 0.1	4.9 ± 0.4
T04	48 ± 12	110 ± 10	20 ± 1	48 ± 2	6.4 ± 0.4	32 ± 3
T05	6.4 ± 1.6	19 ± 5	7.5 ± 2.1	14 ± 4	1.9 ± 0.6	9.5 ± 2.9
LoD [ng g^{-1}]	0.16	0.26	1.3	2.6	0.27	0.90
LoQ [ng g^{-1}]	0.52	0.86	4.3	8.6	0.88	3.0

sample	Sm	Gd	*Tb*	*Dy*	Ho	*Er*
F01	78 ± 5	71 ± 12	*12 ± 3*	*66 ± 6*	13 ± 1	*33 ± 2*
F02	47 ± 4	55 ± 13	*9.1 ± 1.3*	*48 ± 3*	9.3 ± 0.9	*23 ± 1*
F03	66 ± 4	72 ± 12	*11 ± 3*	*63 ± 3*	11 ± 1	*27 ± 2*
S01	31 ± 2	46 ± 11	*5.8 ± 1.3*	*41 ± 2*	7.7 ± 0.5	*20 ± 1*
S01II	44 ± 3	56 ± 8	*7.3 ± 2.1*	*53 ± 3*	9.9 ± 0.6	*27 ± 2*
S02	55 ± 15	74 ± 23	*12 ± 2*	*70 ± 20*	13 ± 4	*33 ± 9*
S03	63 ± 4	92 ± 17	*13 ± 2*	*78 ± 4*	14 ± 1	*34 ± 2*
S04	45 ± 3	48 ± 9	*6.9 ± 2.0*	*43 ± 2*	8.1 ± 0.5	*21 ± 2*
S05	38 ± 3	64 ± 14	*8.9 ± 2.6*	*55 ± 3*	10 ± 0	*25 ± 1*
S06	30 ± 2	31 ± 7	*5.1 ± 1.1*	*35 ± 2*	6.6 ± 0.3	*18 ± 1*
T01	1.2 ± 0.3	2.7 ± 2.6	*<LoD*	*1.4 ± 0.2*	0.099 ± 0.019	*0.89 ± 0.15*
T02	6.4 ± 0.6	12 ± 6	*0.98 ± 0.33*	*9.5 ± 0.5*	1.7 ± 0.1	*4.6 ± 0.5*
T03	1.2 ± 0.2	1.6 ± 1.7	*<LoD*	*1.3 ± 0.2*	0.090 ± 0.007	*0.91 ± 0.09*
T04	12 ± 1	33 ± 7	*3.5 ± 1.0*	*22 ± 2*	3.9 ± 0.2	*9.0 ± 1.0*
T05	1.9 ± 0.6	3.3 ± 2.3	*0.28 ± 0.40*	*2.2 ± 0.7*	0.55 ± 0.17	*1.7 ± 0.4*
LoD [ng g^{-1}]	0.14	0.23	*0.033*	*0.054*	0.012	*0.034*
LoQ [ng g^{-1}]	0.45	0.77	*0.11*	*0.18*	0.039	*0.11*

sample	Tm	Yb	*Lu*	Th
F01	4.8 ± 0.3	22 ± 2	*4.8 ± 0.7*	160 ± 10
F02	2.9 ± 0.2	14 ± 1	*2.6 ± 0.2*	83 ± 5
F03	3.4 ± 0.2	15 ± 1	*2.9 ± 0.2*	120 ± 10
S01	2.5 ± 0.2	13 ± 1	*2.7 ± 0.2*	68 ± 4
S01II	3.2 ± 0.3	16 ± 1	*2.8 ± 0.2*	92 ± 6
S02	4.5 ± 1.2	20 ± 6	*4.3 ± 1.1*	120 ± 10
S03	4.1 ± 0.3	20 ± 1	*4.0 ± 0.2*	93 ± 6
S04	2.6 ± 0.1	13 ± 1	*2.1 ± 0.2*	130 ± 10
S05	3.1 ± 0.2	16 ± 1	*3.3 ± 0.3*	67 ± 4
S06	2.4 ± 0.2	13 ± 1	*2.4 ± 0.2*	90 ± 6
T01	<LoD	0.88 ± 0.27	*0.18 ± 0.02*	0.74
T02	0.40 ± 0.05	2.9 ± 0.4	*0.33 ± 0.02*	2.0 ± 0.1
T03	<LoD	0.97 ± 0.22	*0.17 ± 0.01*	1.6 ± 0.1
T04	0.79 ± 0.08	5.0 ± 0.3	*0.68 ± 0.07*	15 ± 1
T05	0.28 ± 0.08	1.2 ± 0.3	*0.13 ± 0.04*	0.55
LoD [ng g^{-1}]	0.010	0.029	*n.d.*	0.47
LoQ [ng g^{-1}]	0.035	0.096	*n.d.*	1.6

italic values: with reservations due to quality control, n.d. not determinable,
values below LoQ are semiquantitative (no uncertainty stated)

Tab. 31 REE and Th concentration in dry prehistoric wood samples with expanded uncertainties (k=2)

	concentration [ng g^{-1}]									
sample	Sc	Y	La	Ce	Pr	Nd	Sm	Gd	*Dy*	Yb
RF1	0.31	1.6 ± 0.1	6.2 ± 0.4	3.3	0.28	1.6	0.44	1.2 ± 0.0	*0.060*	0.24 ± 0.29
RF2	<LoD	2.1 ± 0.6	11 ± 3	4.2	0.90 ± 0.26	2.7	0.30	<LoD	*0.30 ± 0.09*	<LoD
RF3	0.51	1.6 ± 0.1	6.5 ± 0.4	2.9	0.30	1.6	0.31	0.71	*<LoD*	0.24 ± 0.15
RF4	0.52	1.3 ± 0.2	3.1	3.4	<LoD	1.2	0.51 ± 0.16	1.1 ± 0.0	*<LoD*	0.23 ± 0.49
RF5	0.37	1.0 ± 0.1	2.4	<LoD	<LoD	0.91	0.44	0.69	*<LoD*	0.22 ± 0.36
RF6	0.25	0.58	<LoD	<LoD	<LoD	<LoD	0.27	0.68	*<LoD*	0.21 ± 0.43
RF7	0.43	0.73	<LoD	<LoD	<LoD	<LoD	0.24	0.79 ± 0.00	*<LoD*	0.23 ± 0.41
RF8	0.23	0.54	<LoD	<LoD	<LoD	<LoD	0.21	0.67	*<LoD*	0.21 ± 0.40
RF9	0.34	0.63	<LoD	<LoD	<LoD	<LoD	0.18	0.68	*<LoD*	0.21 ± 0.41
RF10	0.37	1.9 ± 0.2	11 ± 1	18 ± 1	1.4 ± 0.1	5.3 ± 0.7	1.0 ± 0.2	1.4 ± 0.0	*0.19 ± 0.08*	0.26 ± 0.21
RT1	0.26	1.1 ± 0.1	4.1	3.6	<LoD	1.2	0.32	0.95 ± 0.00	*<LoD*	0.23 ± 0.36
RT2	0.49	1.3 ± 0.2	3.7	<LoD	<LoD	1.3	0.52 ± 0.11	1.0 ± 0.0	*<LoD*	0.25 ± 0.28
RT4	0.31	0.78	2.6	4.2	<LoD	1.1	0.22	1.2 ± 0.0	*<LoD*	0.22 ± 0.45
RT5	0.88 ± 0.61	1.9 ± 0.2	12 ± 1	19 ± 1	0.95 ± 0.09	3.9 ± 0.5	0.61 ± 0.15	0.97 ± 0.00	*<LoD*	0.26 ± 0.22
RT6	0.29	2.6 ± 0.7	11 ± 3	15 ± 4	1.5 ± 0.4	4.5 ± 1.4	0.44	1.5 ± 0.0	*0.29 ± 0.09*	<LoD
RT7	0.33	0.38	<LoD	<LoD	<LoD	<LoD	0.15	0.73	*<LoD*	0.22 ± 0.56
RT8	0.28	<LoD	<LoD	<LoD	<LoD	<LoD	<LoD	0.75	*<LoD*	0.19 ± 0.20
RT9	0.32	1.2 ± 0.1	4.0	5.6	0.44	2.1	0.46 ± 0.16	1.6 ± 0.0	*0.13*	0.23 ± 0.24
RT10	0.41	0.46	1.6	<LoD	<LoD	<LoD	0.16	0.79 ± 0.00	*<LoD*	0.22 ± 0.34
RB1	0.55 ± 0.38	1.5 ± 0.1	3.6	<LoD	<LoD	1.2	0.27	0.75	*<LoD*	0.26 ± 0.17
RB2	<LoD	1.8 ± 0.3	4.9 ± 0.6	<LoD	0.40	1.1	0.28	<LoD	*0.14*	0.029
RB3	<LoD	1.4 ± 0.2	5.4 ± 0.5	<LoD	0.36	1.1	0.20	0.60	*0.10*	<LoD
RB4	0.51	1.9 ± 0.2	2.9	3.3	0.33	1.3	0.42	<LoD	*0.19 ± 0.07*	0.075
RB5	0.20	1.6 ± 0.2	3.3	<LoD	<LoD	<LoD	0.51 ± 0.27	<LoD	*<LoD*	<LoD
RB6	<LoD	1.6 ± 0.3	5.2 ± 0.5	3.9	0.46	1.6	0.35	0.30	*0.14*	0.039
RB7	<LoD	1.0 ± 0.2	1.5	<LoD	<LoD	<LoD	0.30	<LoD	*0.094*	<LoD
RB8	0.53 ± 0.37	1.3 ± 0.4	1.8	2.6	<LoD	1.1	<LoD	0.79 ± 0.00	*0.26 ± 0.08*	<LoD
RB9	0.16	0.85	2.6	<LoD	0.28	0.97	0.21	<LoD	*0.097*	0.035
RB10	0.50	2.2 ± 0.2	8.8 ± 0.7	6.3	1.1 ± 0.1	3.9 ± 0.5	0.73 ± 0.15	0.98 ± 0.00	*0.37 ± 0.27*	0.039
LoD [ng g^{-1}]	0.16	0.26	1.3	2.6	0.27	0.90	0.14	0.23	*0.054*	0.029
LoQ [ng g^{-1}]	0.52	0.86	4.3	8.6	0.88	3.0	0.45	0.77	*0.18*	0.096

italic values: with reservations due to quality control, n.d. not determinable, values below LoQ are semiquantitative (no uncertainty stated)

Tab. 32 REE concentrations in dry recent wood samples with expanded uncertainties (k=2)

	concentration [ng g^{-1}]							
SM extracts	Sc	Y	La	Ce	Pr	Nd	Sm	Gd
average	1.9	2.4	1.1	1.4	0.17	0.71	0.22	0.2
minimum	0.61	1.1	0.24	<LoD*	0.026	0.18	0.065	<LoD*
maximum	3.6	7.1	5.6	8.2	0.92	3.8	1	1.2
average prehistoric wood (S01-S06)	320	240	170	360	43	170	44	59
LoD for SM extracts	0.34	0.63	0.91	0.85	0.51	0.57	0.59	0.071
LoQ for SM extracts	1.1	2.1	3	2.8	1.7	1.9	2	0.24
LoD* from digestion blanks	0.015	0.025	0.12	0.25	0.025	0.086	0.013	0.022
LoQ* from digestion blanks	0.05	0.082	0.41	0.82	0.084	0.29	0.043	0.074

SM extracts	*Tb*	*Dy*	Ho	*Er*	Tm	Yb	*Lu*
average	*0.028*	*0.18*	0.05	*0.085*	0.012	0.12	*0.012*
minimum	*<LoD**	*0.034*	<LoD*	*0.026*	<LoD*	0.035	*n.d.*
maximum	*0.12*	*0.77*	0.21	*0.36*	0.043	0.25	*0.036*
average prehistoric wood (S01-S06)	*8.4*	*53*	9.9	*26*	3.2	16	*3.1*
LoD for SM extracts	*0.038*	*0.42*	0.56	*0.66*	0.52	0.38	*0.043*
LoQ for SM extracts	*0.13*	*1.4*	1.9	*2.2*	1.7	1.3	*0.14*
LoD* from digestion blanks	*0.0031*	*0.0051*	0.0011	*0.0032*	0.0010	0.0027	*n.d.*
LoQ* from digestion blanks	*0.01*	*0.017*	0.0037	*0.011*	0.0033	0.0091	*n.d.*

italic values: with reservations due to quality control, n.d. not determinable,
values below LoD included, but below LoD* (determined from digestion blanks) excluded

Tab. 33 Results from REE measurement of mine material

VI.2.4 Measurement of Sr isotope ratios

sample name	c(Sr) [µg g^{-1}]	^{87}Sr/^{86}Sr ± SU (k=2)	RSU (k=2)
SM01	162	0.70759 ± 0.00014	0.019%
SM02	53	0.70791 ± 0.00013	0.018%
SM03	39	0.70787 ± 0.00014	0.019%
SM03A	33	0.70797 ± 0.00014	0.019%
SM04	52	0.70794 ± 0.00012	0.017%
SM05	23	0.70834 ± 0.00013	0.019%
SM06	33	0.70821 ± 0.00013	0.018%
SM07	6.5	0.70835 ± 0.00019	0.026%
SM08	87	0.70760 ± 0.00015	0.022%
SM09	75	0.70783 ± 0.00014	0.019%
SM10	60	0.70800 ± 0.00015	0.022%
average SM*	57	0.70796 ± 0.00051	0.072%

* 2 (R)SD is given instead of (R)SU (k=2)

Tab. 34 Sr concentration and Sr isotope ratios for extracts of surrounding mine material

sample	mineralogy	c(Sr) [µg g^{-1}]	^{87}Sr/^{86}Sr ± 2σ	2σ$_{rel}$
TS 26	anhydrite	1265	0.709773 ± 0.000011	0.0015%
TS 37	anhydrite	1471	0.708839 ± 0.000020	0.0028%
A 12	anhydrite	542	0.707643 ± 0.000012	0.0017%
E 6	anhydrite	1034	0.707269 ± 0.000008	0.0011%
FJ 17	gypsum, anhydrite	4336	0.708240 ± 0.000026	0.0037%

all data from Spötl and Pak [1996]

Tab. 35 Sr concentrations and Sr isotope ratios for Permian and Lower Triassic evaporites from Hallstatt

sample name	c(Sr) [µg g^{-1}]	^{87}Sr/^{86}Sr ± SU (k=2)	RSU (k=2)
T01_L1	2.8 ± 0.2	0.70793 ± 0.00018	0.025%
T01_L2	0.93 ± 0.06	0.70807 ± 0.00061	0.086%
T01_L3	0.39 ± 0.02	0.70787 ± 0.00047	0.066%
T01_L4	2.7 ± 0.2	0.70787 ± 0.00016	0.022%
T01_L5	1.1 ± 0.1	0.70789 ± 0.00025	0.035%
S01_L1	1.8 ± 0.1	0.70788 ± 0.00025	0.035%
S01_L2	0.39 ± 0.02	0.70827 ± 0.00058	0.082%
S01_L3	0.13 ± 0.01	0.70820 ± 0.00057	0.080%
S01_L4	3.9 ± 0.2	0.70785 ± 0.00017	0.024%
S01_L5	2.0 ± 0.1	0.70792 ± 0.00013	0.019%

Tab. 36 Sr concentrations and Sr isotope ratios for leaching solutions of prehistoric wood samples T01 and S01

| sample name | measurement results | | RSU (k=2) | uncertainty contributions | | |
	c(Sr) [µg g^{-1}]	^{87}Sr/^{86}Sr ± SU (k=2)		U$_{blank}$	U$_{Rb}$	U$_{mb}$
RB1	3.8 ± 0.2	0.70917 ± 0.00034	0.048%	60%	38%	2%
RB2	4.6 ± 0.3	0.70912 ± 0.00033	0.047%	77%	13%	10%
RB3	3.8 ± 0.2	0.70913 ± 0.00030	0.042%	88%	11%	1%
RB4	4.8 ± 0.3	0.70966 ± 0.00031	0.043%	76%	23%	1%
RB5	3.9 ± 0.3	0.71787 ± 0.00035	0.049%	79%	20%	1%
RB5a	*2.2 ± 0.1*	*0.72371 ± 0.00056*	*0.077%*	*6%*	*92%*	*2%*
RB6	1.9 ± 0.1	0.71105 ± 0.00047	0.066%	86%	13%	1%
RB6a	2.0 ± 0.1	0.71098 ± 0.00043	0.061%	38%	60%	2%
RB7	3.7 ± 0.2	0.70949 ± 0.00029	0.041%	60%	40%	1%
RB8	2.3 ± 0.1	0.70888 ± 0.00042	0.060%	60%	39%	0%
RB9	4.2 ± 0.3	0.71200 ± 0.00018	0.025%	78%	20%	1%
RB9a	2.4 ± 0.2	0.71235 ± 0.00040	0.056%	20%	80%	1%
RB10	3.8 ± 0.2	0.70971 ± 0.00018	0.026%	59%	40%	1%
RT1	5.7 ± 0.4	0.71108 ± 0.00029	0.040%	88%	12%	1%
RT1a	*2.9 ± 0.2*	*0.71957 ± 0.12069*	*17%*	*0%*	*100%*	*0%*
RT2	6.5 ± 0.4	0.71054 ± 0.00017	0.023%	81%	18%	1%
RT4	1.8 ± 0.1	0.70974 ± 0.00040	0.057%	80%	20%	1%
RT5	3.5 ± 0.2	0.70983 ± 0.00054	0.076%	79%	21%	0%
RT6	2.3 ± 0.2	0.71035 ± 0.00056	0.079%	80%	20%	0%
RT7	1.6 ± 0.1	0.70924 ± 0.00043	0.060%	86%	13%	1%
RT8	1.2 ± 0.1	0.70868 ± 0.00041	0.058%	88%	11%	1%
RT9	2.5 ± 0.2	0.71377 ± 0.00037	0.052%	88%	11%	1%
RT9a	*1.6 ± 0.1*	*0.71476 ± 0.00412*	*0.58%*	*0%*	*98%*	*1%*
RT10	3.6 ± 0.2	0.70961 ± 0.00036	0.051%	82%	17%	1%
RF1	11.3 ± 0.7	0.70902 ± 0.00020	0.028%	80%	19%	1%
RF2	11.4 ± 0.7	0.70922 ± 0.00018	0.025%	85%	14%	1%
RF3	14.2 ± 0.9	0.70905 ± 0.00024	0.034%	70%	29%	1%
RF4	5.8 ± 0.4	0.71025 ± 0.00015	0.020%	71%	28%	1%
RF5	5.5 ± 0.4	0.71085 ± 0.00025	0.035%	66%	34%	1%
RF6	4.0 ± 0.3	0.70995 ± 0.00025	0.035%	88%	11%	1%
RF7	8.6 ± 0.6	0.71099 ± 0.00017	0.024%	85%	14%	1%
RF8	6.1 ± 0.4	0.70913 ± 0.00028	0.040%	88%	12%	1%
RF9	9.1 ± 0.6	0.71067 ± 0.00026	0.036%	71%	28%	1%
RF10	10.2 ± 0.7	0.71115 ± 0.00045	0.064%	85%	15%	1%

italic values: with reservations (see text)

Tab. 37 Sr concentrations, Sr isotope ratios with SU (k=2) and uncertainty contributions of blank, Rb correction and mass bias correction for recent wood samples

sample name	c(Sr) [μg g^{-1}]	^{87}Sr/^{86}Sr ± SU (k=2)	RSU (k=2)
S01_I	2.0 ± 0.1	0.71171 ± 0.00016	0.023%
S01_II	3.3 ± 0.2	0.71084 ± 0.00015	0.021%
S02	5.1 ± 0.3	0.71047 ± 0.00034	0.048%
S03	2.1 ± 0.1	0.71116 ± 0.00056	0.078%
S04	2.4 ± 0.1	0.71331 ± 0.00057	0.080%
S05	2.9 ± 0.2	0.70968 ± 0.00038	0.053%
S06	2.0 ± 0.1	0.71190 ± 0.00060	0.084%
T01	0.85 ± 0.05	0.70799 ± 0.00064	0.090%
T02	1.00 ± 0.06	0.70782 ± 0.00066	0.094%
T03	0.59 ± 0.04	0.70762 ± 0.00103	0.15%
T04	1.1 ± 0.1	0.70890 ± 0.00054	0.076%
T05_I	0.72 ± 0.04	0.70801 ± 0.00028	0.040%
T05_II	6.0 ± 0.4	0.70839 ± 0.00133	0.19%
F01	7.5 ± 0.5	0.71108 ± 0.00033	0.046%
F02	4.6 ± 0.3	0.71039 ± 0.00039	0.055%
F03	7.2 ± 0.4	0.71009 ± 0.00034	0.047%

Tab. 38 Sr concentrations and Sr isotope ratios for prehistoric wood samples

VI.3 List of Abbreviations

°C	degree Celsius
a	year
amu	atomic mass unit
asl	above sea level
BC	before Christ
c	concentration
CCD	charge-coupled device
CITAC	Cooperation on International Traceability in Analytical Chemistry
cps	counts per second
CRDS	cavity ring down spectroscopy
CRM	certified reference material
DNA	desoxyribonucleic acid
DRC	dynamic reaction cell
equ.	equation
et al.	et alii
ETV	electrothermal vaporisation
eV	electron volt
fig.	figure
FTIR	Fourier transform infrared
g	gram
HPLC-PDA	high performance liquid chromatography with photo diode array detection
HR	high resolution
HREE	heavy rare earth elements
Hz	Hertz
ICP	inductively coupled plasma
INAA	instrumental neutron activation analysis
int	intensity
IRMS	isotope ratio mass spectrometry
IUPAC	International Union of Pure and Applied Chemistry
J	Joule
k	coverage factor
L	litre
LA	LASER ablation
LASER	light amplification by stimulated emission of radiation
LDA	linear discriminant analysis
LREE	light rare earth elements
m	mass
M	molar
MC	multiple collector
MS	mass spectrometry
n.c.	not certified
n.d.	not determined
NAA	neutron activation analysis
Nd:YAG	neodymium doped yttrium aluminium garnet

p.a.	pro analysi
PCA	principal component analysis
PE	polyethylene
PFA	perfluoroalkoxy
PP	polypropylene
PTFE	polytetrafluoroethylene
QC	quality control
QMS	quadrupole mass spectrometry
R	resolution
REE	rare earth elements
RM	reference material
rpm	revolutions per minute
RSU	relative standard uncertainty
SD	standard deviation
SEM/EDS	scanning electron microscopy / energy dispersive X-ray spectroscopy
SF	sector field
SM	surrounding (mine) material
SU	standard uncertainty
tab.	table
TIMS	thermal ionisation mass spectrometry
U	voltage
UV	ultraviolet
V	volt
VIRIS	Vienna Isotope Research, Investigation and Survey
VSMOW	Vienna standard mean ocean water
W	watt
wlr	weighted linear regression
z	charge
Ω	ohm

VI.4 List of Tables

VI.5 List of Figures

VI.6 List of Equations

VI.7 Curriculum Vitae

Angaben zur Person

Name	Monika Horsky
Adresse	Felbigergasse 62/8, 1140 Wien, Österreich
Geburtsdatum, -ort	08. Mai 1985, Wien
Familienstand	ledig

Ausbildung

2008/12 – 2010/03	Diplomarbeit im VIRIS-Labor, Department für Chemie, Universität für Bodenkultur
2007/02	Erste Diplomprüfung
2003/10 –	Diplomstudium der Chemie an der Universität Wien
2003/06	Matura mit ausgezeichnetem Erfolg
1995/09 – 2003/06	Goethegymnasium Astgasse 3, 1140 Wien, Schulzweig Gymnasium
1991/09 – 1995/06	Volksschule Felbigergasse 97, 1140 Wien

Relevante Arbeitstätigkeiten

2008/03–07	Tutorin, Chemische Übungen für Biologen und Ernährungswisschenschafter, Universität Wien, Institut für Organische Chemie
2007/08–09	Praktikum Archivrecherche, Abteilung Verfahrensentwicklung, Fresenius Kabi Austria GmbH, 4020 Linz
2007/03–07	Tutorin, Chemische Übungen für Biologen und Ernährungswissenschafter, Universität Wien, Institut für Organische Chemie
2006/08	Praktikum Labortätigkeit, Abteilung Verfahrensentwicklung, Fresenius Kabi Austria GmbH, 4020 Linz